12. SITE 697[1]

Shipboard Scientific Party[2]

HOLE 697A

Date occupied: 3 March 1987, 1130 local time

Date departed: 4 March 1987, 1645, local time

Time on hole: 29 hr, 15 min

Position: 61°48.634′S, 40°17.27′W

Bottom felt (m, drill pipe): 3491

Distance between rig floor and sea level (m): 11

Water depth (drill-pipe measurement from sea level, m): 3480

Penetration (m): 20.9

Number of cores: 3

Total length of cored section (m): 20.9

Total core recovered (m): 26.60

Core recovery (%): 130

Oldest sediment cored:
Depth sub-bottom (m): 19.5
Nature: Clayey mud
Age: Quaternary
Measured velocity (km/s): 1.498

HOLE 697B

Date occupied: 4 March 1987, 1645 local time

Date departed: 7 March 1987, 1330 local time

Time on hole: 69 hr, 15 min

Position: 61°48.626′S, 40°17.749′W

Bottom felt (m, drill pipe): 3491

Distance between rig floor and sea level (m): 11

Water depth (drill-pipe measurement from sea level, m): 3480

Penetration (m): 322.9

Number of cores: 32

Total length of cored section (m): 304.9

Total core recovered (m): 188.27

Core recovery (%): 62

Oldest sediment cored:
Depth sub-bottom (m): 320.1
Nature: Silty mud
Age: early Pliocene
Measured velocity (km/s): 1.601

Principal results: Site 697 lies in Jane Basin, in 3480 m water depth, and is the deepest member of a three-site depth transect on the northern margin of the Weddell Gyre. Jane Basin formed at 25–30 Ma ago as a back-arc basin separating the then-active island arc of Jane Bank from the South Orkney microcontinent (SOM). Sediments in Jane Basin extend back to the upper Oligocene, but a prominent reflector of probable middle Miocene age, at 550 ms twt (two-way traveltime), separates a lower terrigenous and volcaniclastic turbidite sequence from an upper hemipelagic sequence which was the target for Leg 113 drilling. Antarctic Bottom Water flows northward through Jane Basin, and the hemipelagic sediments promised a high-resolution record of bottom-water production and sediment transport in the past.

Two holes were drilled in 4 days, 2 hr, and 30 min, 3–7 March, 1987. With Hole 697A we penetrated to 20.9 mbsf and recovered 26.60 m (130%) in 3 APC cores. We abandoned the hole when the Advanced Hydraulic Piston Corer (APC) could not be retracted. In Hole 697B we washed to 18.0 mbsf, cored to 322.9 mbsf, recovering 188.27 m (62%) in 11 APC and 21 Extended Core Barrel (XCB) cores; the hole was abandoned when time ran out.

The sedimentary sequence is mainly hemipelagic, with a minor siliceous biogenic component and numerous thin, altered, volcanic ash layers. Ice-rafted detritus (IRD) occurs throughout, but is abundant only near the base of the sequence.

Lithologic units are Unit I: 0–293.0 mbsf, silty and clayey mud, with variable diatom content, as thin laminae and disseminated. Subunit IA, 0–15.5 mbsf, is upper Quaternary silty mud and diatom-bearing silty mud; Subunit IB, 15.5–85.7 mbsf, is upper Pliocene to Pleistocene clayey mud and clay, devoid of diatoms but for one core; Subunit IC, 85.7–293.0 mbsf, is Pliocene, mainly diatom-bearing clayey mud. Unit II: 293.0 to 322.9 mbsf is lower Pliocene silty and clayey mud, without diatoms.

Only four thin turbidites were found, three beween 161 and 162 mbsf. Volcanics are ash altered to smectite, disseminated glass, and thin vitric ash layers. Illite and chlorite dominate the clay minerals, varying more smoothly than at other sites.

The biogenic component is siliceous: diatoms dominate, fluctuating in abundance and preservation but including a few, thin, pristine ooze interbeds. Generally, biosiliceous abundance and preservation vary with time and between taxonomic groups as at other, shallower sites, but with less amplitude.

Magnetostratigraphic zonation is precise, and indicates high and smoothly-varying sedimentation rates, of as much as 150 m/m.y. for the Gilbert to the middle Gauss and 40 m/m.y. to the upper Brunhes. The biostratigraphy is in agreement.

The expanded section at Site 697 provides a high-fidelity magnetostratigraphic record with opportunities for calibration of high-latitude biosiliceous zonations and paleoceanographic studies. The Blake Subchron occurs as a doublet at 4 mbsf, confirming its global range and reversed nature. Whole-core susceptibilities may reflect orbitally-induced changes in sediment composition. Volcanic ash beds can provide additional correlation between South Orkney transect sections, particularly useful for high-resolution studies of bottom-water variability.

Quaternary sedimentation rates are more than five times higher than at any other Leg 113 site, and indicate continued sediment supply and bottom-water nepheloid transport in the Weddell Gyre despite contrary indications elsewhere. This suggests changes in the distribution and mode of formation of turbidity currents along the West Antarctic and Antarctic Peninsula margins of the Weddell Sea.

BACKGROUND AND OBJECTIVES

Site 697 is the deepest of a three-site depth transect of the southeast margin of the South Orkney microcontinent (SOM). It lies near 61°49′S, 40°17′W, in 3480 m of water, in Jane Basin (Fig. 1). It is located on the single-channel seismic reflection profile BRAN801-E (Birmingham University/British Antarctic Survey; Figs. 2 and 3).

[1] Barker, P. F., Kennett, J. P., et al., 1988. *Proc. ODP, Init. Repts.*, 113: College Station, TX (Ocean Drilling Program).

[2] Shipboard Scientific Party is as given in the list of participants preceding the contents.

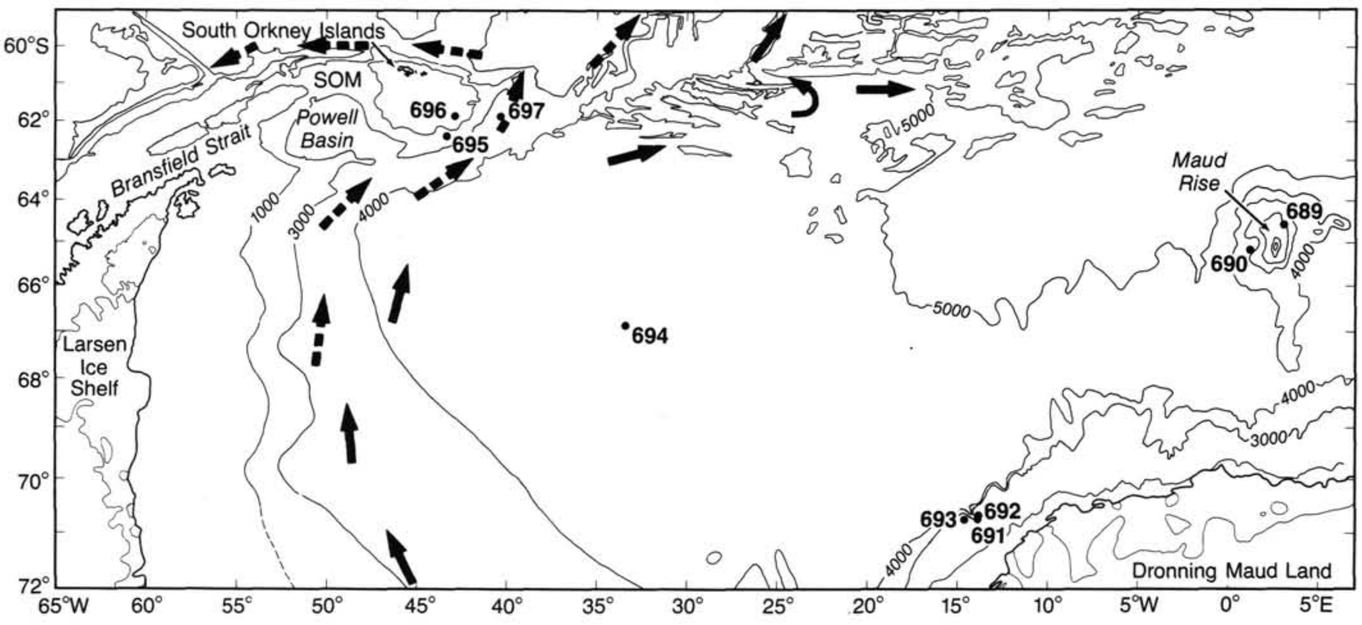

Figure 1. Regional setting of Site 697 showing deep-water pathways (arrowed) available for bottom-water flow into and out of Jane Basin (after Pudsey, et al., in press). SOM = South Orkney microcontinent.

Jane Basin was formed as a back-arc basin 25–30 Ma ago, when Jane Bank, then an active island arc subducting oceanic lithosphere of the South American plate, separated from the SOM (Barker et al., 1984; Lawver et al., 1986; King and Barker, 1988). The sediments in Jane Basin thus extend back into the upper Oligocene. At a depth of about 500 m at the site, a prominent reflector marks a change in the dominant mode of sedimentation. The overlying sediments appear hemipelagic, in that they are draped evenly over the subdued topography of the reflector and pinch out at the western, SOM margin of the basin (Fig. 3). The underlying sediments, in contrast, do not pinch out, and appear to be derived directly from both the SOM and the now-dead island arc of Jane Bank. From radiometric ages of dredged rocks from the island arc, volcanic activity ceased 15–20 Ma ago, shortly after subduction stopped (Barker et al., 1984). The younger, hemipelagic mode of deposition therefore extends back no further than the early middle Miocene.

Site 697 forms part of a depth transect intended to examine the history of the circum-Antarctic water masses. At present, Antarctic Bottom Water (AABW) flows through Jane Basin as part of the general clockwise circulation of the Weddell Gyre (for an overview, see Foster and Middleton, 1979, 1980). The densest variety of AABW, designated Weddell Sea Bottom Water (WSBW), is probably formed by a series of mixing processes in the southern Weddell Sea, which modify the Warm Deep Water by the addition of brine from beneath forming sea-ice, and water which has been supercooled beneath the floating ice shelves. Most of the densest AABW so formed either flows northward out of the Weddell Sea along deep pathways, or recirculates within the gyre. Some, slightly less dense, bottom water flows north along Jane Basin and into the Scotia Sea through gaps in the South Scotia Ridge.

Sediments in Jane Basin should therefore provide information about bottom-water production, circulation, and transport in the past. Gravity cores near the site recovered fine-grained hemipelagic sediments which show fluctuations in grain size, and diatom abundance and preservation, which may reflect Quaternary glacial/interglacial cyclicity (Pudsey et al., in press). Sedimentation rates appear high (average about 30 m/m.y.); if these high rates extend through the Pleistocene, Site 697 would have the highest Pleistocene rate by far of any Leg 113 site. During the Pliocene too, the higher siliceous biogenic productivity and apparently abundant hemipelagic component found at Sites 693 and 695 promise an expanded section. In the time available at the end of the leg, it seemed possible to sample also the lowermost Pliocene and uppermost Miocene, to see what was the fine-grained equivalent of the massive coarse sands found at Site 694 in the Weddell Basin.

The site was moved about 10 km west from the original location, to make the deeper layers more accessible, in view of the limited time available for drilling. A single APC/XCB hole was intended, to consume all of the time remaining on the leg.

OPERATIONS

Site 697 is 74.9 nmi east of Hole 696B. The ship reached full speed ahead at 0432 hr on 2 March 1987, and the area of Site 697 was reached late on the morning of the same day.

Hole 697A

The dropping of the beacon was delayed 3 hr while waiting on approval from the Pollution Prevention and Safety Panel to move the location about 6 mi. Beacon # 335, 15.5 kHz, was launched at 61°48.74′S, 40°17.40′W, at 1420 on 2 March.

The hole was to be APC/XCB cored. A used 11-7/16-in. bit MSDS-S695 with the mechanical release was run. The remainder of the bottom-hole assembly was the usual 14-drill-collar one which had been run on nearly all the holes. Weather conditions were deteriorating as the drill pipe was started in the hole. Winds were gusting to 40–50 kt and the seas were building past 20 ft in height. The weather did not stop the pipe-running operation but the resulting ship motion did slow the trip. This was the first time on the leg that weather hampered operations, excluding ship transit.

The water depth indicated by the precision depth recorder (PDR) was 3495.3 m. The bit was positioned at 3491 m for the first core. Ship heave was in the range of 3 m, and coring the mud line under these conditions is at best unpredictable. The first core contained 8.93 m and established the seabed at 3491 m below the rig floor (3480 mbsf). The co-chief requested the first four cores be double-cored because of the large amount of heave;

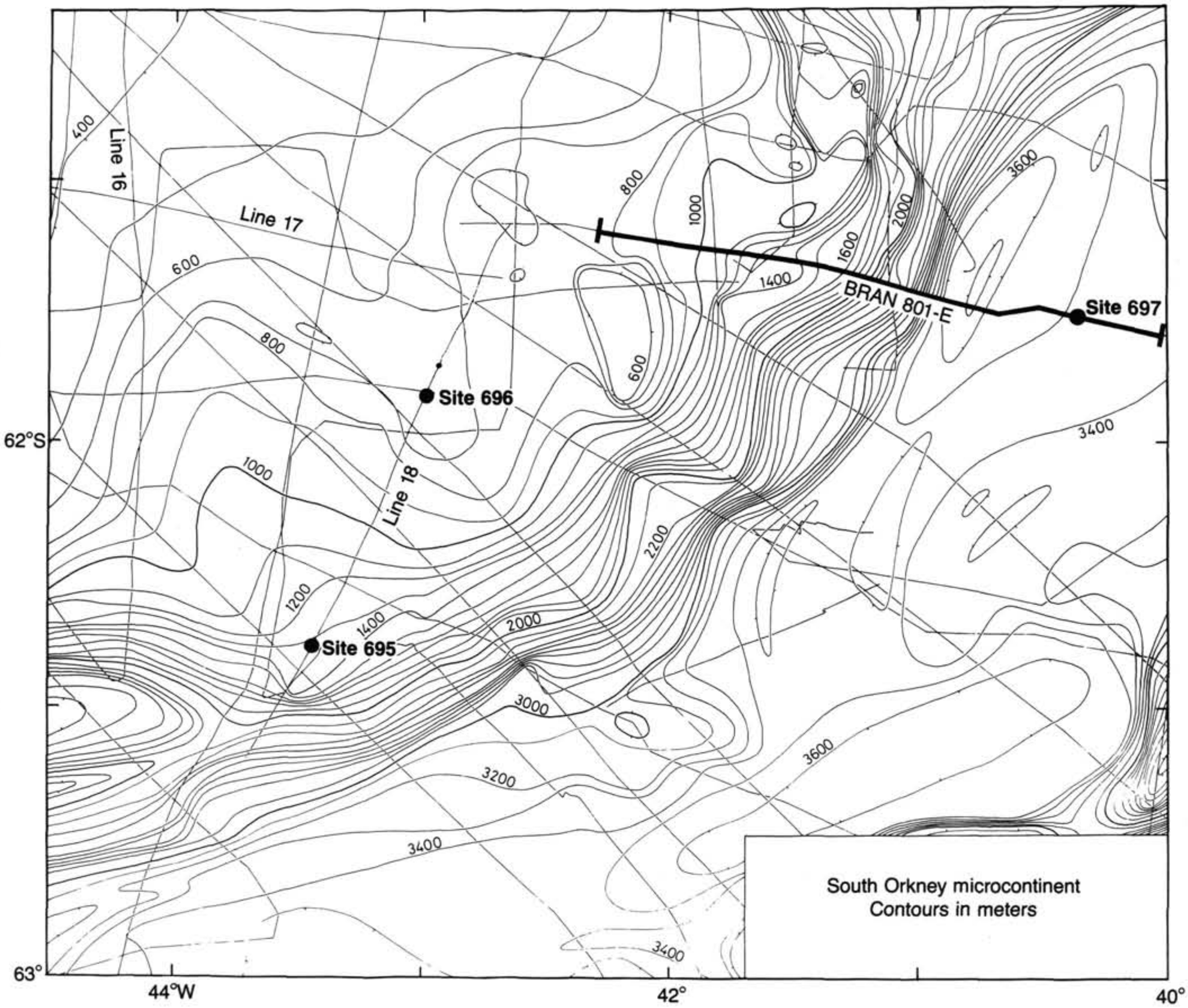

Figure 2. ODP sites on southeast margin of SOM and in Jane Basin, showing location of single channel seismic profile BRAN801-E.

the bit was advanced less than the normal 9.5 m each core. It was hoped that this practice would reduce the amount of missing section caused by ship heave.

Three piston cores were taken to a depth of 20.9 mbsf (Table 1). After shooting the third core, the inner core barrel became stuck and could not be pulled out of the bottom hole assembly with the wire line. It was necessary to trip the drill pipe out of the hole. It was expected that the reason the barrel could not be pulled was that it had been bent, either from hitting a rock or by the ship heaving. When the bit reached the surface about 65% of the barrel was projecting below the bit and the barrel was not damaged. The latch, a suspected problem, had released properly and the seals of the piston were positioned inside the outer barrel in a normal location. There was no visible sand or other material holding the inner barrel in place. There is little doubt that the seals were stuck, but there were no marks on the seals or on the metal retainers that hold them in place. It is speculated that a piece of shear pin may have been caught between the seals and outer barrel where the clearance is only 0.05 in., but there was no damage or mark to support this conclusion.

As a precaution against unseen damage the outer barrel was laid down and replaced. The bottom-hole assembly was run down the hole a few stands and the APC was test fired and retrieved with no problem.

Hole 697B

The mechanical bit release was laid down and the drill pipe run in the hole. Hole 697B was spudded at 0400 on 4 March. The first core was washed to 18.0 m to provide a little overlap with Hole 697A. Piston coring continued to 119.8 mbsf where a pullout of 60,000 lb indicated the necessity of switching to the XCB system. A total of 75.61 m was recovered from the 101.8-m APC interval (Table 1). Coring was routine except for the continued problem of ship heave which resulted in the shearing of the pins in the core retrieve overshot.

Cores 113-697B-12X to 113-697B-32X were from 119.8 to 322.9 mbsf. Except for one shattered liner the operation was routine. The last core reached the surface at 0330 on 7 March. The proposed total depth had not been reached but there was no time remaining in the leg to continue the operation. The drill pipe was secured on the ship in the early afternoon of 7 March,

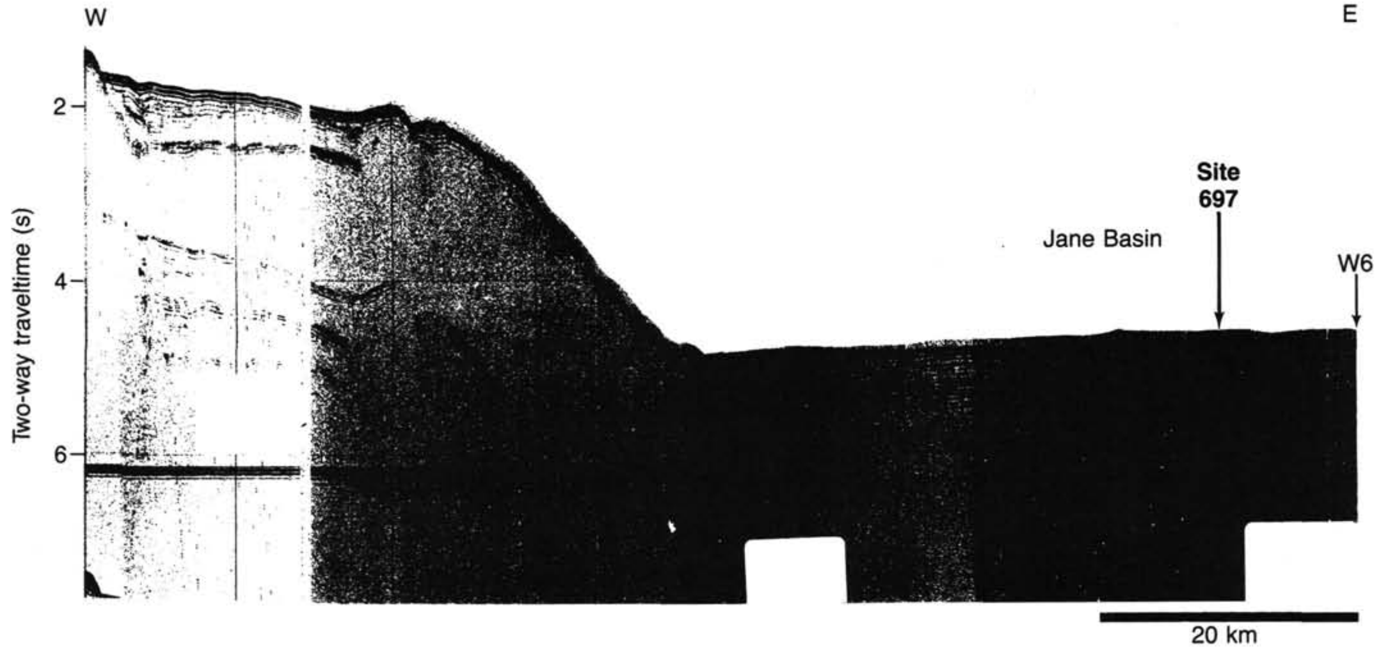

Figure 3. Seismic profile BRAN801-E showing original (W6) and revised position of Site 697.

thrusters were pulled, and the *JOIDES Resolution* departed for East Cove in the Falkland Islands at 1330.

LITHOSTRATIGRAPHY

Introduction

Site 697 was cored to a depth of 322.9 mbsf and a total of 215 m of sediment recovered from two holes (Fig. 4). The sedimentary sequence is mainly of hemipelagic origin, with a small siliceous biogenic component and numerous thin, altered ash layers. Ice-rafted detritus (IRD) is only abundant near the base of the sequence. Two lithologic units are recognized, the upper one being divided into three subunits (Table 2). Recovery at this site was generally good and drilling disturbance is severe in only a few cores (Cores 113-697A-2H, 113-697B-5H, 113-697B-12X, and 113-697B-23X).

Unit I (0–293.0 mbsf; Age late Pleistocene to early Pliocene)
Cores 113-697A-1H through 113-697A-3H; 113-697B-1H through 113-697B-29X

Unit I is nearly 300 m thick and has been divided into three subunits using the proportion of diatoms in the sediment, estimated from smear slides (Fig. 5). The unit includes silty and clayey mud, diatom-bearing silty and clayey mud, clay, and diatom clayey mud as major lithologies. Each subunit is described in detail below but the following remarks apply to the whole unit.

Volcanic ash (altered to clay) occurs throughout Unit I and comes in two main varieties: (1) dark gray (N 4/0) to very dark gray (N 3/0) clay, forming laminae or filling burrows; (2) greenish gray (5G 5/1) to dark greenish gray (5G 4/1) clay, forming very thin beds 1–2 cm thick. The occurrence of these two types, termed gray and green respectively, is shown in Figure 4. The amount of ash varies downcore but has not been used to create subunits; color contrasts with the surrounding sediment are faint, and the ash beds are difficult to see in disturbed cores. Green layers are commonly but not invariably found overlying gray laminae. A few coarser vitric ash beds occur in Subunits IA and IC and are described below.

IRD is present throughout Unit I but is nowhere abundant. Sedimentary dropstones predominate although metamorphic and igneous rocks are also found. Most are less than 2 cm across but some are as large as core-liner diameter in size (7 cm). Most are rounded or subrounded.

Subunit IA (0–15.5 mbsf; late Pleistocene)
Core 113-697A-1H through Sample 113-697A-3H-3, 125 cm; thickness 15.5 m

Subunit IA consists of silty mud and diatom-bearing silty mud, predominantly gray (5Y 6/1, 5Y 5/1) in the upper 5 m and greenish gray (5G 5/1, 5GY 5/1, 5BG 5/1) from 5 to 13 mbsf, becoming dark gray to dark greenish gray (N 4/0, 5G 4/1, 5BG 4/1) at the base. This color change is accompanied by a downward increase in fine-grained sediments (Fig. 6). Minor bioturbation is present where not obliterated by drilling disturbance. Diatom-bearing and barren silty mud alternate in cycles about 2 m thick (Fig. 7) continuing the pattern seen in nearby gravity cores (see "Background and Objectives" section, this chapter). Diatom occurrence is not related to color changes. In Sample 113-697A-2H-5, 45–85 cm, there is a diatom ooze layer composed mainly of *Corethron criophilum*. The proportion of other diatom species and of clay increases toward the base of this ooze layer.

Two very dark grayish brown (2.5Y 3/2) fine-grained ash beds occur in 113-697A-1H-2; they have sharp contacts with the surrounding mud. Subunit IA contains 5%–10% of volcanic glass (estimated from smear slides: Fig. 5).

Subunit IB (15.5–85.7 mbsf; late Pliocene to Pleistocene)
Sample 113-697A-3H, 125 cm, through Section 113-697A-3H, CC; Cores 113-697B-1H through 113-697B-7H; thickness 70.2 m

Subunit IB consists of clayey mud and clay, with diatoms rare to absent except for one interval in Core 113-697B-4H. Color is very uniform, mainly dark gray (N 4/0) shading to dark greenish gray (5GY 4/1), 5G 4/1, 5BG 4/1); all color changes are subtle and gradational. Faint minor to moderate bioturbation is seen throughout the subunit. Very small (1–2 mm) clasts of angular quartz silt occur sparsely in all cores except Core 113-

Table 1. Coring summary, Site 697.

Core No.	Date (March 1987)	Time	Depth (mbsf)	Cored (m)	Recovered (m)	Recovery (%)
113-697A-						
1H	3	0145	0–8.9	8.9	8.93	100.0
2H	3	0345	5.3–14.9	9.6	9.57	99.7
3H	3	1515	11.3–20.9	9.6	8.10	84.4
				28.1	26.60	
113-697B-						
1H	4	0615	18.0–27.5	9.5	2.86	30.1
2H	4	0830	27.5–37.1	9.6	9.54	99.4
3H	4	1200	37.1–46.8	9.7	10.15	104.6
4H	4	1430	46.8–56.5	9.7	9.12	94.0
5H	4	1800	56.5–66.2	9.7	7.27	74.9
6H	4	2000	66.2–76.0	9.8	5.16	52.6
7H	4	2130	76.0–85.7	9.7	6.32	65.1
8H	4	2330	85.7–95.4	9.7	8.25	85.0
9H	5	0130	95.4–104.7	9.3	5.70	61.3
10H	5	0330	104.7–114.3	9.6	5.78	60.2
11H	5	0630	114.3–119.8	5.5	5.46	99.3
12X	5	0915	119.8–128.6	8.8	4.20	47.7
13X	5	1145	128.6–138.2	9.6	6.59	68.6
14X	5	1345	138.2–147.9	9.7	9.74	100.0
15X	5	1530	147.9–157.5	9.6	9.56	99.6
16X	5	1715	157.5–167.2	9.7	8.64	89.1
17X	5	1915	167.2–176.9	9.7	9.71	100.0
18X	5	2045	176.9–186.6	9.7	0.37	3.8
19X	5	2230	186.6–196.2	9.6	7.22	75.2
20X	6	0030	196.2–205.9	9.7	9.63	99.3
21X	6	0400	205.9–215.5	9.6	3.12	32.5
22X	6	0600	215.5–225.2	9.7	3.63	37.4
23X	6	0800	225.2–234.8	9.6	1.46	15.2
24X	6	1000	234.8–244.5	9.7	1.12	11.5
25X	6	1215	244.5–254.2	9.7	3.36	34.6
26X	6	1415	254.2–263.9	9.7	5.40	55.7
27X	6	1615	263.9–273.6	9.7	2.54	26.2
28X	6	1830	273.6–283.3	9.7	5.37	55.3
29X	6	2030	283.3–293.0	9.7	3.90	40.2
30X	6	2230	293.0–302.6	9.6	5.64	58.7
31X	7	0015	302.6–312.2	9.6	4.61	48.0
32X	7	0315	312.2–322.9	10.7	6.88	64.3
				304.9	188.27	

697B-5H which has been homogenized by drilling. An (as yet) unidentified mineral, probably a zeolite, forms as much as 20% of the sediment in Subunit IB (Fig. 5). Its occurrence is cyclic on a scale of 10 m.

Diatoms occur abundantly only in Sections 113-697B-4H-3, 113-697B-4H-4, and 113-697B-4H, CC; these sections contain a total of eight laminae of diatom ooze and clayey diatom ooze, which are lighter colored than the surrounding mud, i.e., gray (5Y 5/1).

Subunit IC (85.7–293.0 mbsf; Pliocene)

Cores 113-697B-8H through 113-697B-29X; thickness 207.3 m

Subunit IC consists mainly of diatom-bearing clayey mud, with clayey mud near the top, diatom clayey mud around 150 mbsf and clay toward the base (Figs. 5 and 6). Color variations are minor and include dark gray (N 4/0) and dark greenish gray (5G 4/1, 5GY 4/1, 5BG 4/1) with some dark bluish gray (5B 4/1). The exact color appears to depend more on the recorder than on grain size or composition. Bioturbation is generally minor (moderate in Cores 113-697B-14X and 113-697B-19X). Very small (1–2 mm) gray (5Y 6/1) clasts of quartz silt occur in most cores in Subunit IC but are less common in Cores 113-697B-27X through 113-697B-29X.

Diatoms commonly form 10%–30% of the sediment in Subunit IC and even in those sediments classified as clay or clayey mud, the diatom content is usuallly at least 5% (Fig. 5). Diatom ooze and clayey diatom ooze occur in laminae in Cores 113-697B-13X (9 laminae, silicoflagellates common in addition to diatoms; Fig. 8), 113-697B-14X (11 laminae), 113-697B-15X (12 laminae); and as rare small clasts or thin beds in Cores 113-697B-16X, 113-697B-17X, 113-697B-19X, and 113-697B-21X. Also, Core 113-697B-15X contains abundant diatom ooze laminae forming 10%–20% of the sediment from Sample 113-697B-15X-1, 120 cm, to 113-697B-15X-2, 76 cm.

Authigenic pyrite occurs widely in Subunit IC, generally filling small burrows 3–4 mm in diameter and 1–2 cm long. It is most abundant in Cores 113-697B-26X through 113-697B-28X. Unusual occurrences include pyritized diatom ooze layers in Section 113-697B-9H-4 at 78 cm; Section 113-697B-15X-2 at 32 cm; and Section 113-697B-19X-4 at 90 cm. Fine-grained carbonate, probably dolomite or siderite, forms 10%–20% of the sediment around 200 mbsf (Fig. 5; Sections 113-697B-19X-5 through 113-697B-20X-3). Carbonate silt also occurs rarely as small clasts or burrowed layers in Cores 113-697B-8X, 113-697B-14X, 113-697B-15X, 113-697B-17X, and 113-697B-20X.

In Section 113-697B-16X-3 there are three graded silt layers interpreted as fine-grained turbidites (Fig. 9). Each has a sharp base (slightly disturbed by coring) and a burrowed top. Another silt layer in Section 113-697B-29X-3 is not apparently graded, contains three small dropstones and is burrowed throughout: this may be a lag deposit representing a period of relatively strong bottom currents (Fig. 10). Five very dark grayish brown (2.5Y 3/2) vitric ash laminae occur at around 150 mbsf (Samples 113-697B-13X-3, 30 cm (Fig. 8); 113-697B-14X-1, 42, 81, and 111 cm; 113-697B-15X-2, 75 cm).

Unit II (293–322.9 mbsf; Age Pliocene)

Cores 113-697B-30X through 113-697B-32X; thickness 29.9 m

Unit II is distinguished from Unit I by the absence of diatoms (Fig. 4), a coarser grain-size (Fig. 5) and the abundance of IRD. Silty mud and clayey mud are the major lithologies, with "weathered minerals" and rock fragments prominent in the smear slides. Colors are similar to Unit I: dark gray (N 4/0) and dark greenish gray (5G 4/1, 5BG 4/1). Thin layers of altered volcanic ash continue down from Unit I (Fig. 4) and pyrite is present as a few small (2 cm) concretions. The sediment is transitional between mud and mudstone and is severely biscuited, making it difficult to observe sedimentary structures. Minor bioturbation is noted, including identifiable Zoophycos, Chondrites, and Planolites.

Sand-sized IRD is common in this unit and 28 dropstones were identified in the 17 m of recovered sediment, compared with 42 in the 171 m recovered in Unit I. Again, rounded to subrounded sedimentary rocks predominate although igneous and metamorphic rocks also occur.

Core 113-697B-32X contains two distinctive minor lithologies. In Samples 113-697B-32X-2, 74–75 cm, and 146–147 cm, there are very thin beds of vitric ash containing pristine glass, and in Sample 113-697B-32X-4, 94–101 cm, there is a graded laminated silt bed with some cross-lamination at the base (Fig. 11). This may be a turbidite.

Conclusion

Hemipelagic and pelagic sedimentation processes are responsible for the great majority of sediment recovered at Site 697. It is evident from Figures 5 and 6 that productivity and/or preservation of diatoms, and grain-size of terrigenous sediment, have varied considerably in Jane Basin. Diatom content and grain size are cyclic on a scale of tens to hundreds of meters (unit and subunit scale) and also on a scale of meters (Fig. 7). Diatom content may be related to sea-ice cover, and grain size to bottom-water velocity or to changes in sediment sources: further study of this sequence may therefore yield valuable data on the history of glaciation and bottom-water flow.

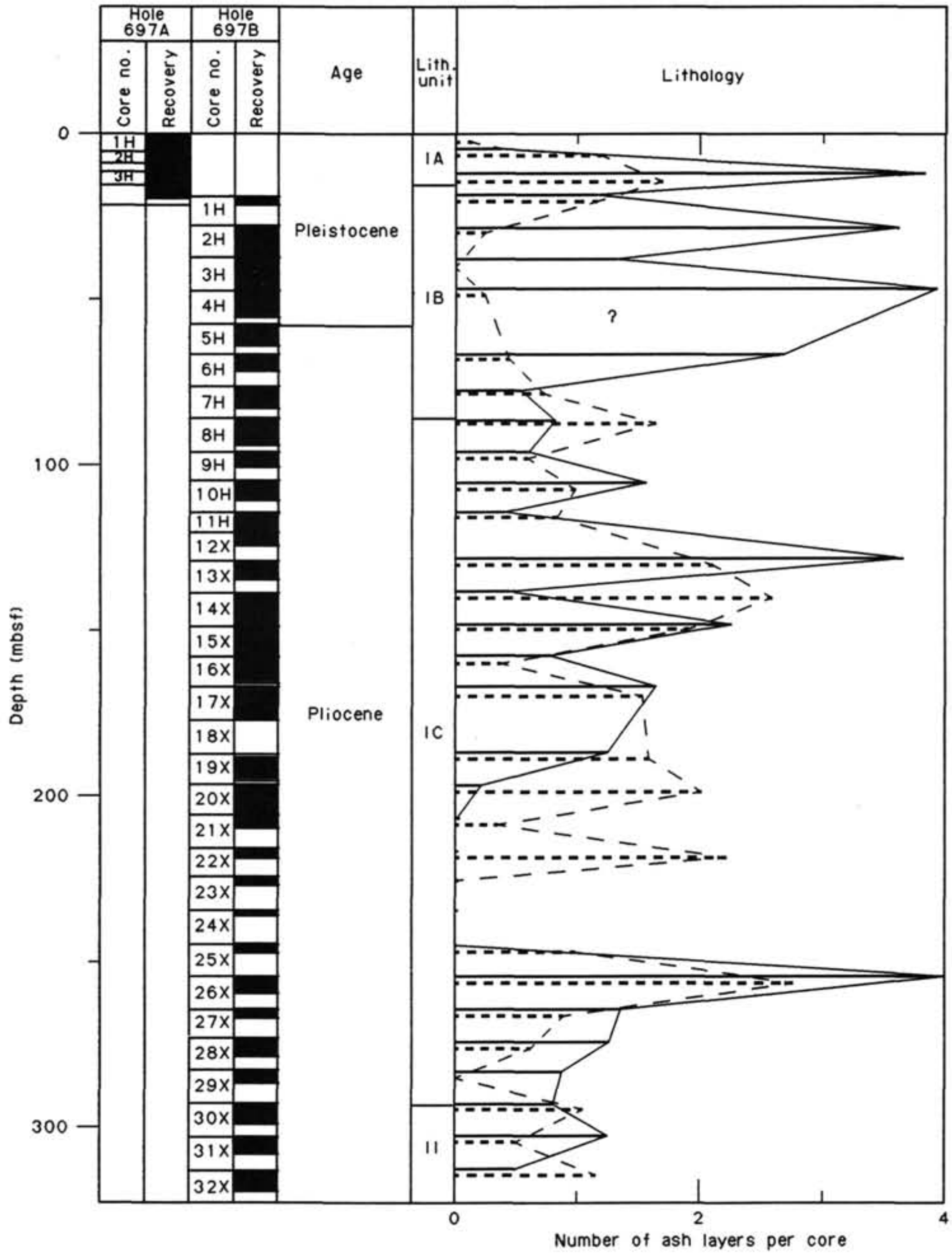

Figure 4. Recovery, lithologic units, and occurrence of altered volcanic ash layers, Site 697. Number of ash layers normalized for core recovery. Solid line = gray ash; dotted line = green ash.

Table 2. Lithologic units at Site 697.

Unit	Subunit	Lithology	Depth (mbsf)	Age
I	IA	Silty mud and diatom-bearing silty mud	0–15.5	Late Pleistocene
	IB	Clayey mud and clay	15.5–85.7	Late Pliocene to Pleistocene
	IC	Diatom-bearing clayey mud; also mud, diatom clayey mud clay	85.7–293.0	Pliocene
II		Silty mud and clayey mud with ice-rafted detritus	293.0–322.9	Pliocene

Clay Mineralogy

X-ray diffraction analyses were completed on 34 samples from Holes 697A and 697B (Fig. 12). The objectives of the clay mineral studies at Site 697 are (1) to recognize the major paleoenvironmental changes as expressed by the clay associations (using a sampling interval of one per core); (2) to examine the cyclical variations of the clay associations, in relation to slight lithological changes expressed by the changing color of the sediment (using a sampling interval of one per color change); (3) to compare the clay associations with those observed at other sites in the Weddell Sea and in the adjacent Falkland Plateau area.

Results

The clay minerals identified include chlorite, illite, kaolinite, and smectite (Fig. 12). Based on the relative abundances of the

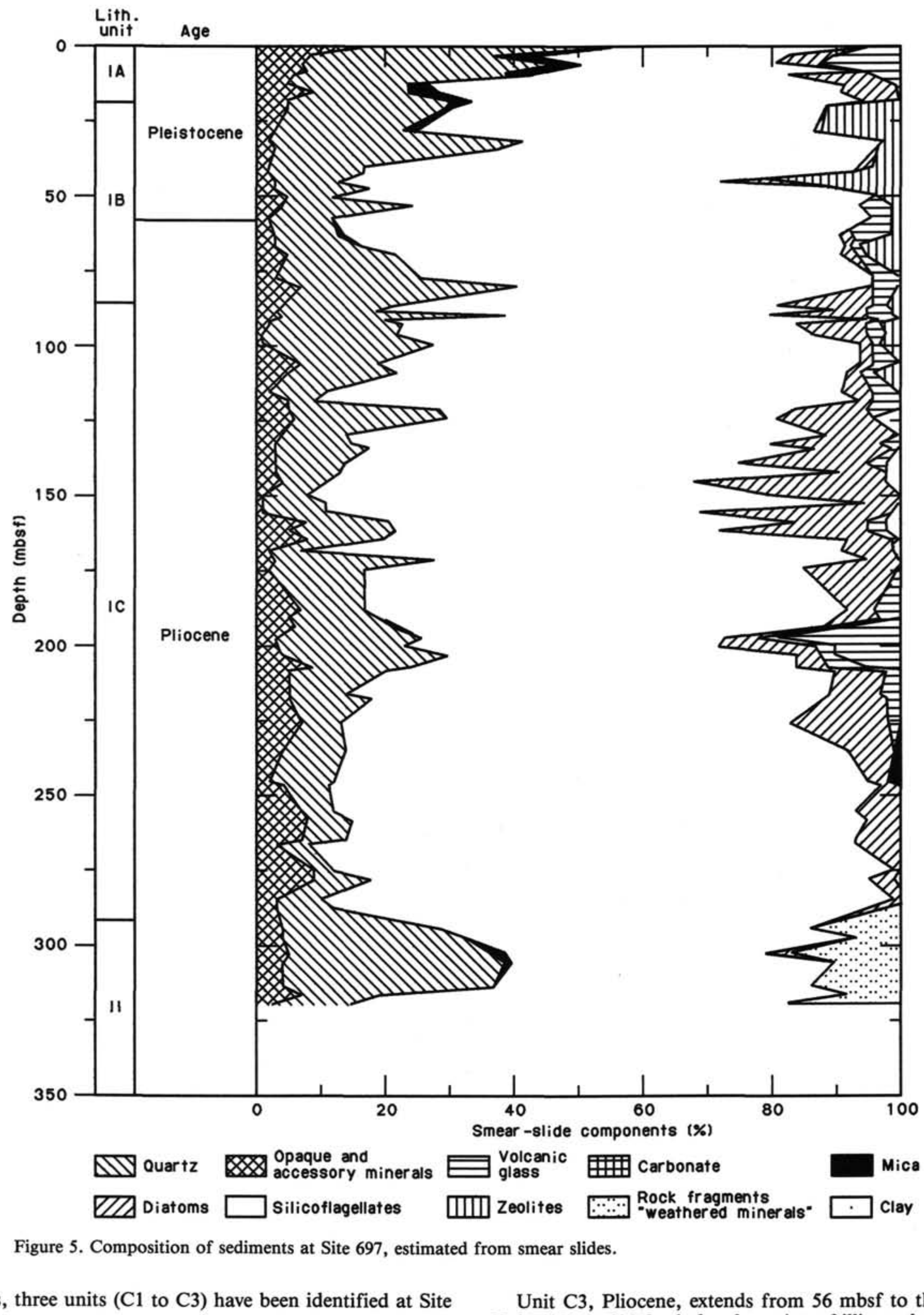

Figure 5. Composition of sediments at Site 697, estimated from smear slides.

clay species, three units (C1 to C3) have been identified at Site 697.

Unit C1 extends from the seafloor to 33 mbsf, is Pleistocene, and consists of illite (abundant), chlorite (common), smectite (rare to abundant), and kaolinite (rare to common).

Unit C2 extends from 33 to 56 mbsf, is Pleistocene, and has a clay association of illite (abundant), chlorite (common to abundant), kaolinite (rare to common), and smectite (absent to common).

Unit C3, Pliocene, extends from 56 mbsf to the bottom of Hole 697B at 322.9 mbsf and consists of illite and chlorite (common to abundant), and kaolinite and smectite (rare to common).

Paleoenvironmental History

At Site 697, clay associations contain common to abundant smectite throughout the sedimentary sequence, and differ from the clay mineral associations of the shallower sites on the South Orkney microcontinent (Sites 695 and 696). At these sites, smec-

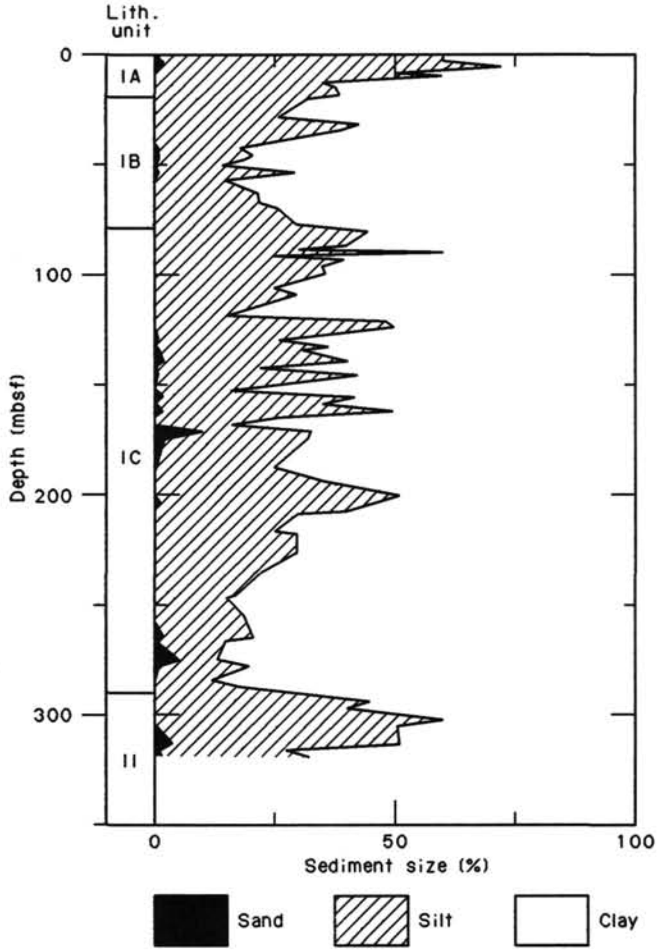

Figure 6. Grain size of sediments at Site 697, estimated from smear slides.

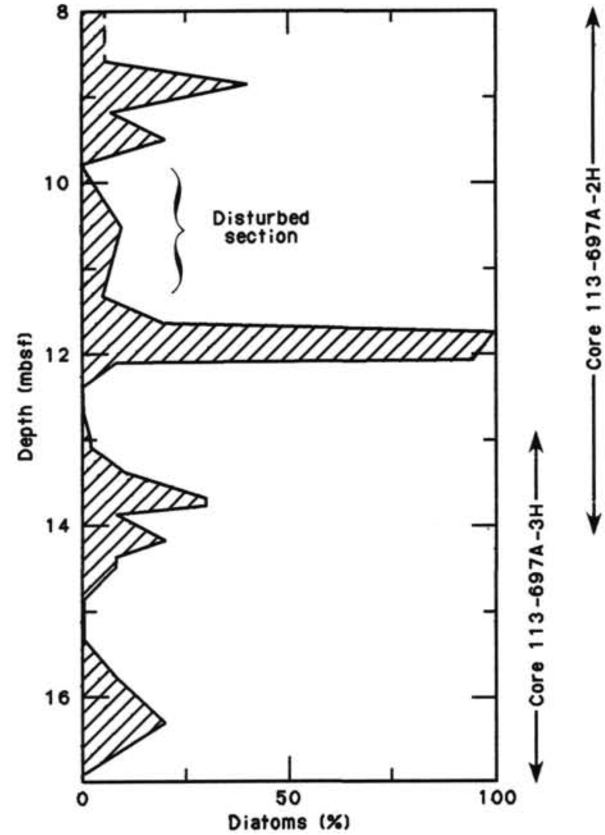

Figure 7. Percentage of diatoms, estimated from smear slides, in Sections 113-697A-2H-3 through 113-697A-2H-7 and 113-697A-3H-1 through 113-697B-3H-3. This cyclicity does not show on the scale of Figure 5.

tite was less abundant than at Site 697 during the late Neogene and especially during Pliocene time.

Site 697 clay associations probably originate partly from the removal of ancient smectite- and kaolinite-rich sediments cropping out on the Antarctic margin, as was also observed on Maud Rise (Sites 689 and 690) and in the Weddell Basin (Site 694) during the Neogene. Very similar clay associations at Site 697 and 694 also suggest that the clay minerals in Jane Basin originate mainly from southern regions of West Antarctica.

Unit C3 (lower Pliocene to Pleistocene) is characterized by common or abundant smectite, mainly eroded from ancient sediments of the Antarctic margin. This unit stratigraphically corresponds to Units C1 to C3 at Site 695, but Unit C2 at Site 695 was characterized by sporadic rare smectite and abundant chlorite. This unit is lacking at the adjacent Site 697 (located in deeper water). However, a slight increase of the chlorite content occurs in Cores 113-697B-17X through 113-697B-21X. From Core 113-697B-13X upward, a slight increase in kaolinite (which has not been recorded in shallower waters) could correspond to a modification of the detrital supply.

Unit C2 (Pleistocene) is characterized by higher chlorite and lower kaolinite and smectite contents, suggesting that erosion of sediments decreased while detrital supply from poorly developed soils (extending over the partially glaciated areas) increased. A similar event has been recorded at DSDP Site 513 in the Falkland Plateau area (Robert and Maillot, 1983). The mineralogic change correlates with a decrease in Antarctic Bottom Water production observed in the South Atlantic Subantarctic area (Ledbetter and Ciesielski, 1982).

Unit C1 (Pleistocene) is characterized by increasing smectite and decreasing chlorite contents. Low abundances of chlorite probably result from reduced pedogenesis in the source area, and increased abundances of smectite may reflect a resumption of erosion of ancient sediments on the Antarctic margin. The mineralogic change suggests that a cooling, associated with enhanced circulation, occurred just above the Matuyama/Brunhes boundary.

Alternating gray (5Y 5/1) and greenish gray (5G 5/1) sediments, and also dark greenish gray (5G 4/2) laminae of devitrified volcanic ash have been studied in Section 113-697A-1H-3. Smectite content is higher in the gray than in the greenish gray. Gray sediments were probably deposited during colder periods. Similar variations have been previously described from the upper Pleistocene sediments off East Antarctica (Grobe, 1986). Dark greenish gray laminae contain abundant smectite, this mineral being rare in the surrounding greenish gray sediment. This difference in the smectite content suggests that the volcanic materials in the dark greenish gray laminae are partially altered into smectite. This result correlates with data obtained from similar laminae of devitrified volcanic ash from the Southwest Pacific (Gardner et al., 1985). Further detailed studies will elucidate the influence of greenish gray laminae upon clay assemblages.

BASEMENT ROCKS

No Basement Rocks section was done for Site 697.

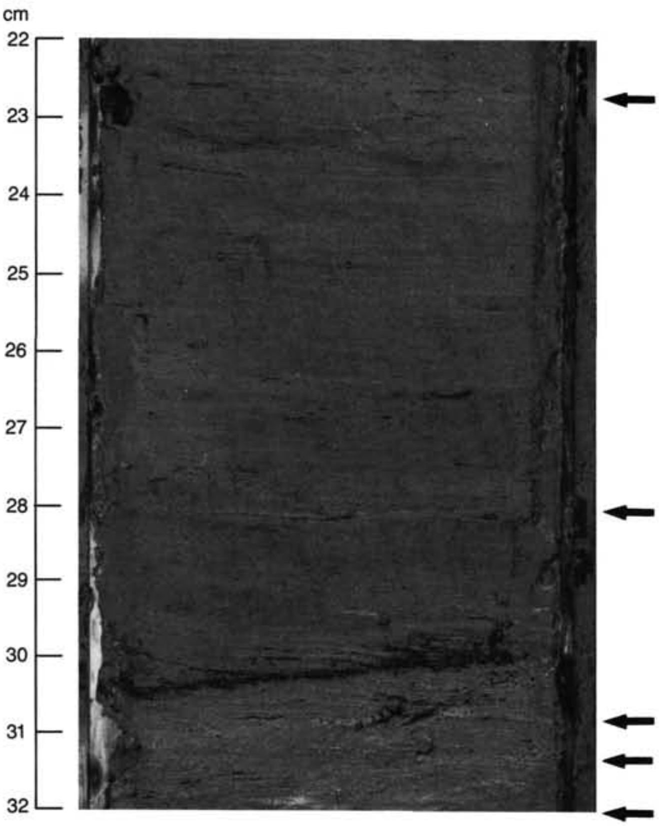

Figure 8. Subunit IC, laminae of diatom ooze (arrows) in Section 113-697B-13X-3. Lamina of dark brown vitric ash at 30 cm. Section 113-697B-13X-3, 22–32 cm.

PHYSICAL PROPERTIES

Index properties measured on samples selected from the most intact portions of cores are listed in Table 3. Profiles of bulk density, water content (dry basis), and grain density are illustrated in Figure 13. A profile of porosity is illustrated in Figure 14.

The clayey sediments of Site 697 display index properties, bulk density, water content, and porosity that are typical of a normally-consolidated clayey marine section. The bulk density increases at a steady rate below 14.4 mbsf. The rate of increase is 0.0116 $g/cm^3/m$ for the upper 14.4 m and 0.00077 $g/cm^3/m$ for the interval between 14.4 and 313.7 mbsf. Bulk density ranges from 1.34 g/cm^3 at 12.1 mbsf to 2.15 g/cm^3 at 275.7 mbsf. Water content decreases steadily downhole below 14.4 mbsf. The water content gradient for the upper 14.4 mbsf is 2.58%/m, and 0.08%/m for the interval between 14.4 to 313.7 mbsf. The water content ranges from 179% at 12.1 mbsf to 34% at 284.1 mbsf. Grain density increases downhole and averages approximately 2.79 g/cm^3. Porosity decreases at the rate of 0.979 %/m over the interval from 0 to 14.4 mbsf and 0.022%/m from 14.4 to 240 mbsf. From 240 to 313.7 mbsf the rate of decrease is 0.136%/m. The average porosity for Site 697 is 58%.

Shear Strength

The undrained shear strength of the sediment was determined using the ODP Motorized Vane Shear Device. Standard 1.2-cm equidimensional miniature vanes were used with the device. Its operation and calculations follow procedures outlined in the *Physical Properties Handbook* (used on the ship). Strength measurements were made on the least disturbed sections of the cores.

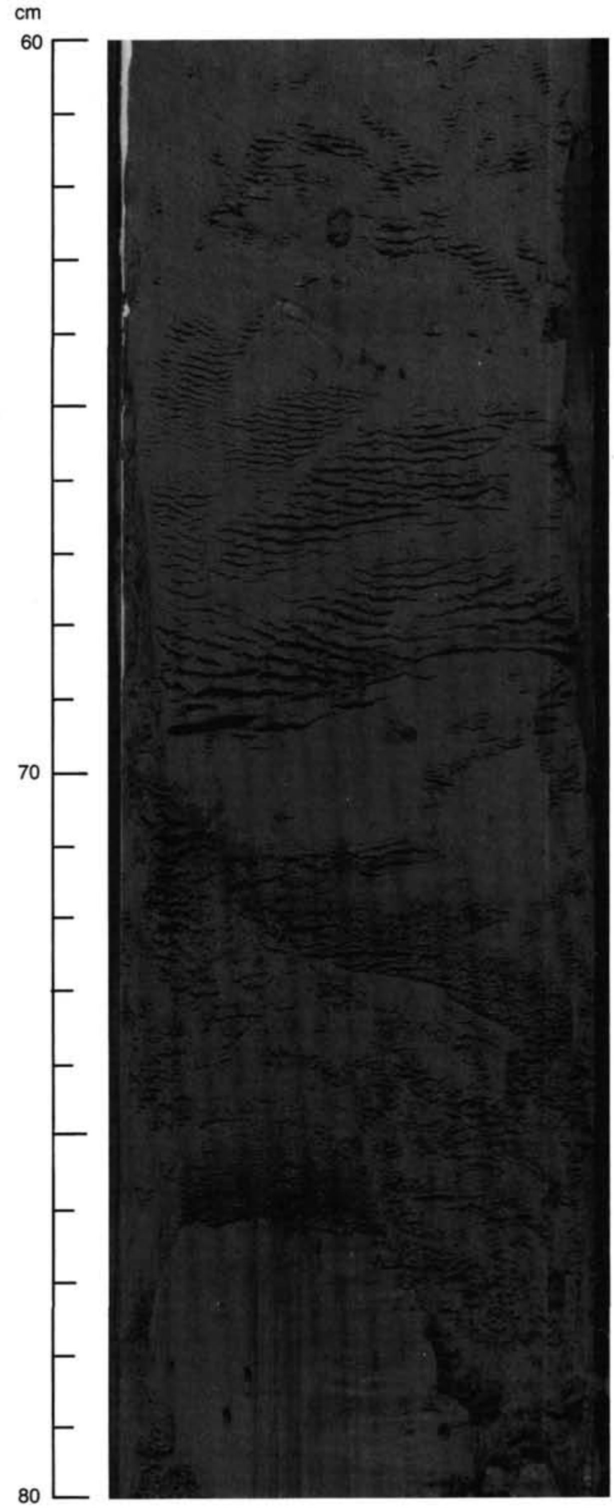

Figure 9. Subunit IC, graded silt beds (bases at approximately 68, 73, 76 cm) interpreted as distal turbidites. Minor coring disturbance. Sample 113-697B-16X-3, 60–80 cm.

The shear strengths determined for Site 697 are listed in Table 4 and illustrated in Figure 15. The shear strength varied over a wide range of values at similar depths in the interval between 90 and 318 mbsf. Shear strength steadily increased at the rate of

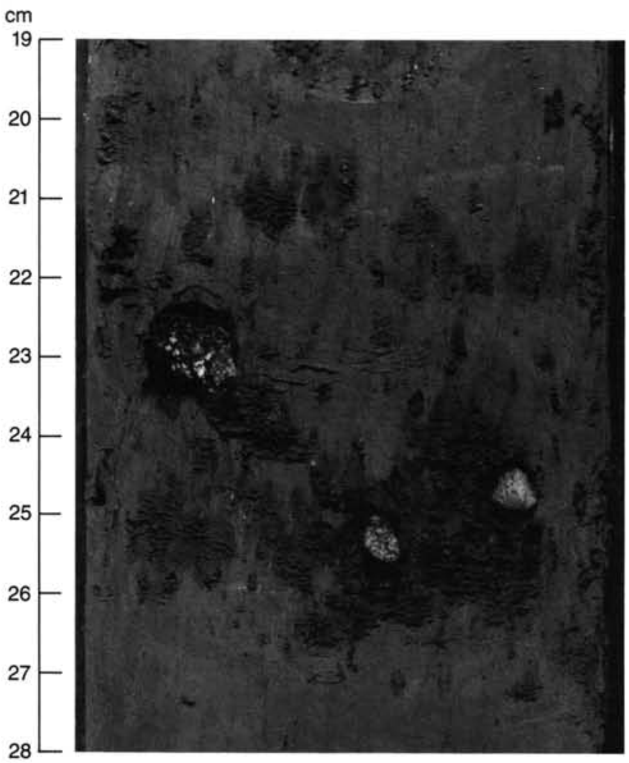

Figure 10. Subunit IC, ungraded silt bed containing three dropstones. The largest dropstone is biotite schist and the other two are mudstones. Sample 113-697B-29X-3, 19–28 cm.

1.23 kPa/m from 0 to 90 mbsf. From 90 to 250 mbsf it increased at the rate of 0.316 kPa/m but fluctuated by as much as 150 kPa over several meters. From 250 to 313 mbsf the shear strength increased 2.86 kPa/m, the largest shear strength gradient at Site 697. The overall gradient for shear strength is 0.083 kPa/m.

Shear strength reflects the condition of the cored sediments more than any other parameter. Examination of Figure 15 indicates that the recovered sediments are obviously highly disturbed and in some cases completely remolded or reconstituted. The age of the sediments and the index properties indicate that the sediments at Site 697 are normally consolidated; the strength data suggest otherwise. Assuming hydrostatic pressure as the equilibrium pore pressure of this site, vertical stresses were calculated using bulk density data. Effective overburden stresses (P′) were determined so that the ratio of undrained shear strength (Cu) to effective overburden stress (Cu/P′) could be calculated. The ratio (Cu/P′) gives an indication of the degree of consolidation or strength deviation from that expected of a normally-consolidated clayey sediment. Clayey sediments that are normally consolidated have (Cu/P′) values between 0.2 and 0.5. Site 697 sediments have average (Cu/P′) values that are much less than 0.2 and in many samples, values less than 0.1. This indicates that the sediments at Site 697 are highly underconsolidated. The age of the sediment and the character of the index properties contradict the interpretation that the sediments are highly underconsolidated. The reduced strength is therefore interpreted to be a result of disturbance due to the remolding of the sediment during the drilling and coring process.

Compressional Wave Velocity

Sonic velocity (V_p) in sediments is measured using two methods. First, a continuous measurement of V_p was made through the unsplit core using a *P*-wave logger (PWL) installed next to the Gamma Ray Attenuation Porosity Evaluator (GRAPE) source and detector. Second, measurements were made by the use of the Hamilton Frame on individual samples removed from the core with one measurement from every other core section. Velocity was measured in only one direction, usually perpendicular to the long axis of the core.

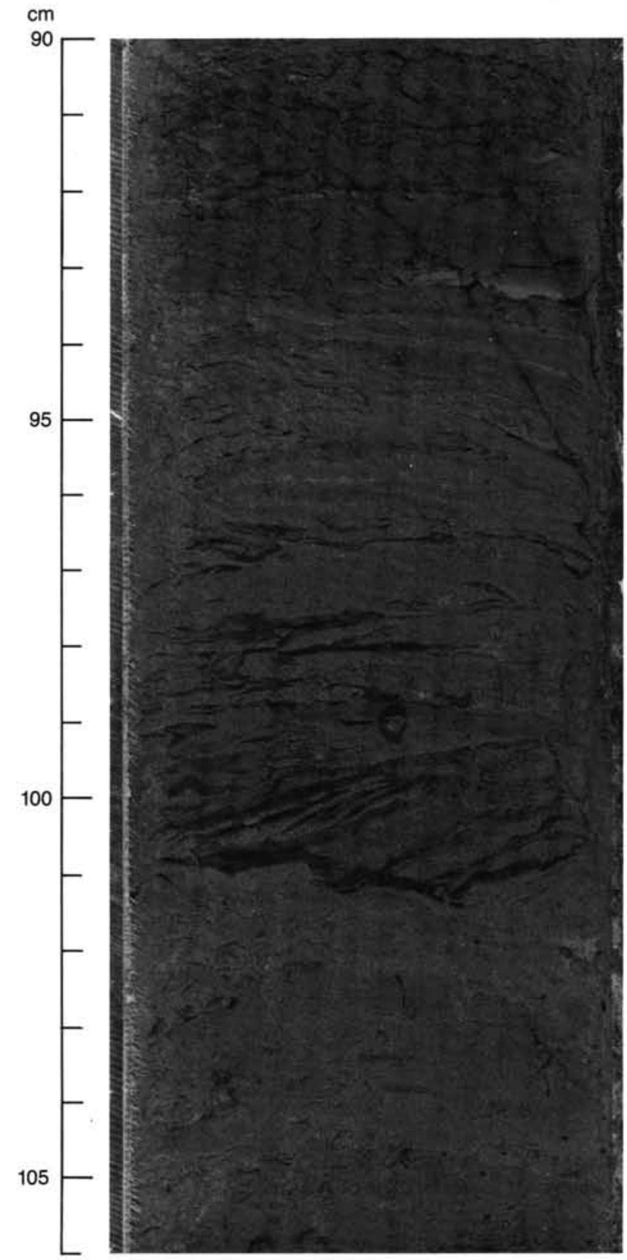

Figure 11. Unit II, graded silt bed (90–100 cm), cross-laminated near the base. Note sand-sized IRD (black spots) in underlying silty mud. Sample 113-697B-32X-4, 90–106 cm.

The results of velocity measurements made on the Hamilton Frame are listed in Table 5 and illustrated in Figure 16. Some of the velocity data were lost due to a malfunction of the Hamilton Frame Velocimeter. Velocity increased downhole at an overall rate of 0.50 m/s/m. Over the interval, 0–18.9 mbsf, the rate of increase is 2.30 m/s, 4.6 times larger than the overall gradient. The average velocity in the upper 18.9 m is 1480 m/s, a very low average velocity, the lowest for Leg 113. The average velocities for Site 697 over the following intervals are:

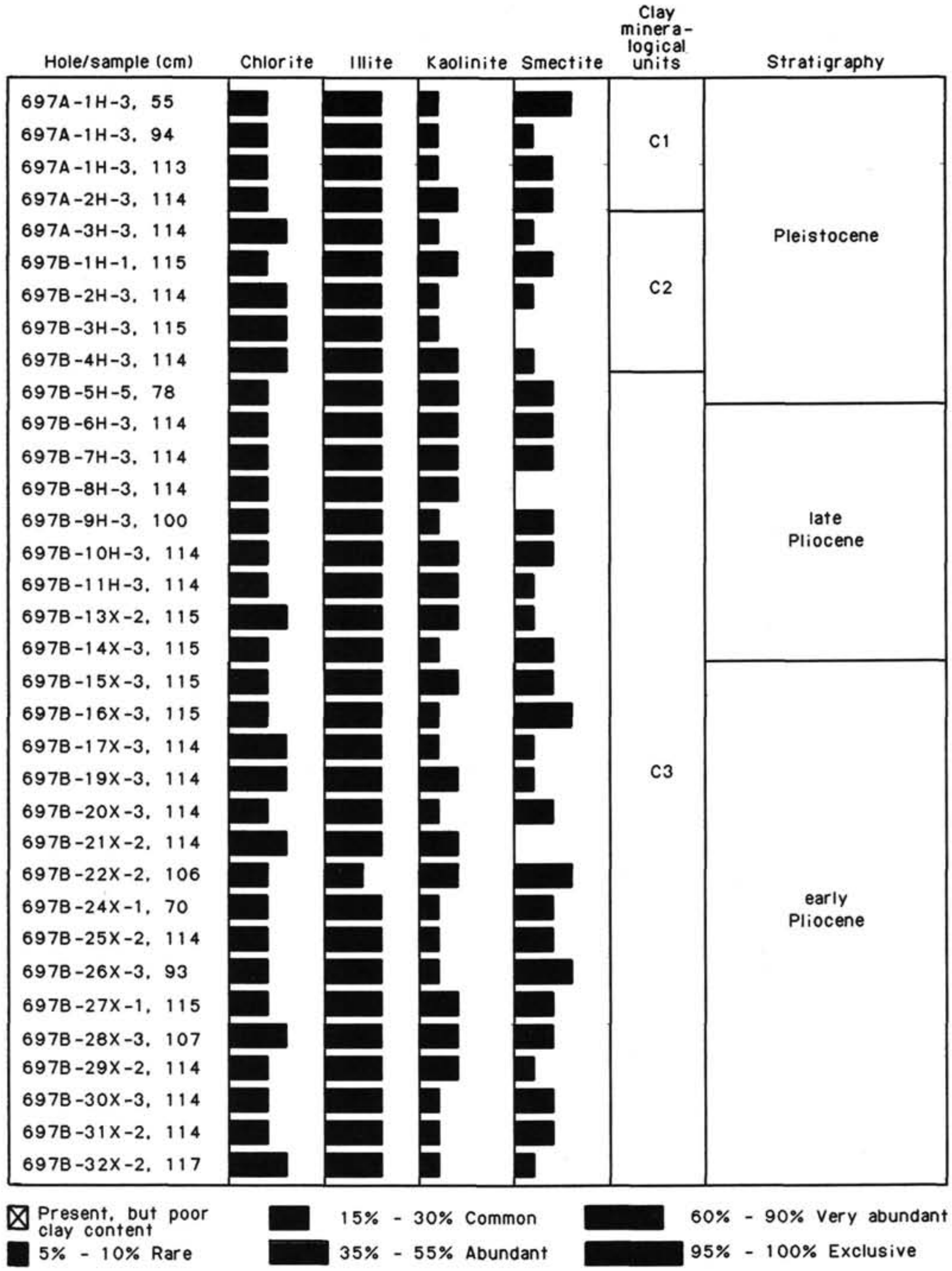

Figure 12. Clay mineralogy, Site 697.

0–18.9 mbsf	1479 m/s
18.9–100 mbsf	1507 m/s
100–235.4 mbsf	1575 m/s
234.5–318.5 mbsf	1621 m/s

Thermal Conductivity

The thermal conductivity of the sediments sampled at Site 697 was measured following the methods of Von Herzen and Maxwell (1959) using the needle-probe technique. The results of the thermal conductivity tests are listed in Table 6 and illustrated in Figure 17. Thermal conductivity ranges from 1.155 to 1.471 W/m-k. The average value is 1.380 W/m-k. The thermal conductivity gradient for Site 697 sediment is 0.0025 W/m-k/m.

Summary

The sediments at Site 697 have index properties that are typical of a normally-consolidated marine clayey sediment. The shear strength data suggests that the sediments of the area are highly underconsolidated. The reduced shear strengths, which lead to the underconsolidated appearance of the sediment, are the result of core disturbance due to the drilling and coring process. The age and other properties indicate that a state of normal consolidation exists for the sediments at Site 697. The acoustic

Table 3. Index properties, water content, porosity, bulk density, and grain density measured on samples from Site 697.

Core, section top (cm)	Depth (mbsf)	Water content (%WW)	(%DW)	Porosity (%)	Bulk density (g/cm³)	Grain density (g/cm³)
113-697A-						
1H-2, 90	2.4	47.55	90.64	73.57	1.59	2.94
1H-4, 90	5.4	47.15	89.22	72.54	1.58	2.62
1H-6, 90	8.4	42.36	73.50	68.35	1.65	2.68
2H-3, 90	9.2	46.24	86.02	68.87	1.53	2.60
2H-5, 76	12.1	64.18	179.18	84.05	1.34	2.41
2H-6, 90	13.7	51.02	104.16	76.17	1.53	2.84
2H-7, 10	14.4	41.76	71.69	67.03	1.64	2.73
3H-4, 95	16.7	35.52	55.08	59.81	1.73	2.77
3H-5, 94	18.2	37.13	59.05	62.39	1.72	2.67
113-697B-						
1H-1, 90	18.9	38.04	61.40	63.65	1.71	2.84
1H-2, 90	20.4	34.61	52.93	62.08	1.84	3.07
2H-2, 90	29.9	35.92	56.05	61.70	1.76	2.80
2H-4, 90	32.9	32.59	48.36	60.98	1.92	3.00
2H-6, 90	35.9	34.24	52.06	60.88	1.82	2.82
3H-4, 90	39.5	34.27	52.14	61.66	1.84	2.99
3H-6, 90	42.5	35.96	56.15	61.91	1.76	2.85
4H-2, 68	49.0	39.74	65.94	64.72	1.67	2.69
4H-4, 90	52.2	35.31	54.59	63.18	1.83	2.83
4H-6, 90	55.2	35.66	55.41	61.52	1.77	2.65
6H-2, 11	67.8	31.07	45.08	56.38	1.86	2.71
6H-4, 12	70.8	33.36	50.06	57.58	1.77	2.62
7H-2, 90	78.4	33.31	49.96	59.84	1.84	2.94
7H-4, 80	81.4	37.41	59.76	63.63	1.74	2.83
7H-CC, 18	82.2	35.86	55.91	61.43	1.75	2.72
8H-1, 90	86.6	41.33	70.45	69.97	1.73	2.69
8H-2, 90	88.1	35.52	55.10	61.27	1.77	2.68
8H-3, 90	89.6	38.09	61.53	63.49	1.71	2.81
8H-4, 90	91.1	33.86	51.20	57.87	1.75	2.79
8H-5, 90	92.6	33.48	50.32	56.75	1.74	2.49
8H-6, 40	93.6	38.88	63.62	63.22	1.67	3.32
9H-1, 90	96.3	37.06	58.88	62.83	1.74	2.34
9H-3, 13	98.5	32.26	47.63	56.73	1.80	2.71
9H-3, 90	99.3	33.87	51.21	59.17	1.79	2.64
9H-4, 90	100.8	35.49	55.02	62.69	1.81	2.98
10H-1, 56	105.3	32.38	47.88	58.67	1.86	2.89
10H-2, 60	106.8	33.62	50.65	58.59	1.79	2.67
10H-3, 110	108.8	31.62	46.24	56.00	1.81	2.76
10H-4, 90	110.1	30.97	44.86	55.69	1.84	2.78
11H-2, 90	116.7	32.68	48.55	57.73	1.81	2.66
11H-3, 90	118.2	31.70	46.42	56.87	1.84	2.82
11H-4, 10	118.9	34.15	51.86	57.49	1.72	2.62
13X-2, 29	130.4	36.53	57.55	61.55	1.73	1.94
13X-5, 8	133.2	29.78	42.41	55.35	1.90	2.86
14X-2, 108	140.8	36.44	57.34	62.99	1.77	2.78
14X-3, 115	142.4	35.89	55.99	61.55	1.76	2.68
14X-5, 115	145.4	35.40	54.79	59.74	1.73	2.59
15X-4, 82	153.2	34.59	52.88	61.17	1.81	2.74
15X-6, 90	156.3	35.98	56.20	60.69	1.73	2.69
15X-CC, 15	157.3	29.54	41.93	55.22	1.91	2.78
16X-2, 115	160.2	31.25	45.46	56.83	1.86	2.87
16X-4, 90	162.9	32.96	49.16	57.72	1.79	2.65
16X-6, 65	165.6	28.63	40.12	52.85	1.89	2.77
17X-2, 113	169.8	25.96	35.06	49.64	1.96	2.88
17X-4, 113	172.8	29.39	41.62	56.58	1.97	2.88
17X-6, 90	175.6	28.09	39.06	51.68	1.89	2.69
19X-2, 90	189.0	31.95	46.95	56.14	1.80	2.68
19X-4, 90	192.0	40.43	67.87	67.09	1.70	2.88
19X-5, 60	192.7	30.39	43.67	57.39	1.93	2.93
20X-1, 90	197.1	32.34	47.80	59.86	1.90	2.95
20X-2, 90	198.6	28.94	40.73	54.39	1.93	2.95
20X-3, 90	200.1	33.05	49.37	59.12	1.83	2.72
20X-4, 85	201.6	28.05	38.98	53.09	1.94	2.89
20X-5, 83	203.0	32.86	48.94	58.68	1.83	2.79
20X-6, 46	204.2	36.21	56.76	63.01	1.78	2.87
21X-2, 90	208.3	31.72	46.45	56.72	1.83	2.82
22X-1, 102	216.5	31.72	46.45	58.11	1.88	2.79
22X-3, 17	218.4	31.99	47.04	57.43	1.84	2.77
24X-1, 64	235.4	30.68	44.25	57.88	1.93	2.89
24X-CC, 16	235.7	29.79			1.86	
25X-2, 123	247.2	26.88			2.03	
25X-CC, 26	247.6	33.88	51.24	60.95	1.84	2.88

Table 3 (continued).

Core, section top (cm)	Depth (mbsf)	Water content (%WW)	(%DW)	Porosity (%)	Bulk density (g/cm³)	Grain density (g/cm³)
113-697B- (Cont.)						
26X-2, 55	256.3	26.98	36.94	52.57	2.00	2.95
26X-4, 16	258.9	27.41	37.76	53.32	1.99	2.97
27X-2, 53	265.9	26.29	35.67	51.58	2.01	2.88
28X-2, 64	275.7	25.40	34.04	53.40	2.15	2.84
28X-4, 31	278.4	25.21	33.71	46.98	1.91	2.74
29X-1, 78	284.1	25.86	34.88	47.09	1.87	2.55
29X-2, 49	285.3	26.34	35.76	49.88	1.94	2.66
30X-2, 10	294.1	24.82	33.01	46.64	1.93	2.70
31X-1, 96	303.6	28.33	39.54	53.18	1.92	2.73
32X-1, 90	313.1	26.64	36.32	50.28	1.93	2.70
32X-2, 0	313.7	25.86	34.88	49.60	1.96	2.74

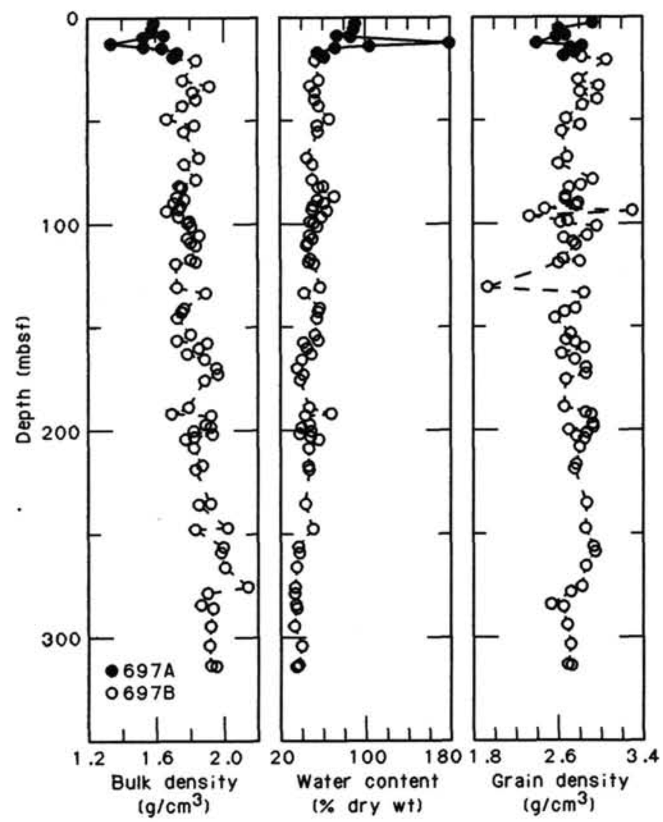

Figure 13. Profile of bulk density, water content, and grain density, Site 697. Data given in Table 3.

velocities in the upper 18.9 mbsf are very low, averaging only 1480 m/s. The overall velocity gradient is 0.59 m/s/m.

SEISMIC STRATIGRAPHY

Site 697 lies in Jane Basin on single-channel seismic line BRAN801-E (Birmingham University/British Antarctic Survey), illustrated in Figure 3 ("Background and Objectives" section, this chapter). *JOIDES Resolution* approached the site from the west (from Site 696) along the same track. The location of the site had been moved about 10 km westward from that selected originally to try to find a slightly thinner sedimentary sequence (given the limited time available for drilling).

The reflection profile shows a prominent reflector at about 550 ms twt which separates two different sedimentary se-

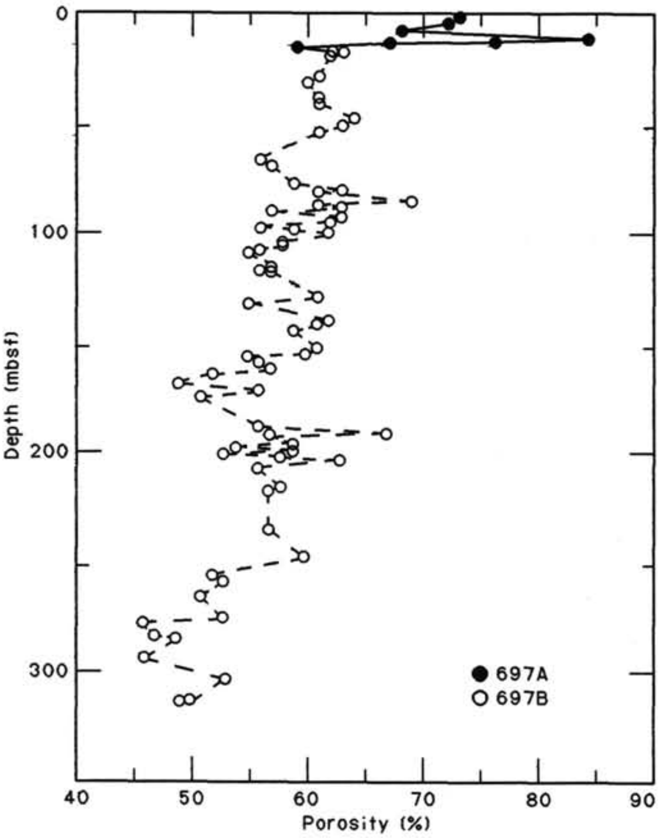

Figure 14. Profile of porosity, Data given in Table 3.

quences. The lower sequence is interpreted as being derived from the now-dead island arc of Jane Bank in the east and from the South Orkney microcontinent in the west; the upper sequence is draped over the subdued topography of the reflector and pinches out at the western edge of the basin under the influence of bottom currents, and from the evidence of gravity cores is hemipelagic (Fig. 3). The only strong reflector in the upper sequence lies just below the seabed, which is exceptionally *weakly* reflective.

The two holes drilled at Site 697 penetrated 323.9 mbsf, to within perhaps 150 m of the prominent reflector at 550 ms. Recovery was generally good, and only a few cores were thoroughly disturbed by the drilling process. The sequence drilled consists of hemipelagic clays with small siliceous biogenic and volcanic ash components. There is no major compositional change within it, only subtle, second-order changes. No large acoustic impedance changes producing strong seismic reflectors were to be expected.

Velocity measurements were made on core samples at regular intervals (see "Physical Properties" section, this chapter), but complete PWL data were not available aboard ship. The PWL and Hamilton Frame velocities which were available showed a variation with depth markedly different from those of the other APC/XCB-drilled sites, 689 and 690. There is a thin, low-velocity zone at shallow depth (near 12 mbsf, within Subunit IA, Fig. 16). This could explain the weak seabed reflector and the strong reflector directly beneath (Fig. 18). At greater depths the velocities increase steadily (see "Physical Properties" section, this chapter, Fig. 16), rather than remaining low initially, then increasing sharply at around 200 mbsf as diagenetic alteration develops. The curve for Site 697 is lower than but parallel to the Carlson et al. (1986) empirical curve. Since laboratory measurements have to be corrected for the change from *in-situ* conditions, and since the physical properties measurements show signs of subtle disturbance of the clay fabric by coring, the measured values are probably too low. It seems most reasonable therefore to use the Carlson et al. (1986) velocity-depth relation to establish the time on the reflection profile equivalent to the depth drilled. The results are shown in Figure 18. Since the only potential sequence boundary, the reflector at 550 ms, was not recorded by drilling our speculation that the underlying sequence is largely turbiditic cannot be tested. However, the presence of three thin turbidites near the base of the hole suggests a downhole change toward a greater turbiditic component.

BIOSTRATIGRAPHY

Site 697 was drilled east of the South Orkney Platform in 3480 m of water in the Jane Basin to obtain a biosiliceous hemipelagic to pelagic record for the Neogene. This site was the deepest component of a three-site transect down the flank of the South Orkney microcontinent to obtain information about changes in water-mass characteristics during the Neogene and to examine the deep-water circulation history of the region. The site was chosen to examine the vertical position of deep-contour-following currents and the evidence for significant velocity fluctuations, in addition to the study of the Neogene-Quaternary glacial history of the region.

At Site 697 a 500-m section was targeted, and 322.9 m was drilled with an average recovery of 64.5%. The recovered section consists of Quaternary to lowermost Pliocene hemipelagic clayey to silty mud with varying amounts of biosiliceous components, ice-rafted debris, and volcanic ash. Biostratigraphic information is derived from siliceous microfossils, because the section is barren of all calcareous microfossils. Preservation and abundance of siliceous microfossils, however, is variable; overall preservation is poorer and abundance less than in Pliocene sections at previously drilled sites of Leg 113. The Quaternary section is much thicker (58 m) than at other Leg 113 Sites.

All depths referred to are sub-bottom depths and samples are from the core-catcher (CC) section unless otherwise specified. On the summary biostratigraphic correlation chart (Fig. 19) the age or biostratigraphic zone assigned to a given core-catcher section is extrapolated to the midpoint of the overlying and underlying cores. The section is described from the top down.

Planktonic Foraminifers

All core-catcher sections from Holes 697A and 697B were examined for the occurrence of planktonic foraminifers; none were found.

Benthic Foraminifers

All core-catcher sections from Holes 697A and 697B, a sample from the top of Core 113-697B-11H, and a sample from the mud line were processed and the residues examined for benthic foraminifers. Most of the samples are barren, with the exception of the mud-line sample (four *Cyclammina pusilla*, two *Textularia wiesneri*, one *Haplophragmoides* sp.), Section 113-697A-2H, CC (one *C. pusilla*), Section 113-697B-8H, CC (one *Martinotiella antarctica*, one *Sigmoilina tenuis*), the sample from the top of Core 113-697B-11H (five *M. antarctica*, one *S. tenuis*), Section 113-697B-12X, CC (one *C. pusilla*), and Section 113-697B-23X, CC (one *M. antarctica*). No interpretations of these poor faunas can be made; presently the area of Site 697 is characterized by low benthic foraminiferal abundances and is in an area of mixed faunas of *M. antarctica* and *C. pusilla* (Echols, 1971).

Calcareous Nannofossils

No calcareous nannofossils were observed at this site.

Table 4. Undrained shear strengths determined on samples from Site 697.

Core, section top (cm)	Depth (mbsf)	Shear strength (kPa)
113-697A-		
1H-2, 84	2.3	4.7
1H-4, 84	5.3	4.1
1H-6, 84	8.3	6.1
2H-3, 84	9.1	5.8
2H-5, 76	12.1	16.5
2H-6, 84	13.6	14.0
2H-7, 10	14.4	9.3
3H-4, 81	16.6	25.6
3H-5, 81	18.1	18.6
113-697B-		
1H-1, 86	18.9	16.3
1H-2, 86	20.4	22.1
2H-2, 86	29.9	29.1
2H-4, 86	32.9	31.4
2H-6, 86	35.7	27.9
3H-4, 86	39.5	44.2
3H-6, 86	42.5	34.9
4H-2, 86	49.2	45.4
4H-4, 81	52.1	39.6
4H-6, 86	55.2	53.5
6H-2, 80	68.5	100.1
6H-4, 18	70.9	107.0
7H-2, 84	78.3	79.1
7H-4, 84	81.4	76.8
7H-CC, 5	82.1	81.4
8H-1, 84	86.5	81.4
8H-2, 84	88.0	123.3
8H-3, 140	90.1	114.0
8H-4, 84	91.0	114.0
8H-5, 84	92.5	121.0
8H-6, 36	93.6	72.1
9H-1, 82	96.2	83.8
9H-2, 84	97.7	128.0
9H-3, 18	98.6	114.0
9H-3, 84	99.2	151.3
9H-4, 84	100.7	104.7
10H-2, 54	106.7	151.3
10H-3, 84	108.5	153.6
10H-4, 84	110.0	230.4
11H-2, 84	116.6	95.4
11H-2, 94	116.7	111.7
11H-3, 84	118.1	132.6
11H-4, 3	118.8	122.2
11H-4, 84	119.6	88.4
11H-4, 84	119.6	111.7
13X-2, 33	130.4	51.2
13X-5, 5	133.2	132.6
14X-2, 105	140.8	62.8
14X-3, 110	142.3	93.1
14X-5, 110	145.3	76.8
14X-7, 32	147.5	146.6
15X-2, 114	150.5	88.4
15X-4, 81	153.2	135.0
15X-6, 86	156.3	169.9
15X-CC, 10	157.2	209.4
16X-2, 110	160.1	80.3
16X-4, 85	162.9	74.5
16X-6, 61	165.6	102.4
17X-2, 110	169.8	137.3
17X-4, 110	172.8	153.6
17X-6, 84	175.6	128.0
17X-CC, 10	176.4	162.9
17X-CC, 20	176.5	114.0
19X-2, 107	189.2	79.1
19X-4, 84	191.9	95.4
19X-5, 54	192.6	137.3
19X-5, 38	192.5	221.1
19X-5, 83	192.9	211.8
19X-CC, 17	193.6	214.1
20C-1, 84	197.0	151.3
20X-2, 84	198.5	142.0
20X-3, 99	200.2	102.4

Table 4 (continued).

Core, section top (cm)	Depth (mbsf)	Shear strength (kPa)
113-697B-		
20X-4, 84	201.5	95.4
20X-5, 70	202.9	200.1
20X-6, 45	204.2	125.7
20X-7, 24	205.4	176.9
21X-1, 134	207.8	109.4
21X-2, 36	207.8	109.4
21X-2, 94	208.3	95.4
22X-2, 87	217.9	155.9
22X-3, 13	218.6	48.9
22X-CC, 16	218.9	102.4
24X-1, 62	235.4	74.5
24X-CC, 20	235.7	69.8
25X-1, 126	245.8	169.9
25X-CC, 16	247.6	148.9
26X-4, 20	258.9	307.2
26X-4, 42	259.1	311.8
27X-2, 55	266.0	144.3
27X-2, 68	266.2	323.5
28X-3, 71	277.3	237.4
28X-4, 27	278.4	358.4
29X-3, 10	286.4	216.4
29X-3, 52	286.8	242.0

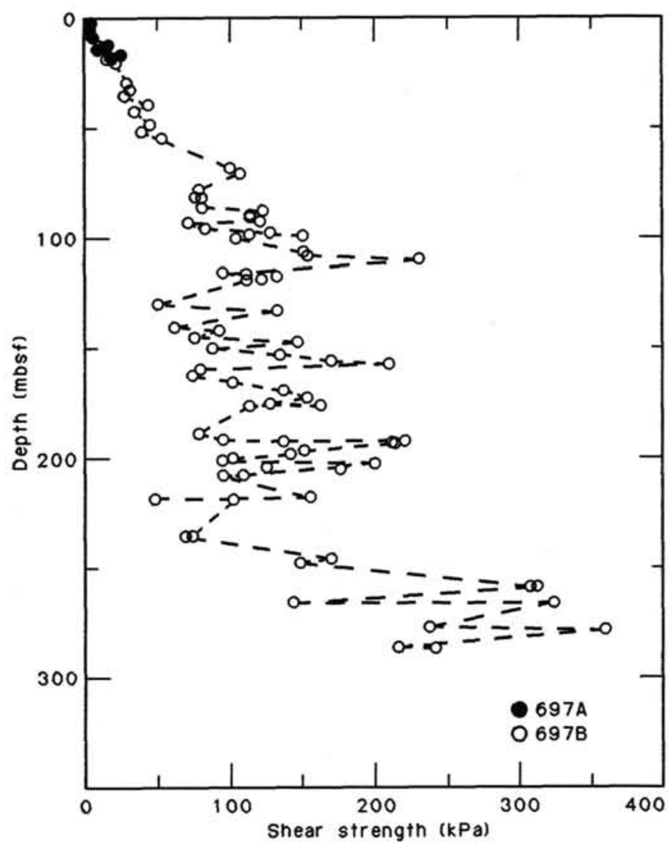

Figure 15. Undrained shear strength profile, Site 697. Data given in Table 4.

Diatoms

Hole 697A

Section 113-697A-1H, CC, contains few, poorly preserved diatoms belonging to the "*Coscinodiscus*" (*Thalassiosira*) *lenti-*

Table 5. Compressional wave velocities (Hamilton Frame) measured on samples from Site 697.

Core, section top (cm)	Depth (mbsf)	Velocity (m/s)
113-697A-		
1H-2, 90	2.4	1457
1H-4, 90	5.4	1460
1H-6, 90	8.4	1464
2H-3, 90	9.2	1471
2H-5, 76	12.1	1485
2H-6, 90	13.7	1478
2H-7, 10	14.4	1491
3H-4, 95	16.8	1497
3H-5, 94	18.2	1498
113-697B-		
1H-1, 90	18.9	1498
1H-2, 90	20.4	1510
2H-2, 90	29.9	1515
2H-4, 90	32.9	1501
2H-6, 90	35.9	1508
3H-4, 90	39.5	1506
3H-6, 90	42.5	1493
4H-2, 68	49.0	1488
4H-4, 90	52.2	1510
4H-6, 90	55.2	1510
6H-2, 11	67.8	1517
6H-4, 12	70.8	1503
7H-2, 90	78.4	1511
7H-4, 80	81.4	1495
7H-CC, 18	82.2	1501
8H-1, 90	86.6	1497
8H-2, 90	88.1	1502
8H-4, 90	91.1	1517
8H-5, 90	92.6	1540
16X-2, 115	160.2	1577
16X-4, 90	162.9	1530
17X-2, 113	169.8	1569
17X-4, 113	172.8	1581
17X-6, 90	175.6	1610
19X-2, 90	189.0	1536
20X-1, 90	197.1	1563
20X-3, 90	200.1	1558
20X-4, 85	201.6	1545
20X-6, 46	204.2	1623
21X-2, 90	208.3	1590
22X-1, 102	216.5	1639
22X-3, 17	218.7	1550
24X-1, 64	235.4	1580
24X-CC, 16	235.7	1609
25X-2, 123	247.2	1602
27X-2, 53	265.9	1615
31X-1, 96	303.6	1655
32X-1, 90	313.1	1643
32X-2, 60	313.7	1624
32X-5, 30	318.5	1601

ginosus Zone (upper Pleistocene). Other species include *Eucampia antarctica, Actinocyclus actinochilus, Nitzschia linearis, N. kerguelensis, Melosira sulcata*, and *Thalassiothrix longissima*. A few reworked specimens of *Rouxia antarctica* were also present. Section 113-697A-2H, CC, also belongs to the "*C.*" *lentiginosus* Zone but diatoms are rare and poorly preserved. Additional samples in this core support this age designation. In Sample 113-697A-2H-5, 48-80 cm, we found a diatom ooze with abundant, well-preserved diatoms. Within this layer occur such forms as *Corethron criophilum* (abundant at 113-697A-2H-5, 48 cm), *Nitzschia curta, N. ritscherii, N. kerguelensis, N. angulata* (O'Meara) Hasle, *Thalassiosira gracilis, T. lentiginosa*, and *A. actinochilus*. Preservation was so good that diatoms in parts of the layer resembled a fresh net haul. This layer was interbedded with thin, clayey layers which had fewer diatoms.

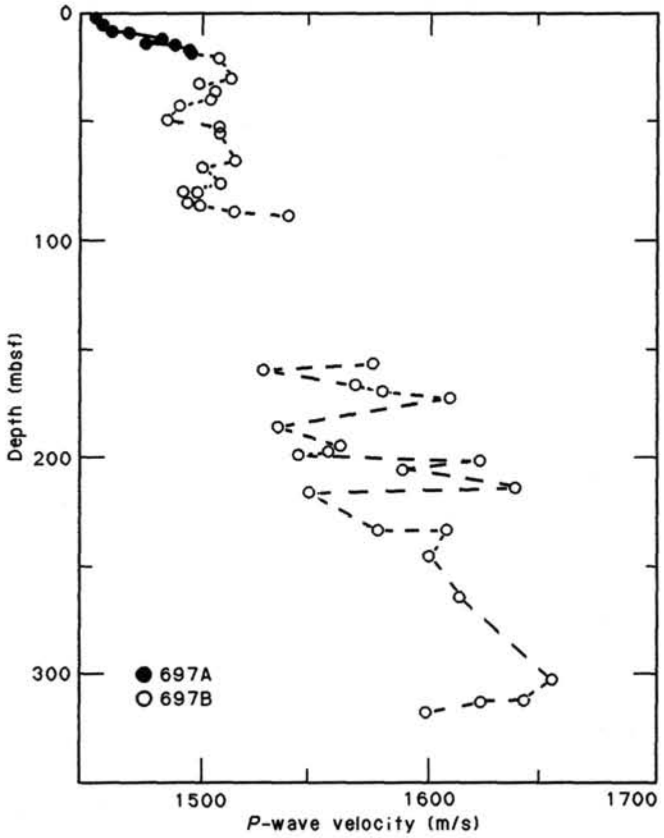

Figure 16. Compressional wave velocities (Hamilton Frame) for Site 697. Data given in Table 5.

Table 6. Thermal conductivities of sediments from Site 697. An "oblique insert" method was used when the measurements were taken from split cores. On whole cores the probe was inserted perpendicular to the core axis.

Core, section top (cm)	Depth (mbsf)	K (W/m-K)	Remarks
113-697A-			
1H-2, 90	2.4	1.260	#119
1H-4, 90	5.4	1.155	#110
1H-6, 90	8.4	1.290	#116
3H-4, 91	16.7	1.349	#110 Oblique
3H-5, 91	18.2	1.339	#115 Oblique
113-697B-			
1H-1, 90	18.9	1.279	#110
1H-2, 90	20.4	1.310	#115
2H-2, 90	29.9	1.290	#115
2H-4, 90	32.9	1.441	#110
3H-4, 90	39.5	1.298	#116
3H-6, 90	42.4	1.276	#119
4H-2, 65	49.0	1.398	#116 Oblique
4H-2, 83	49.1	1.521	#119 Oblique
6H-4, 31	71.0	1.400	#119 Oblique
8H-2, 116	88.4	1.471	#110 Oblique
8H-4, 113	91.3	1.362	#115 Oblique
9H-2, 110	98.0	1.452	#110 Oblique
9H-4, 42	100.3	1.603	#115 Oblique
10H-2, 90	107.1	1.211	#110 Oblique

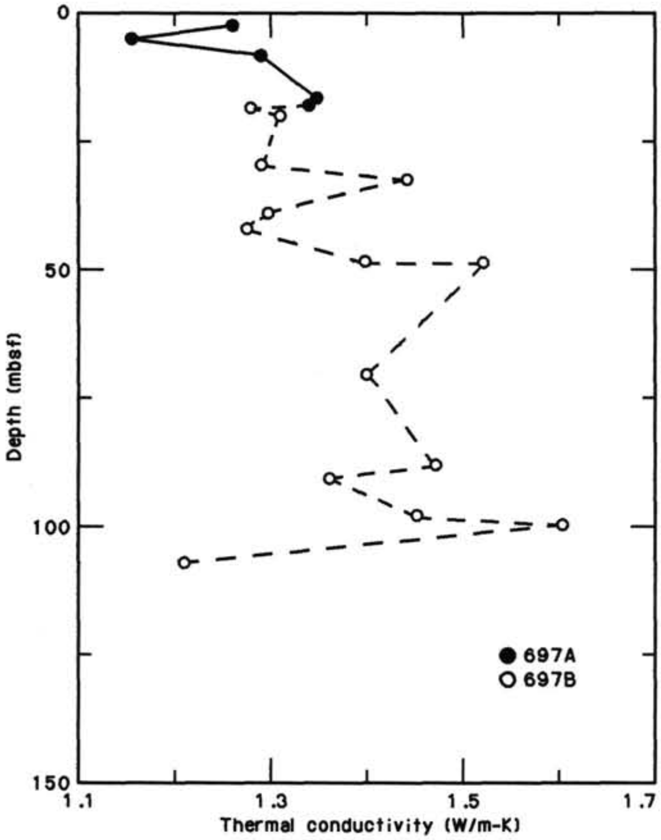

Figure 17. Profile of thermal conductivity, Site 697. Data given in Table 6.

Section 113-697A-3H, CC, is barren of diatoms. Sample 113-697A-3H-1, 100 cm, contains few, poorly preserved, diatoms including *N. kerguelensis, Stellarima microtriaxs, Odontella weissflogii*, and common *E. balaustium*. Based on the absence of *Actinocyclus ingens* this interval is also placed in the "*C.*" *lentiginosus* Zone. Hole 697A was abandoned due to technical problems after reaching 20.9 mbsf.

Hole 697B

Hole 697B was washed down to 18 mbsf. Section 113-697B-1H, CC, had a few diatom fragments, none of which were from recognizable stratigraphic markers. Section 113-697B-2H, CC, however, is tentatively placed in the *Coscinodiscus elliptopora/Actinocyclus ingens* Zone based upon the occurrence of *Actinocyclus ingens*. This placement is tentative, however, since the sample has rare, generally poorly preserved, diatoms. Section 113-697B-3H, CC, was barren of diatoms. Sample 113-697B-4H-3, 145 cm, however, contains abundant, well-preserved diatoms belonging to the lower Pleistocene *A. ingens/C. elliptopora* Zone. Other species in this sample include *N. curta, N. obliquecostata, N. angulata* (O'Meara) Hasle, *T. lentiginosa, A. actinochilus, E. antarctica*, and *Thalassiosira* cf. *T. lineata*.

We are unsure of the stratigraphic position of Sections 113-697B-4H, CC, and 113-697B-5H, CC. The former sample contains abundant, well-preserved diatoms, of which *T. longissima* is the most abundant, but no stratigraphic markers. The latter sample contains only diatom fragments and cannot be zoned. Section 113-697B-6H, CC, is tentatively placed in the *Coscinodiscus kolbei/Rhizosolenia barboi* Zone in spite of the fact that only a questionable *C. kolbei* is present. Other taxa include *R. antarctica, T. lentiginosa, T. gracilis*, and *E. antarctica*.

Because of the presence of only a few, poorly preserved, diatoms we are unable to zone Section 113-697B-7H, CC. Species present in this sample include *A. ingens, R. antarctica, S. antarctica, E. antarctica*, and *M. sulcata*. Sections 113-697B-8H, CC, and 113-697B-9H, CC, definitely belong to the upper Pliocene *C. kolbei/R. barboi* Zone based upon the presence of *Coscinodiscus vulnificus* and the absence of *Cosmiodiscus insignis*. Other species include *T. gracilis, E. antarctica, R. antarctica, N. curta*, and *Cosmiodiscus intersectus*, the latter species probably displaced. We are unable to date Section 113-697B-10H, CC, because of rare, poorly preserved diatoms.

The interval from Section 113-11H, CC, to Sample 113-697B-13X-3, 31 cm, is in the *Nitzschia interfrigidaria* Zone (upper Pliocene) because of the occurrence of the nominate taxon. Sample 113-697B-13X-3, 31 cm, is from a thin (several millimeters) diatom-bearing layer. The assemblage is dominated by extremely well-preserved *Thalassiothrix longissima*. Other species are *N. curta, Rouxia antarctica, T. lentiginosa*, and *Schimperiella antarctica*. Sections 113-697B-13X, CC, and 113-697B-14X, CC, have rare, poorly preserved diatoms which lack biostratigraphic markers.

The transition from *N. praeinterfrigidaria* to *N. interfrigidaria* (*N. interfrigidaria*/combined *N. angulata-N.reinholdii* Zone boundary) occurs near Sample 113-697B-15X-2, 48 cm (149.88 mbsf). In addition to the nominate taxa, the sample also contains *T. longissima* (common), *Rouxia naviculoides, T. gracilis, S. turris* (few), and *E. balaustium* (rare).

Section 113-697B-15R, CC, contains no marker species and few, poorly to moderately preserved diatoms, but the interval from Sample 113-697B-16X-2, 10 cm, to Section 113-697B-24X, CC, can be placed in the combined *N. angulata/N. reinholdii* Zone. Diatoms are rare to common and preservation is poor to moderate. Other species are *C. intersectus, R. naviculoides, Stephanodiscus turris, S. microtriaxs, T. gracilis, T. oestrupii*, and rare *N. angulata*. A several-millimeter-thick layer containing abundant, unusually well-preserved diatoms was sampled at 113-697B-21X-2, 16 cm. The dominant species was *T. longissima*, but *N. angulata, C. intersectus, T. oestrupii, N. curta, R. barboi*, and *N.* cf. *N. praeinterfrigidaria* were also present.

Sections below 113-697B-24X, CC (below 244.5 mbsf), contain rare to few, poorly preserved diatoms, which do not include biostratigraphically useful species. These assemblages are dominated by strongly fragmented *T. longissima*. Some of the diatoms from these samples are pyritized. One exception is Section 113-697B-29X, CC (diatoms are few, preservation is poor), which contains rare *Denticulopsis hustedtii, Synedra jouseana*, and *Cosmiodiscus intersectus*. We do not find indications that Miocene sediments have been penetrated at the base of Hole 697B.

Summary

At Site 697 we recovered 322.9 m of lower Pliocene to Quaternary sediment in two holes. Although the extent of Pliocene recovery at this site is matched elsewhere in the western Weddell Sea region, Site 697 has the most expanded Quaternary section sampled on Leg 113.

Compared to the Pliocene, diatom abundance in Quaternary sediments is generally poor but some levels (indicated in the text) contain abundant diatoms. Pliocene sediments at Site 697 contain rare to few and moderately to poorly preserved diatoms in contrast to Sites 689, 690, 693, 695, and 696 where, except for the lowermost Pliocene, common to abundant and moderately to well-preserved diatoms are present. At Site 697 abundant and well-preserved diatoms are generally restricted to discrete layers of several millimetere to decimeters in thickness. Such horizons, some of which have unusually well-preserved assemblages, occur in both the Quaternary and Pliocene. Examples are assemblages

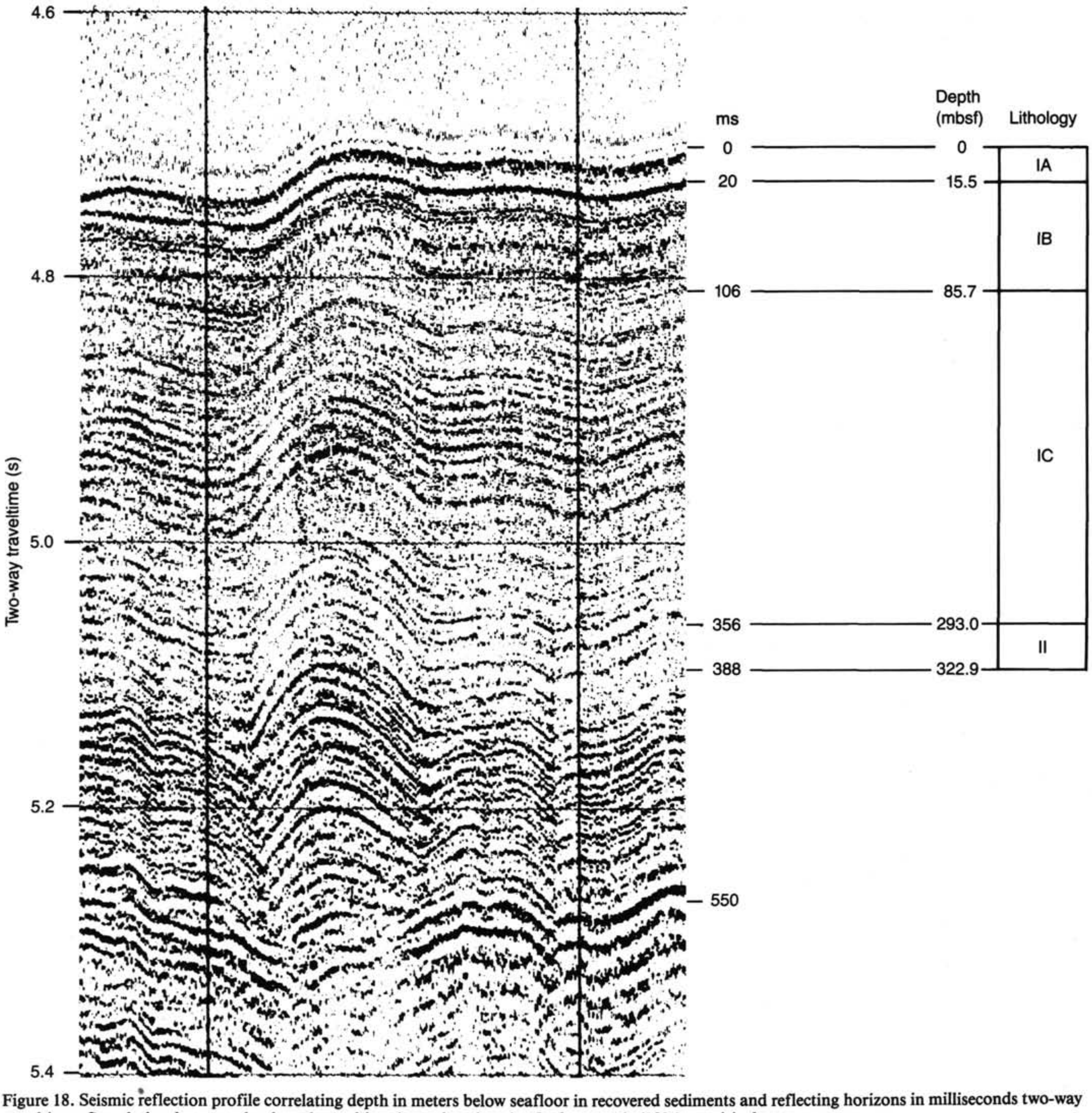

Figure 18. Seismic reflection profile correlating depth in meters below seafloor in recovered sediments and reflecting horizons in milliseconds two-way traveltime. Correlation between depth and traveltime is made using the Carlson et al. (1986) empirical curve.

dominated by *Corethron criophilum* (Sample 113-697A-2H-5, 48 cm) and *Thalassiothrix longissima* (Section 113-697B-4H, CC and Samples 113-697B-13X-3, 31 cm, and 113-697B-15X-2, 48 cm).

At Site 697, all Quaternary and Pliocene diatom zones of Weaver and Gombos (1981) could be identified, except the *Rhizosolenia barboi/Nitzschia kerguelensis* Zone (uppermost Pliocene) and the *Cosmiodiscus insignis* Zone (upper Pliocene). The latter, very-short-ranging zone was possibly not encountered because of poor diatom preservation, but the other zone could not be determined because the marker species were not found. According to independently interpreted paleomagnetic results, the transition from *N. praeinterfrigidaria* to *N. interfrigidaria* occurs within the lower part of the Gauss Chron. This finding supports the preliminary redating of the transition described in the Diatoms discussion in "Biostratigraphy" section, "Site 695" chapter (this volume).

With supporting bio- and magnetostratigraphic data, this site may provide us with useful insights into latest Neogene climate and ocean dynamics in a high southern latitude environment.

General Biostratigraphic Comment

Since this is the last Site of ODP Leg 113, we take the opportunity to discuss the biostratigraphic scheme used during the

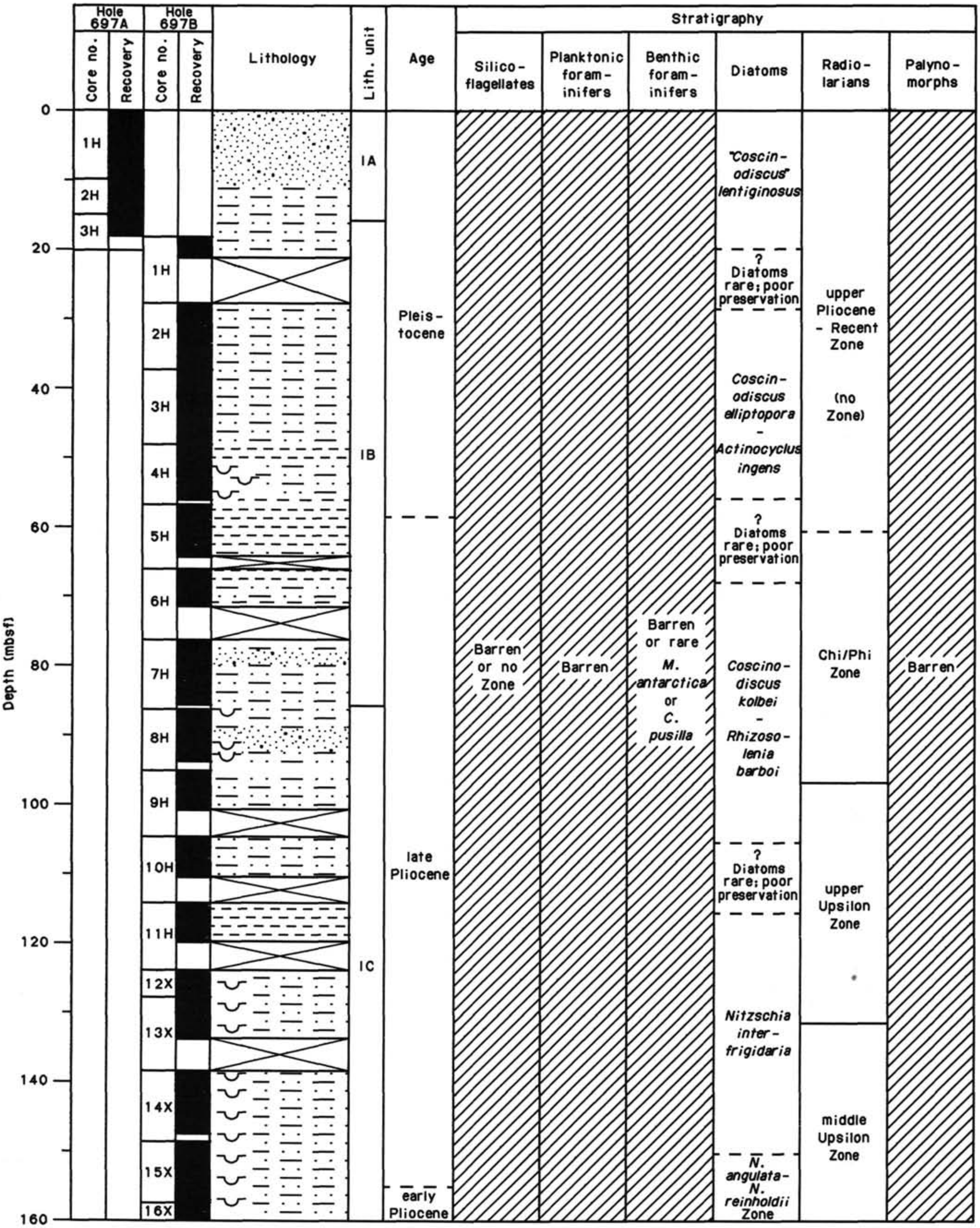

Figure 19. Summary biostratigraphic correlation chart, Site 697.

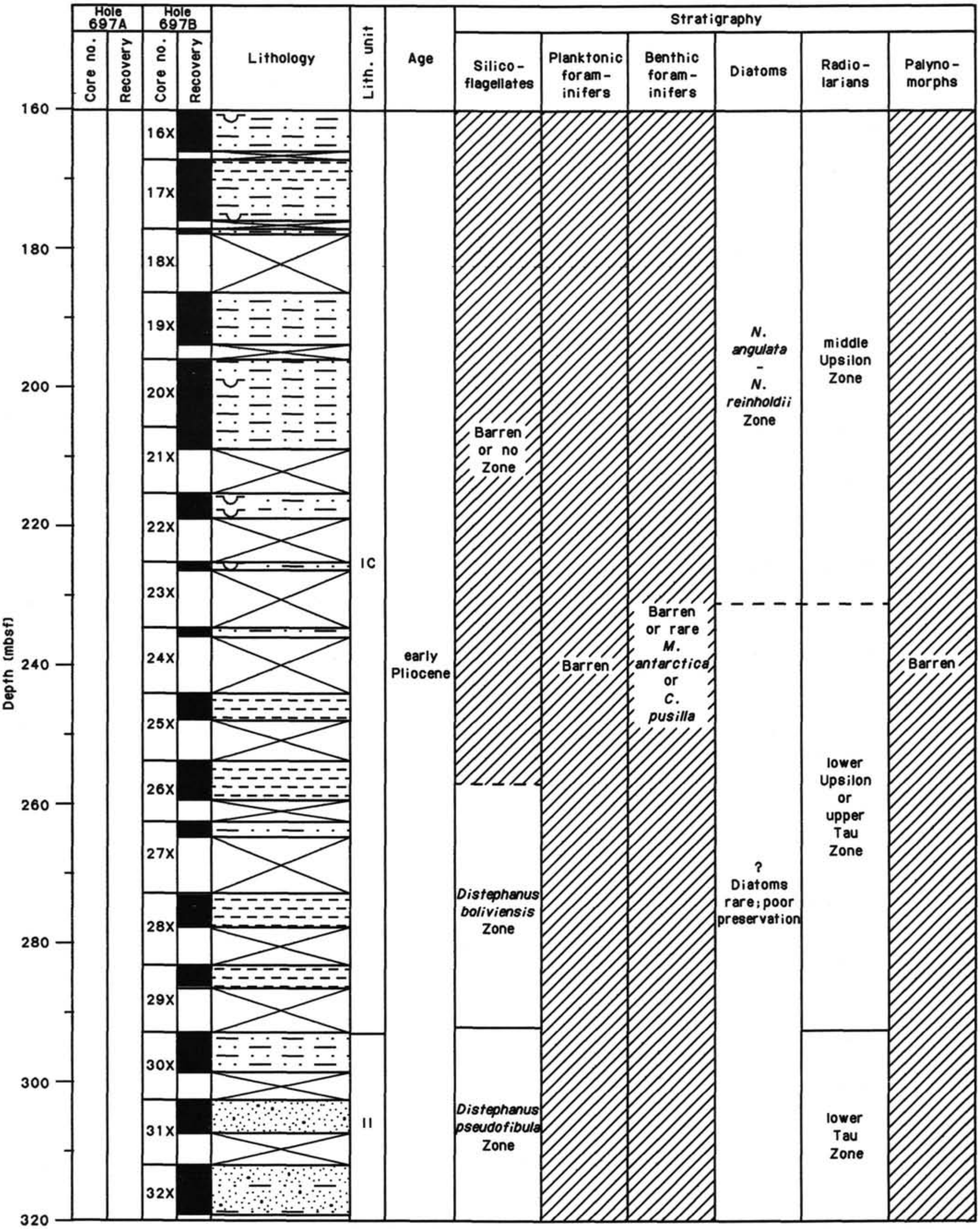

Figure 19 (continued).

course of this leg. In our opening comments on biostratigraphy, we indicated that the zonal scheme of Weaver and Gombos (1981) would be used for the Neogene and that of Fenner (1984) for the Paleogene. At the time, we expressed some misgivings about using what are essentially Subantarctic zonations in high southern latitudes. These were the only zonations available, however, so we were constrained to use them. We found difficulties in applying these zonations in many parts of the section and make some brief comments.

Upper Pliocene Diatom Zones

The *Rhizosolenia barboi/Nitzschia kerguelensis* Zone could not be determined because the former species was rare or absent from this interval while *C. kolbei* was variable in its last appearance. Similar comments can be made for the *Coscinodiscus kolbei/Rhizosolenia barboi* Zone. This zone was in most cases identified by the occurrence of *Coscinodiscus vulnificus* and the absence of *Cosmiodiscus insignis. C. vulnificus* was generally easy to identify, particularly in the western Weddell Sea region. On the eastern side, however, the species was rare to absent. The underlying *Cosmiodiscus insignis* Zone was in general easy to determine.

The *Nitzschia praeinterfrigidaria/N. interfrigidaria* transition

The presumed evolutionary transition of *N. praeinterfrigidaria* to *N. interfrigidaria* defines the zonal boundary of the *Nitzschia interfrigidaria* Zone and the underlying *Nitzschia angulata* Zone. Based on correlations to the magnetostratigraphy established for Holes 693A, 695A, and 697B, we tentatively changed the age assignment for the transition from the upper Gilbert (C3N-1, 3.88–3.97 Ma), as published by Weaver and Gombos (1981) and Ciesielski (1983), to the lower part of the Gauss Chron (about C2AN-2 to C2AN-3, 2.99–3.4 Ma). Shore-based studies will provide a more restricted time interval for the transition, possibly in the lowermost part of the Gauss Chron (C2AN-3; for further comments compare Diatom discussion in "Biostratigraphy" section, "Site 695" chapter, this volume).

The *Nitzschia angulata* enigma

We have already (in the "Site 689" chapter, this volume) indicated that the form referred to as *Nitzschia angulata* and used as a Pliocene marker by a number of authors (Gombos, 1977; Weaver and Gombos, 1981; Ciesielski, 1983) is not synonymous with the extant *N. angulata* (O'Meara) Hasle. We point out here that these authors were very likely referring to similar forms; one form appears to dominate in the Subantarctic region while a group of other forms is found in sediments farther to the south. We do not know the time of final occurrence of these forms; it appears from our study of Leg 113 samples, however, that they did not first appear near the base of magnetic subchron C3N-2 as reported by Weaver and Gombos (1981) and Ciesielski (1983). Rather, our study suggests that at least one form made its first appearance in upper Miocene sediments and one may bear an evolutionary relationship to *Nitzschia porteri* sensu Schrader (1976).

The combined *Nitzschia angulata/N. reinholdii* and the *Denticulopsis hustedtii* Zone (lower Pliocene to upper Miocene)

We could not define the base of the *N. angulata* Zone (compare above) and thus we were forced to combine that zone with the underlying *N. reinholdii* Zone. The nominate species of the latter zone could not be found consistently in our samples from lower Pliocene Southern Ocean sediments, as stated by Weaver and Gombos (1981) for these sediments. Forms with some affinity to *N. reinholdii* were very rarely found. In lower Pliocene sediments the Last Abundant Appearance Datum (LAAD) of *Denticulopsis hustedtii* has been used to identify the boundary between the *N. reinholdii* Zone and the underlying *D. hustedtii* Zone (Weaver and Gombos, 1981). We used this criterion in the Weddell Sea sites but find no evidence in the literature that this datum level (the LAAD of *D. hustedtii*) has ever been documented. Weaver and Gombos (1981) defined the top of the *D. hustedtii* Zone but never presented the supporting numerical data. Similarly, they did not present the magnetostratigraphic data for this zonal boundary although they published summary diagrams showing the relationship of this datum to magnetostratigraphy. Finally, we note some preliminary data obtained during Leg 113 suggesting that the last consistent appearance of *D. hustedtii* may be diachronous between the Subantarctic and the high-latitude Weddell Sea region. The last consistent appearance may be in the upper Miocene rather than the lower Pliocene.

The *Denticulopsis hustedtii/D. lauta* Zone (upper Miocene)

Although useful in the western Weddell Sea, we question continued use of the *D. hustedtii/D. lauta* Zone to identify the upper middle Miocene in the eastern Weddell Sea. In our experience, *D. lauta* is so rare and its occurrence so variable that its value as a zonal marker is questionable. The *D. lauta* Last Appearance Datum (LAD) appears to be useful in the Subantarctic region, but we found it of limited value in the eastern and central Weddell Sea. It wasn't until we analyzed diatoms in sites from the western Weddell Sea that we began to recover this species in considerable numbers. As noted in the Diatoms discussion, "Site 696" chapter (this volume), we suspect that this species is biogeographically linked to the Subantarctic and northern Antarctic regions and has limited value as a stratigraphic marker in much higher latitudes. Because we could not identify the *D. hustedtii/D. lauta* Zone, it was combined with the underlying *Nitzchia denticuloides* Zone. The nominate species of the latter zone has its last appearance near the top of the *D. hustedtii/D. lauta* Zone according to Weaver and Gombos (1981).

Middle and lower Miocene Zones

Because of the scarcity or absence of the middle and lower Miocene marker species *Bogorovia veniamini, Coscinodiscus rhombicus*, and *Coscinodiscus lewisianus*, it was not possible to identify, unequivocally, the *Bogorovia veniamini* Zone (uppermost Oligocene to lower Miocene), the *Coscinodiscus rhombicus* Zone (lower Miocene), or the *Coscinodiscus lewisianus* Zone (lower middle Miocene). Similarly, it was not possible to delineate the top and bottom of the *Nitzschia malinterpretaria* and *N. grossepunctata* Zones (lower to lower middle Miocene and lower middle Miocene, respectively), although the nominate taxa were present in considerable numbers. For this reason, we combined the *N. grossepunctata* and *C. lewisianus* Zones and the *N. malinterpretaria* and *C. rhombicus* Zones in some of the Leg 113 sites.

Summary

Although Neogene diatom stratigraphies have been published for the southern high-latitude ocean (Weaver and Gombos, 1981, Barron, 1985), a considerable number of the defined zones could not be used for biostratigraphic age assignment in Leg 113 Sites. This is especially true for the Miocene zonations because of the scarcity or absence of marker species and the poor definition of some zones. Although the Pliocene zonation has been tied to the paleomagnetic time scale we found a number of discrepancies, especially for the middle and lower Pliocene zones. Apparently part of the paleomagnetic time scale used for calibration was not accurately interpreted (e.g., by Ciesielski, 1983) and the taxonomy of some marker species is not well known.

Implicit in the use of the term is the requirement that the designations LAAD and First Abundant Appearance Datum (FAAD) need to be supported quantitatively. In spite of this, we could not find in the literature any quantitative data for the following datum levels: LAAD *D. hustedtii*, LAAD *N. denticuloides*, and LAAD *D. maccollumi*. In our view, LAAD or LAD should be used with caution in defining high southern latitude zonal boundaries because of problems related to reworking and displacement by bottom water. Unfortunately, most of the established Neogene zones are defined by LAAD and LAD.

Based on our preliminary study of the sections recovered during Leg 113 we found a number of species originally described and/or figured by Schrader (1976) and ignored until now which apparently can be used to redefine established Neogene diatom zonations for the Southern Ocean.

For Paleogene sediments, we tried to apply both the Gombos and Ciesielski (1983) and the Fenner (1984) stratigraphic schemes. Although we found problems with both, especially in the upper Oligocene, we think that the Fenner (1984) scheme is more reasonable since very broad zones are defined.

Radiolarians

Radiolarians from Site 697 were rare in the Pleistocene, and only a few samples provided any useful age information. Pliocene radiolarians are common and generally moderate to poorly preserved. Samples from this epoch can be assigned to the standard zonation, except for one interval within the lower Pliocene, where poor preservation makes it difficult to identify the base of the Upsilon Zone. The base of the section recovered at Site 697 (113-697B-32X, CC) is within the lower Tau Zone (basal Pliocene). Patterns of biogenic silica abundance and preservation at Site 697 parallel those at previous sites in this region, with low biogenic silica fluxes in the Pleistocene through latest Pliocene, relatively high fluxes and good preservation in middle and early Pliocene, and, in the basal Pliocene, poorly preserved biosiliceous microfossils with common Subantarctic radiolarians. Biostratigraphic assignments for Site 697 are as follows:

All 697A core-catcher sections, and Sections 113-697B-1H, CC, to 113-697B-4H, CC, contain only rare radiolarians, and no zonal assignment is possible. *Cycladophora davisiana* is present in Sections 113-697A-2H, CC, and 113-697B-4H, CC, indicating that this interval is no older than about 2.5 Ma.

Sections 113-697B-5H, CC, through 113-697B-8H, CC, are upper Pliocene to lower Pleistocene (Phi Zone or Chi Zone), based on the occurrence of *Pterocanium trilobum* in Section 113-697B-5H, CC, *C. davisiana* in Sections 113-697B-5H, CC, and 113-697B-8H, CC, and *Antarctissa ewingi* and *Clathrocyclas bicornis* in Section 113-697B-8H, CC.

Sections 113-697B-9H, CC, through 113-697B-23X, CC, are assigned to the Upsilon Zone, based on the occurrence of *Helotholus vema* and *Desmospyris spongiosa*. The First Appearance Datum (FAD) of *C. davisiana* subdivides this interval into the upper (Section 113-697B-9H, CC, to 113-697B-12X, CC) and middle (Sections 113-697B-13X, CC, to 113-697B-23X, CC) portions of the Upsilon Zone.

Poor preservation below Core 113-697B-23X makes zonal assignments difficult. Cores 113-697B-24X through 113-697B-29X contain common *Prunopyle titan* and are thus within either the lower part of the Upsilon Zone, or the upper part of the Tau Zone. The zonal indicator for the Upsilon Zone, *H. vema*, is absent in these samples, suggesting an upper Tau assignment. *Desmospyris spongiosa* is common, however. This latter species is generally restricted to Upsilon through uppermost Tau Zone sediments, and its presence suggests that the absence of *H. vema* in at least some of the samples from this interval may be due to dissolution. The base of the Upsilon Zone is thus not defined at this site.

The LAAD of *Lychnocanium grande* occurs between Sections 113-697B-29X, CC, and 113-697B-30X, CC. This species is common in all remaining sections (113-697B-30X, CC, to 113-697B-32X, CC), despite poor preservation of radiolarian assemblages. Miocene forms are not observed, and the interval is therefore assigned to the lower Tau Zone. The radiolarian assemblages in this interval appear to be very similar to those seen at Sites 695 and 696. Subantarctic elements occur, including Artostrobids and *Polysolenia* sp., while typical Antarctic elements such as Antarctissids are relatively rare.

Silicoflagellates

Silicoflagellates are generally sparse or absent in the upper 250 m of the siliceous muds at Site 697, therefore these fossils do not provide useful datums for biostratigraphy in Cores 113-697A-1H to 113-697B-25X. The paucity of silicoflagellates may be due to the relatively deep water setting of this site (3480 m), which would have promoted the dissolution of these fossils. Two thin diatomaceous interbeds were sampled, however, at 113-697B-13X-2, 140 cm, and 113-697B-13X-3, 30–32 cm, and these yielded abundant *Distephanus speculum*. Other such acmes have been noted in the Pliocene at previously drilled sites of this leg (example, Core 113-689A-1H).

Distephanus boliviensis is consistently present below 250 m, but its LAD is difficult to establish due to its erratic occurrence above that level. This taxon is common in Section 113-697B-21X-2 with only a few specimens present in Section 113-697B-20X-3 (K. McKartney, written comm., 1987). Core 113-697B-26X contains few *Distephanus boliviensis, D. speculum,* and rare *D. quinquangellus* and *D. crux*. This assemblage closely resembles that of Cores 113-695A-26X and 113-697B-27X on the South Orkney microcontinent.

Section 113-697B-30X, CC, contains few *D. boliviensis, D. quinquangellus*, and rare *D. pseudofibula*. A few specimens of the latter taxon also occur in Section 113-697B-31X, CC, and in Section 113-697B-32X-5, therefore these last three cores can be assigned to the *D. pseudofibula* Zone (Ciesielski, 1975). At this site as well as at others drilled on this leg, this zone coincides closely with the lower portion of the radiolarian Tau Zone (see "Radiolarians" discussion above).

Palynomorphs

All core-catcher sections of Site 697 (Sections 113-697A-1H, CC, through 113-697A-3H, CC, and 113-697B-1H, CC, through 113-697B-32X, CC) were barren of palynomorphs.

Summary

At Site 697 we sampled a 322.9-m thick Quaternary to lower Pliocene sequence consisting predominantly of diatom-bearing silty to clayey mud. Core recovery varied from good to moderate in the Quaternary through upper Pliocene, and from moderate to poor in the lower Pliocene. Recovery was especially poor between 210 and 250 mbsf (Cores 113-697B-21X through 113-697B-25X averaged 26% recovery). The Quaternary section is expanded compared to other Leg 113 sites, and does not contain a carbonate-bearing interval; thus no calcareous microfossils were recovered at this site. Agglutinated benthic foraminifers are very rare throughout the section. All biostratigraphic information is based on the siliceous microfossil groups (radiolarians, diatoms, and silicoflagellates); no hiatuses were observed. The abundance and preservation of siliceous microfossils exhibit strong fluctuations, and thus some zonal boundaries could not be placed with precision. There is good biostratigraphic agreement between diatom, radiolarian, and silicoflagellate data indicating that the sediment at the bottom of the hole is lower Pliocene, although preservation is poor and abundances low in the lower part of the section.

In the Quaternary section, radiolarians and silicoflagellates are rare; the biostratigraphic age assignments are based on diatoms which show strong variations in abundance and preservation. Several core-catcher sections (e.g., 113-697A-3H, CC, and 113-697B-3H, CC) are barren, and from these cores additional samples were studied. Cores 113-697A-1H through 113-697A-3H are placed tentatively in the Pleistocene "*C.*" *lentiginosus* diatom Zone, Cores 113-697B-2H through 113-697B-4H in the lower Pleistocene *C. elliptopora/A. ingens* diatom Zone. The Pliocene/Pleistocene boundary is tentatively placed below Section 113-697B-4H, CC (58 mbsf).

Cores 113-697B-5H through 113-697B-8H are placed in the upper Pliocene through lower Pleistocene radiolarian Phi or Chi Zones; Section 113-697B-5H, CC, cannot be zoned using diatoms, but Sections 113-697B-6H, CC, through 113-697B-9H, CC, are placed in the upper Pliocene *C. kolbei/R. barboi* diatom Zone; Section 113-697B-10H, CC, again cannot be zoned using diatoms. Sections 113-697B-9H, CC, through 113-697B-23X, CC, are placed in the lower to upper Pliocene radiolarian Upsilon Zone. The upper and middle Upsilon subzones could be recognized (the boundary was placed between Sections 113-697B-12X, CC, and 113-697B-13X, CC). Diatoms place the upper part of the interval assigned to the radiolarian Upsilon Zone (Section 113-697B-11H, CC, through Sample 113-697B-15X-2, 48 cm) tentatively in the *N. interfrigidaria* Zone (upper Pliocene). Cores 113-697B-15X through 113-697B-24X (corresponding approximately to the lower part of the radiolarian Upsilon Zone) are placed in the *N. angulata-N. reinholdii* diatom Zone.

The lower part of the hole (Section 113-697B-24X, CC, and below) is difficult to zone because of low abundance and poor preservation of siliceous microfossils, but there are no indications that Miocene sediments were recovered in this hole. No diatom zonation can be given for this part of the hole. Sections 113-697B-23X, CC, through 113-697B-29X, CC, are placed in the radiolarian lower Upsilon or upper Tau Zone. The zones cannot be differentiated because the zonal marker for the Upsilon Zone (*H. vema*) is absent in this interval, while *D. spongiosa* (usually restricted to the uppermost Tau to Upsilon Zones) is common. Sections 113-697B-26X, CC, through 113-697B-29X, CC, are placed in the silicoflagellate *D. boliviensis* Zone, but the upper boundary of the zone cannot be placed precisely because of erratic occurrences of the species higher in the section.

Sections 113-697B-30X, CC, through 113-697B-32X, CC, are in the lower Tau radiolarian Zone because of the absence of Miocene forms and the common presence of *L. grande*, in agreement with silicoflagellate data. Sections 113-697B-30X, CC, and 113-697B-31X, CC, can be placed in the silicoflagellate *D. pseudofibula* Zone, which coincided with the lower Tau Zone at other Leg 113 sites. The radiolarian assemblages in this interval are similar to those at Sites 695 and 696, and contain Subantarctic elements while typical Antarctic elements are rare.

The section recovered at Site 697 will be useful in providing correlations between siliceous biostratigraphic and paleomagnetic datums (see "Sedimentation Rates" section, this chapter), although interpretations will be hampered in some intervals by the erratic preservation and abundance of siliceous microfossils.

PALEOMAGNETISM

Site 697 is the deepest site of the three-site depth transect on the South Orkney microcontinent. It is located in Jane Basin, a back-arc basin formed behind the Jane Bank (King and Barker, 1988). The thick hemipelagic/pelagic sequence at this site offers a unique opportunity to investigate fluctuations in Antarctic Bottom Water (AABW) circulation during the late Neogene and Quaternary. Deciphering the magnetostratigraphy of the sedimentary record of Site 697 is crucial for an understanding of the chronology of major changes in the deep water-mass activity. Previous paleomagnetic study of a few shallow gravity cores from the Jane Basin suggests sediment accumulation rates during the late Brunhes Chron of approximately 20 m/m.y. (Pudsey et al., in press).

We measured the natural remanent magnetization (NRM) vector of 370 samples from the two holes cored at this site. Additionally, whole-core susceptibility measurements were undertaken on a majority of the unsplit core sections; a few sections were unsuitable for such measurements due to disturbance during recovery.

Magnetostratigraphy

The NRM vector-inclination distribution for Site 697 closely parallels that found for Site 695 in showing a bimodal form (Fig. 20). Clearly the coercivity of the dominantly clayey muds recovered here is such as to resist normal polarity overprinting to an extent that the NRM preserves a reasonably good polarity record. Nonetheless, some improvement in quality and resolution is likely after magnetic cleaning.

Figure 21 shows the NRM inclination and intensity variation downhole for Holes 697A and 697B. The magnetic intensities range from weak to moderately strong (0.1–35 mA/m), but the majority of values are greater than 1 mA/m. A number of well-defined normal and reversed magnetozones are evident in the inclination record. We have tentatively assigned these to the established geomagnetic polarity time scale as shown in Figure 22. This correlation allows fairly precise estimates of sedimentation rates to be made independently of any biostratigraphic control, from the lower Pliocene to the upper Pleistocene.

For the first time during Leg 113 we have paleomagnetic data (Hole 697A, Fig. 23) derived from Brunhes Chron sediments

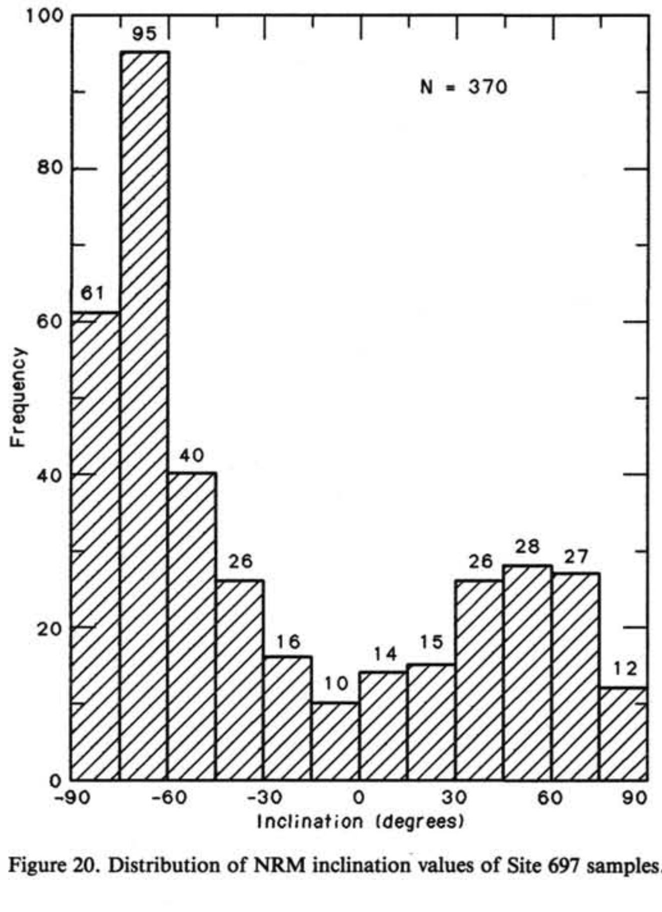

Figure 20. Distribution of NRM inclination values of Site 697 samples.

deposited at a high rate. The downhole NRM inclination plot of Figure 23A indicates that shallow to moderately dipping positive inclinations occur between 3.2 and 4.5 mbsf. It seems probable that these represent a short reversed magnetozone which can be provisionally identified as the Blake Event. Earlier observations of other high sedimentation rate sections have revealed that a split sequence of reversed inclinations may characterize the Blake Event, for example as reported by Creer et al. (1980) for Gioia Tauro, Italy. The record preserved in Hole 697A appears also to show such a split Blake Event. Recognition of its occurrence in Antarctica provides positive verification of the global nature of the Blake Event as a true reversed-polarity geomagnetic event within the Brunhes Chron.

Therefore Site 697 provides a high-fidelity magnetostratigraphic record despite some intervals of poor recovery. Agreement between the magnetostratigraphy and the diatom and radiolarian biostratigraphy is particularly convincing (see "Sedimentation Rates" section, this chapter). This site will be one of key importance in calibrating high-latitude siliceous biozonations using magnetochronology for the late Neogene and Quaternary.

Magnetic Susceptibility

Whole-core susceptibility measurements were made for both holes at Site 697. Figure 23C illustrates the variation in susceptibility with depth for Hole 697A. The apparent overlap of Core 113-697A-2H with Cores 113-697A-1H and 113-697A-3H is not straightforward, but the changes in susceptibility can be used to attempt placement of Core 113-697A-2H in the correct depth position. This is indicated by tie-lines on the figure.

Figure 24 gives the whole-core susceptibility data for Hole 697B. As noted at Site 694 high susceptibility spikes generally correspond to dropstones in the cores but these must be either igneous or metamorphic to give such a response. Cross-checking with lithological descriptions shows that sedimentary dropstones do not produce a change in the background susceptibility. In the upper part of the hole, down to 120 mbsf, quasi-periodic fluctuations in susceptibility are apparent. Visual estimates of the thickness intervals relating to the shortest period between susceptibility maxima are about 1 m. This would correspond to a time span of approximately 23,000 years using the estimated sedimentation rate of 43 m/m.y. determined for the Brunhes through late Gauss, (see "Sedimentation Rates" section, this chapter). We can speculate that a record of Milankovitch orbital cycles may be identified in the susceptibility data we have obtained at Site 697. Spectral analysis is necessary to prove these conjectures.

There is a broad correlation between mean susceptibility (Fig. 25) and the major lithological changes at this site. The clayey muds have the higher susceptibility level of 25–30 10^{-6} G/Oe, while the lower average susceptibility level, approximately 15 10^{-6} G/Oe, corresponds to the diatom-bearing clayey mud. The lowest mean susceptibilities occur between 140 and 196 mbsf. An increase in the amount of ice-rafted debris together with terrigeneous silt in the lowermost cores of the hole is reflected in a trend toward higher susceptibility values.

SEDIMENTATION RATES

Biostratigraphic and Magnetostratigraphic Data

The sedimentation-rate curve for Site 697 (Fig. 26) is constructed from two different sources of data. Biostratigraphic ages derived from diatoms, radiolarians, and silicoflagellates provide one source of age information. The figure was constructed as follows. Biostratigraphic data points (boxes, vertical/horizontal lines) are labeled with identifying numbers. Magnetostratigraphic data in comparison are shown as line segments with unlabeled datum points (solid boxes). Error boxes for paleomagnetic data represent in depth the distance between two samples of different polarities assigned to different magnetozones. From the preceding and the following magnetozone boundaries a sedimentation rate, and from this a corresponding error in the age determination is calculated. This age error is represented by the horizontal box line. Biostratigraphic data are of three types. First and last ocurrences of species which are known to occur only within a finite depth interval are plotted as vertical lines; the age of the datum is generally reported without an associated error estimate. Age ranges for individual samples, by contrast, have a finite age range but do not have a depth uncertainty and are plotted as horizontal lines. Finally, a few FAD's and LAD's for which uncertainty estimates are available are plotted as boxes. Many samples have more than one age-range estimate from different fossil groups. To make the overlap between multiple data clear, small solid circles are used to mark the end of each datum which plots as a line. FAD's and LAD's represent, respectively, the oldest and youngest possible ages for a depth interval. Arrows indicate datums of this type, with the direction indicating the time direction during which the species occurs. Biostratigraphic data used to construct the age-depth relationship (Table 7) consist of selected datum levels and zonal assignments which have been correlated to the chronostratigraphic scale.

Magnetostratigraphy provides a second source of age information. Magnetic polarity data were correlated with the geomagnetic polarity reversal time scale of Berggren et al. (1985) (see "Explanatory Notes" chapter, this volume, and "Paleomagnetism" section, this chapter) without recourse to biostratigraphic data. Magnetostratigraphy for Site 697 provides the most clearly defined polarity pattern of all sites drilled during Leg 113. The polarity record can be completely assigned to the Pleistocene and upper late Pliocene of the geomagnetic polarity time scale. For this site the NRM stratigraphy can be used as a base for comparison and calibration of microfossil zonation for this time interval, although erratic microfossil preservation commonly makes identification of zonal boundaries difficult. A straightforward interpretation leads to a fairly constant sedimentation rate estimate from the upper Gilbert Chron through the Quaternary and a higher scatter in the lower Pliocene due to poor recovery and a less precise definition of reversal boundaries.

Sedimentation Rates

For the Pleistocene and upper Pliocene, sedimentation-rate estimates are derived from both magnetostratigraphic age assignments and diatom datum levels, which are chronostratigraphically calibrated for this time interval. These data sets are in close agreement and suggest a high and continuous sedimentation rate of 40 m/m.y. for the Pleistocene through the upper Gauss Chron (Fig. 26). This high sedimentation rate is in marked contrast to other Leg 113 sites where the Pleistocene and uppermost Pliocene is condensed or absent. Radiolarian age determinations suggest a rate of sedimentation of 130 m/m.y. in the uppermost Gauss Chron. Further shore-based studies are expected to resolve the differences in dating by precise definition of stratigraphic and reversal boundaries and/or perhaps the detection of overprinted polarity intervals, which might require a revised paleomagnetic age assignment.

Sedimentation rate estimates for the lowermost upper and the lower Pliocene are based on combined radiolarian and diatom datum levels. In the middle Gauss Chron, at approximately 3.0 Ma, the sedimentation rate increased to 125–150 m/m.y., continuing at this rate through the lower Gauss and Gilbert Chrons. There is an age difference of 0.5 m.y. between the paleomagnetic data and the placement of the base of the radiolarian middle Upsilon boundary. The paleomagnetic and the diatom datum levels appear to be in close agreement (Fig. 26).

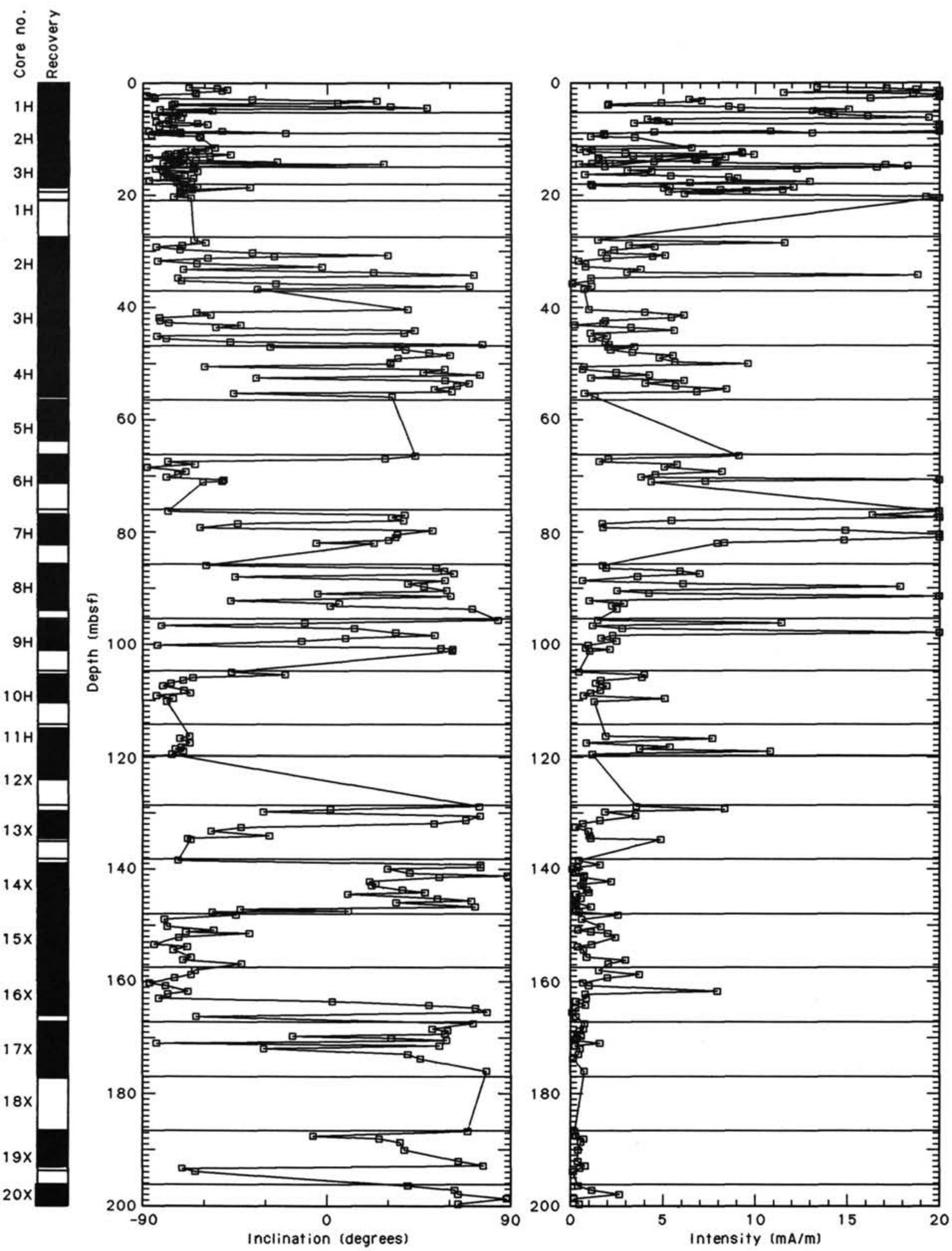

Figure 21. Downhole variation of NRM inclination and intensity for samples from Holes 697A and 697B.

Shorter polarity intervals might remain undetected due to poor recovery in this interval, in which case a late Miocene age would be indicated by paleomagnetic data for the bottom of the hole. Paleomagnetic data, however, allow a clear polarity assignment at the present time and provide a sedimentation-rate estimate of approximately 200 m/m.y. for the middle lower Pliocene.

The middle Gilbert Chron (C3N-1 to C3N-3) sediments accumulated with the highest sedimentation rate of 135 m/m.y. A

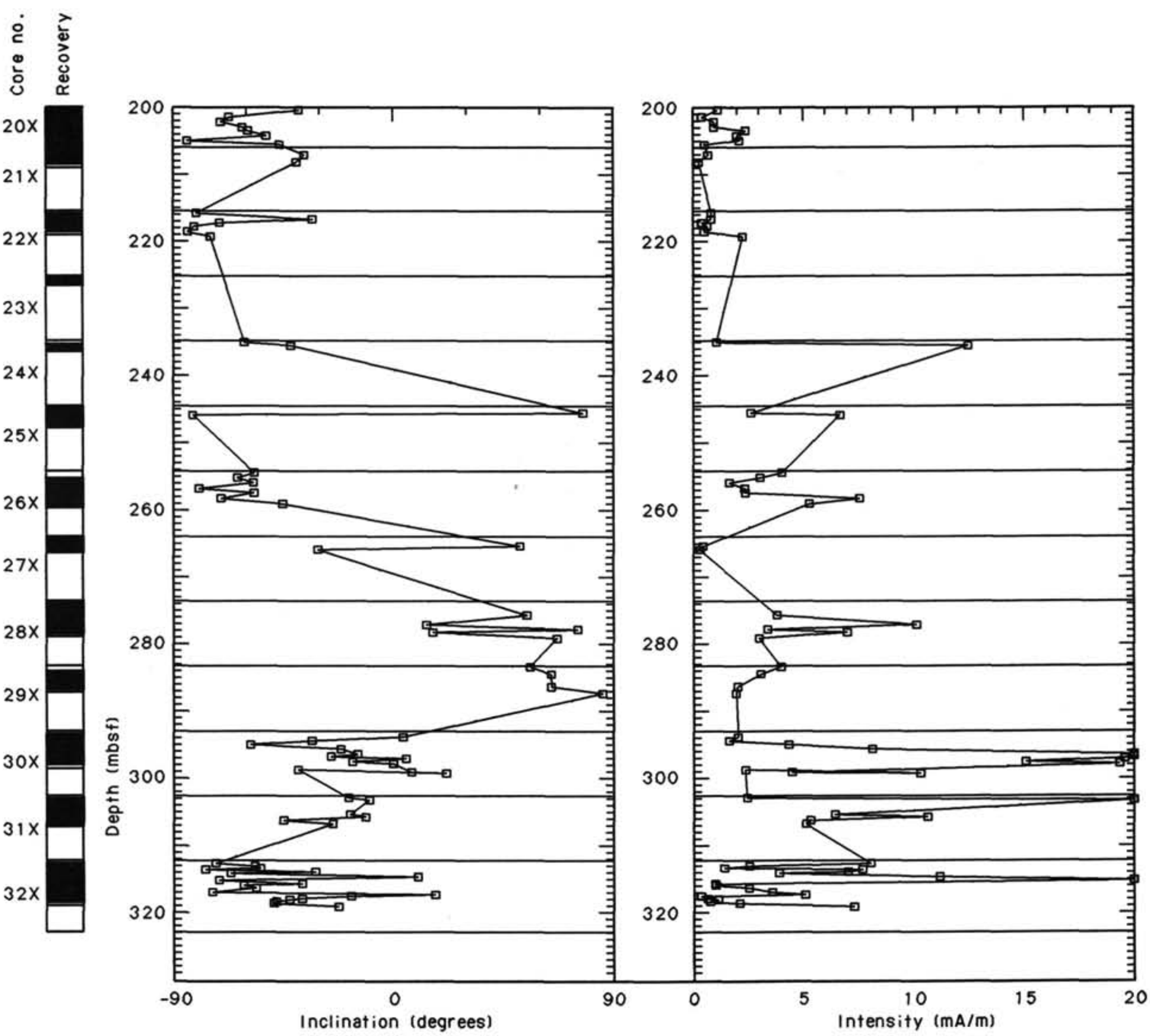

Figure 21 (continued).

decreased rate of 78 m/m.y. followed until middle Gauss Chron times (base of C2AN-1). From then into the late Brunhes, sedimentation slowed to a rate of approximately 43 m/m.y.

The sedimentation record at Site 697 appears to be continuous, with no apparent hiatuses in the Pliocene or Pleistocene. The high sedimentation rate during the early Pliocene is similar to that seen at other Leg 113 sites, reflecting the regional extent of this pattern. Continuously high sedimentation rates in the upper Pliocene and Pleistocene were not observed at other Weddell Sea sites.

INORGANIC GEOCHEMISTRY

Introduction and Operation

Data on the chemical composition of interstitial water are presented for Holes 697A and 697B. Due to a stuck core barrel, Hole 697A was abandoned after APC-coring to 20.9 mbsf. One whole-round sediment sample for squeezing was obtained from the first core (Section 113-697A-1H-4). Hole 697B was XCB-cored from 119.8 to 322.9 mbsf following washing to 18.0 mbsf and APC-coring to 119.8 mbsf. For reasons discussed in the following sections on alkalinity and sulfate, a closer than usual sampling scheme was employed. Thus, 15 whole-round sediment samples (2 of 5-cm and 13 of 10-cm thickness) for squeezing were obtained from Hole 697B.

Chemical data are summarized in Table 8. For details on sampling and analytical methods see "Explanatory Notes" chapter (this volume).

Evaluation of Data

A charge balance based on the assumption of constant Na/Cl ratio equal to that of present-day seawater reveals an erratically increasing excess positive charge to about 1% below 200 mbsf. As with the previous Leg 113 sites, this trend is regarded as being indicative of uptake of sodium (as suggested by Manheim and Sayles, 1974), rather than systematic analytical errors.

From the sulfate profile it is evident that the sample from Section 113-697B-5H-3 is contaminated by seawater. In the visual core description the consistency of this core is described as soupy. Drilling-induced biscuiting of the deeper cores was observed, and it is possible that some contamination by seawater has taken place. As contamination is by nature random, the smooth concentration profiles at depth indicate that it has not seriously affected the results.

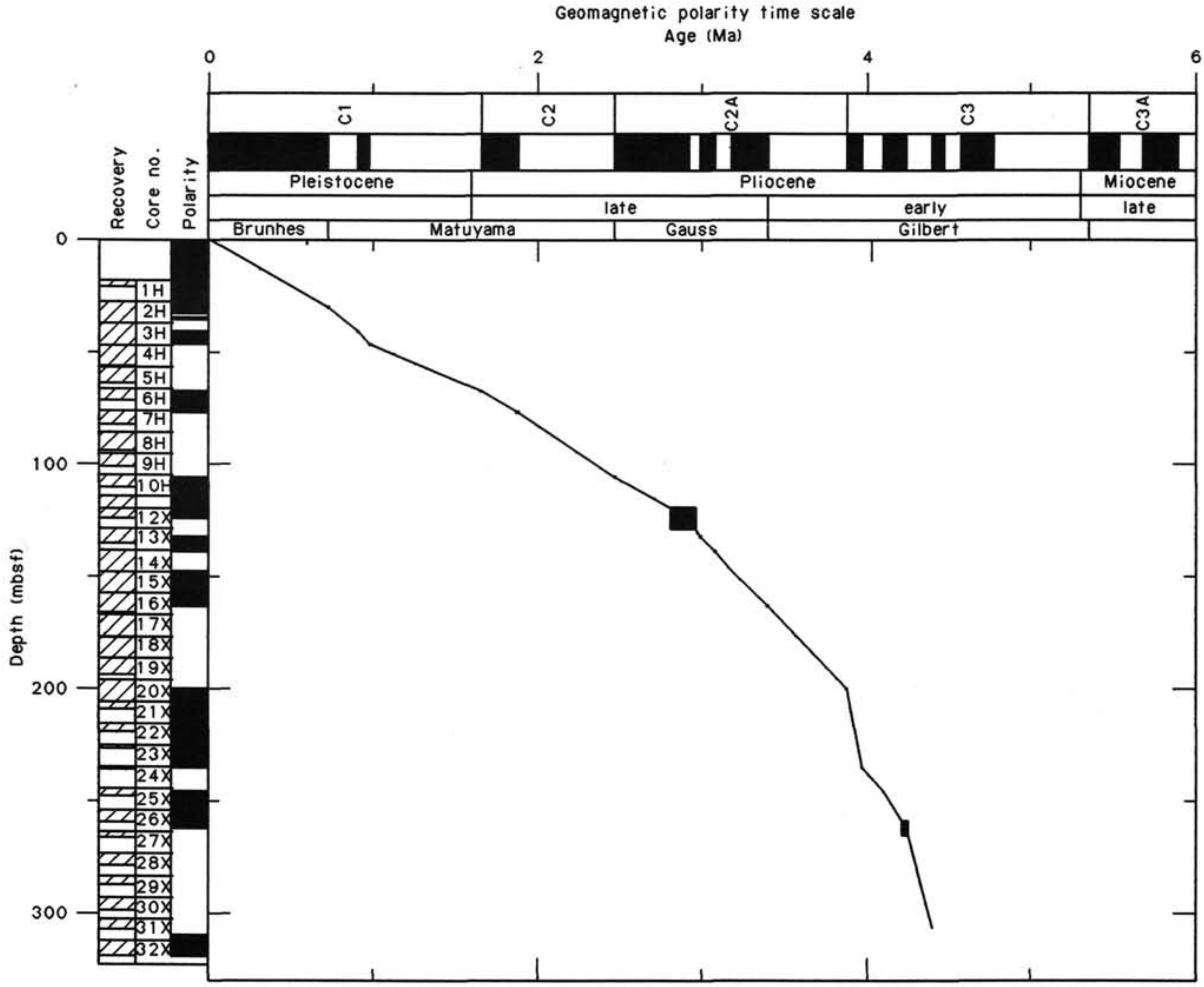

Figure 22. Preliminary assignment of inferred polarity reversal sequence at Site 697 to the geomagnetic polarity time scale and resulting sediment-accumulation rate curve.

Chloride and Salinity

Chloride data are presented in Figure 27A and Table 8. There is a slight general increase in chloride concentration from 555 mmol/L in the upper section (Section 113-697A-1H-4) to a level of about 570 mmol/L below 160 mbsf. Using the chloride/salinity relationship provided by Stumm and Morgan (1981), this corresponds to seawater salinities of 34.3 and 35.2‰, respectively. As the seawater used for circulation during drilling is taken from the upper (less than 10 m) water column, the low chloride concentration in Section 113-697B-5H-3 confirms that this is mainly seawater (see "Sulfate" discussion below).

The average salinity measured by the optical refractometer is 34.4‰. It varies between 32.4‰ in Section 113-697B-19X-3 and 35.0‰ in Section 113-697B-13X-3 (Table 8). The salinity determined by the two methods does not correlate.

pH

The pH (Fig. 27B, Table 8) varies between 7.74 in Section 113-697B-16X-4 (163 mbsf) and 8.27 in the deepest sample (Section 113-697B-31X-2), without showing any trends. The high pH (8.99) in Section 113-697B-5H-3 is caused by contamination (see "Potassium" discussion below).

Alkalinity, Sulfate

The alkalinity data are presented in Figure 27C. The alkalinity increased rapidly from 4.89 meq/L in the shallower section (Section 113-697A-1H-4) to a maximum of 18.35 meq/L at 132.75 mbsf (Section 113-697B-13X-3) below which it decreases to 10.1 meq/L at 305.5 mbsf (Section 113-697B-31X-2).

One of the main objectives of the interstitial water studies of Leg 113 is the investigation of the formation (presumably bacterial) of dissolved organic acids. The rapidly increasing alkalinity indicates high bacterial activity. Thus, based on the alkalinity of the two first samples (5.95 and 19.45 mbsf), it was decided to sample the upper 100 m of the sediment column more frequently (every core) than usual (every third core).

The alkalinity profile is steeper and the alkalinity maximum is higher than observed at any other Leg 113 site. Above the maximum there is a strong correlation between sulfate and alkalinity ($r = -0.99$, $n = 8$). However, the increase in alkalinity is less than half of what one would expect assuming stoichiometric oxidation of organic matter. Probably, alkalinity has been removed by precipitation of carbonate (and possibly as proton acceptor in reversed weathering processes).

The sulfate profile is presented in Figure 27D. The concentration of sulfate decreases from close to seawater value (28.0

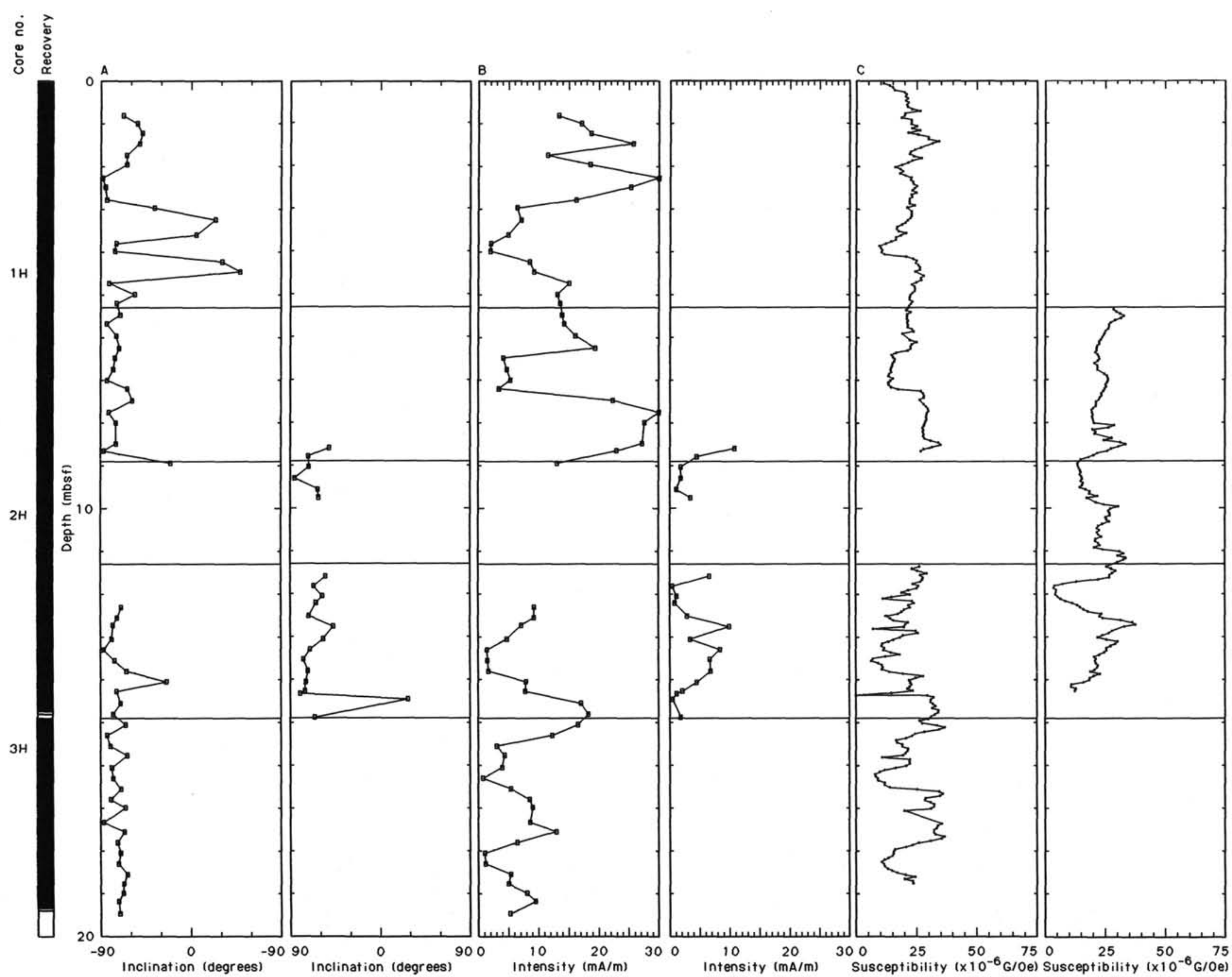

Figure 23. Detailed magnetic parameters for Hole 697A. A. Downhole inclination. B. Downhole NRM intensity. C. Whole-core magnetic susceptibility, tie-lines show suggested location of Core 113-697A-2H with basal part of Core 113-697A-1H.

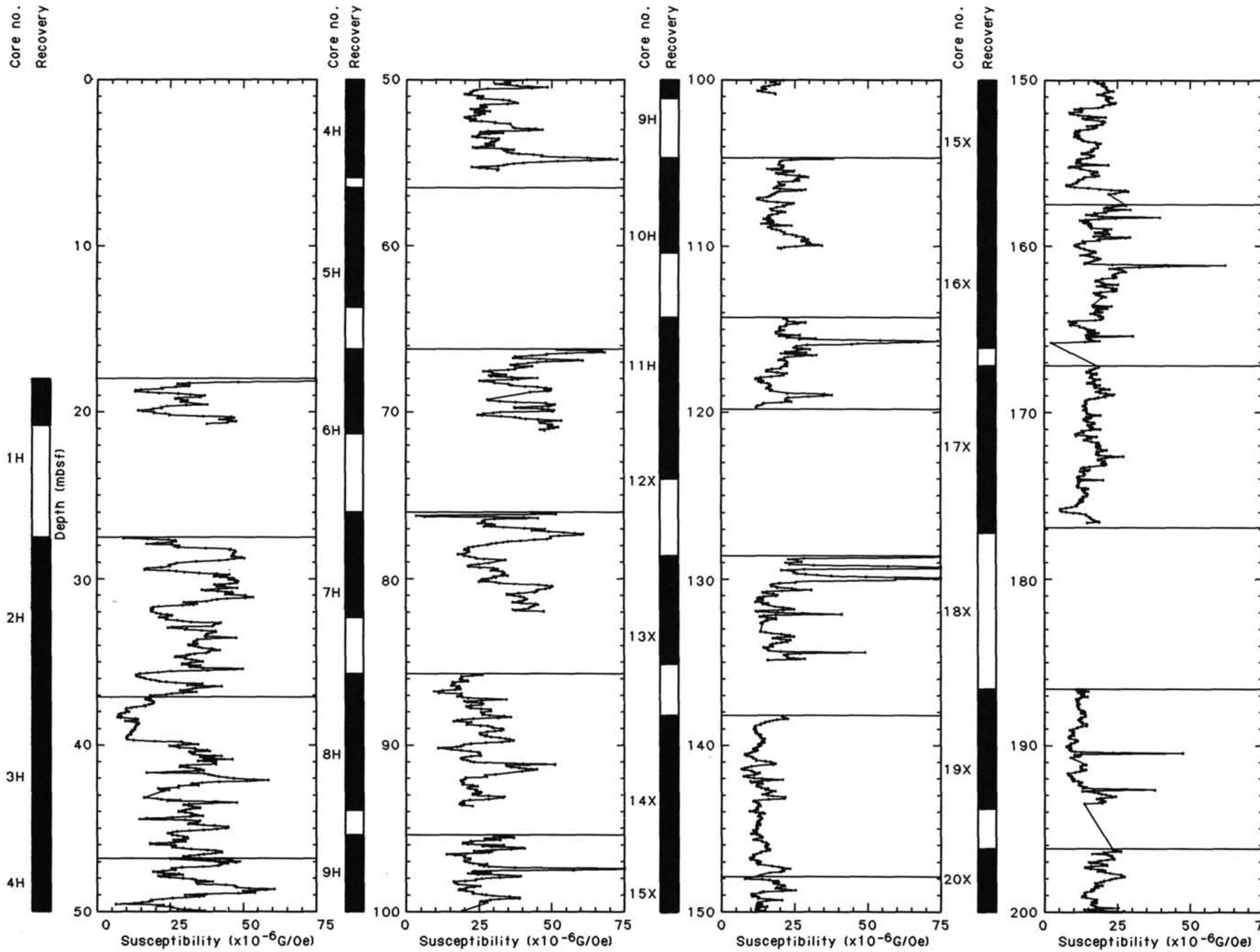

Figure 24. Whole-core susceptibility data for each core of Hole 697B.

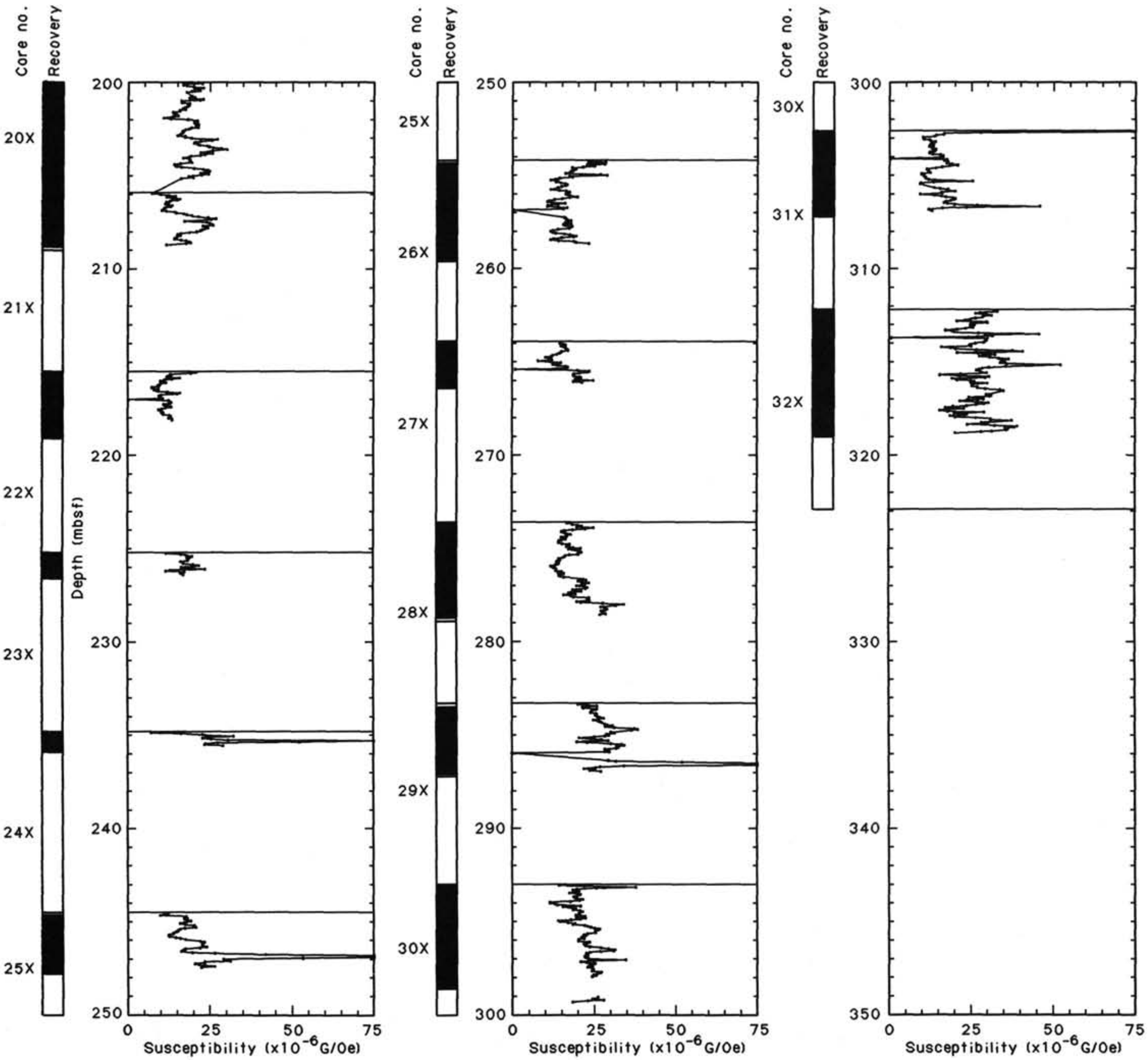

Figure 24 (continued).

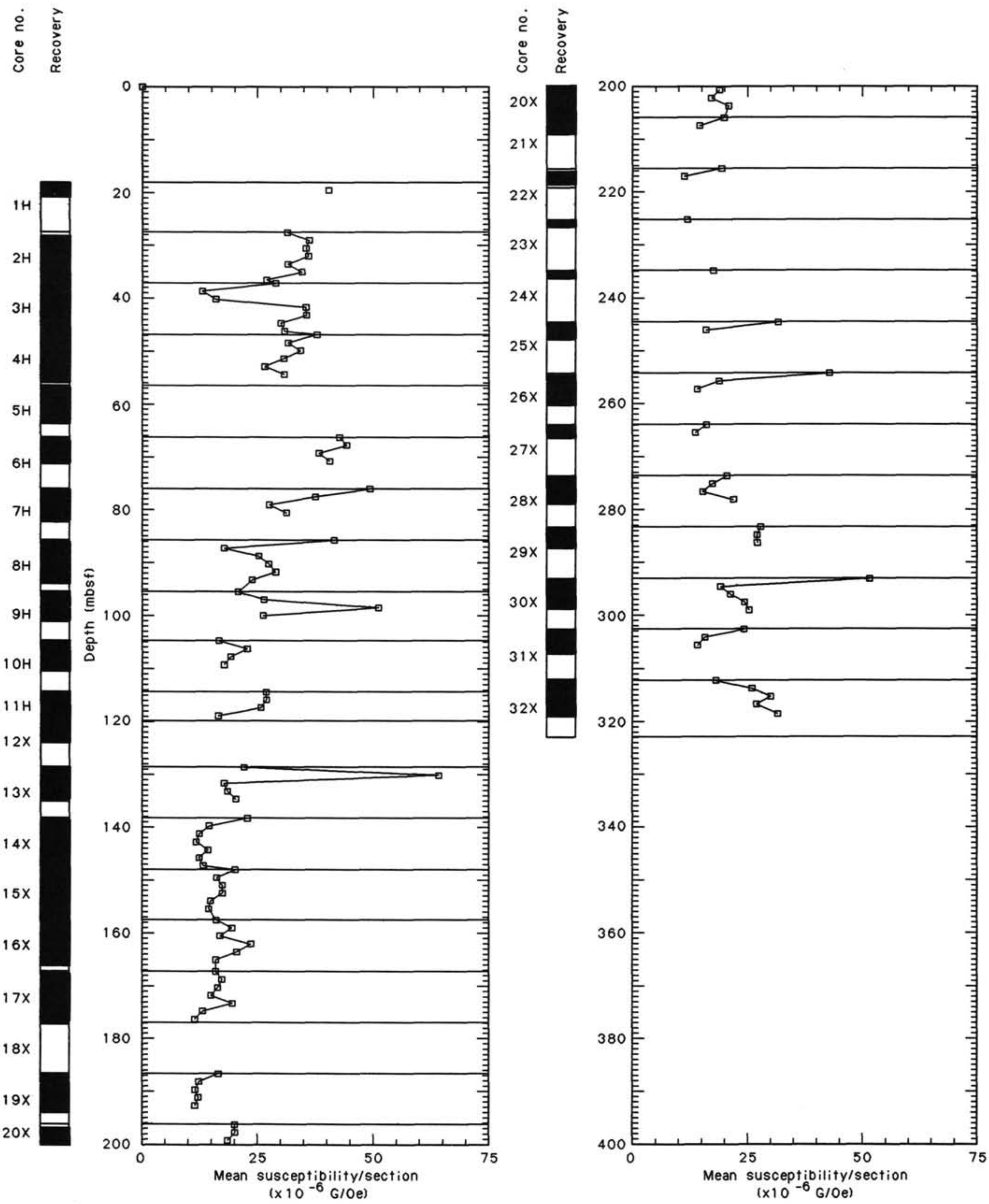

Figure 25. Individual core section mean susceptibility values plotted as a function of depth downhole.

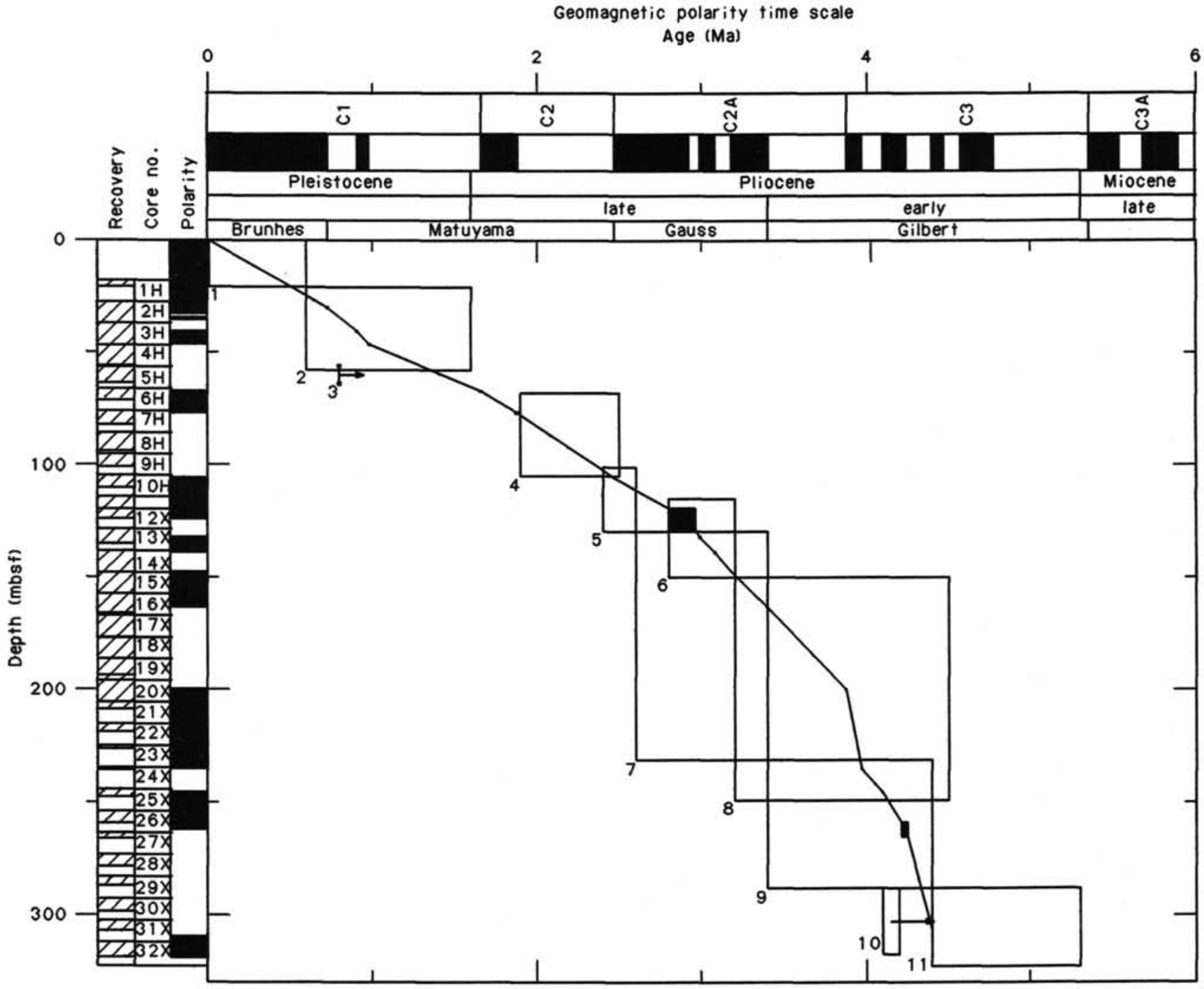

Figure 26. Age-depth interpretation of Site 697. See text for details about how the figure was constructed.

Table 7. Biostratigraphic data used to construct sedimentation-rate curve shown in Figure 26.

Datum number	Depth range (mbsf)	Age range (Ma)	Datum of zone or range
1	0.0–20.9	0.0–0.6	*C. lentiginosus* Zone—D
2	20.9–58.0	0.6–1.6	*C. elliptopora/A. ingens* Zone—D
3	56.1–63.9	0.8–0.8	Top assemblage Phi/Chi—R
4	68.0–105.0	1.9–2.5	*C. kolbei/R. barboi* Zone—D
5	101.1–129.6	2.4–2.6	upper Upsilon Zone—R
6	115.0–150.0	2.8–3.2	*N. interfrigidaria* Zone—D
7	129.6–231.3	2.6–3.4	middle Upsilon Zone—R
8	150.0–249.3	3.2–4.52	*N. angulata/N. reinholdii* Zone—D
9	231.3–288.2	3.4–4.4	upper Tau/lower Upsilon Zone—R
10	288.2–317.6	4.1–4.2	LAD *D. pseudofibula*—S
11	288.2–322.9	4.4–5.3	lower Tau Zone—R

Key to table: Depth range given for First and Last Appearance Datums (FAD's and LAD's). Age range given for zones, and in some instances for uncertainty in age calibration of a FAD or LAD. Letters following each datum name refer to the fossil group: D = diatoms; R = radiolarians; S = silicoflagellates.

mmol/L) in the upper section (Section 113-697A-1H-4) and stabilizes at a value of about 6 mmol/L below 130 mbsf. The sulfate profile is similar to the profile observed at Site 696 which suggests similar rates of sulfate reduction. For a detailed comparison however, sedimentation rates will have to be considered. The consistent values below 130 mbsf indicate that most of the organic matter available to microorganisms is oxidized above this depth. This is consistent with the low and stable methane readings (see "Organic Geochemistry" section, this chapter).

Phosphate and Ammonia

The concentration profile for orthophosphate is presented in Figure 27E. The profile exhibits a broad maximum of 10–12 μmol/L between 80 and 160 mbsf above and below which values of 7–8 μmol/L are observed. The spurious reading of 39 μmol/L in the upper sample (Section 113-697A-1H-4) is probably caused by contamination (since the ammonia value does not indicate extensive mineralization). The level of phosphate is generally higher than observed at any other Leg 113 site. This is caused partly by the higher rate of bacterial activity and partly by the shallower position of the redox boundary (phosphate is desorbed from ferric oxide/oxyhydroxide surfaces as these are reduced upon burial; Stumm and Leckie, 1970).

The concentration of ammonia (Fig. 27F) increases from 0.1 mmol/L near the surface (Section 113-697A-1H-4) to a maximum of 1.1 mmol/L at 132.75 mbsf. The maximum coincides with the alkalinity maximum. The slowly decreasing ammonia concentrations with increasing depth below 150 mbsf indicate

Table 8. Summary of shipboard interstitial water data.

Core, section interval (cm)	Depth (mbsf)	Vol (mL)	pH	Alk. (meq/L)	Sal. (g/kg)	Mg (mmol/L)	Ca (mmol/L)	Cl (mmol/L)	SO_4 (mmol/L)	PO_4 (μmol/L)	K (mmol/L)	NH_4 (mmol/L)	SiO_2 (μmol/L)	Mg/Ca
113-697A-														
1H-4, 145–150	5.95	50	7.85	4.89	34.8	51.68	10.48	555.0	28.0	39.6	10.2	0.10	880	4.93
1H-1, 145–150	19.45	50	7.93	9.48	34.6	49.69	11.38	560.9	23.1	8.2	10.0	0.44	389	4.37
3H-4, 120–125	42.80	35	7.80	12.00	33.2	48.01	11.83	557.5	19.9	9.0	8.8	0.56	663	4.06
4H-4, 115–125	52.45	65	7.82	14.56	34.4	47.45	12.34	567.0	16.8	11.8	9.8	0.71	899	3.84
5H-3, 115–125	60.65	50	8.99	5.62	34.6	47.60	10.31	552.0	26.5	8.6	14.8	0.38	162	4.62
6H-2, 115–125	68.85		7.94	16.64	34.8	45.17	12.66	567.3	13.1	8.3	9.2	0.87	761	3.57
7H-2, 140–150	78.90	40	7.89	16.11	34.6	44.48	12.90	561.0	13.1	10.0	7.9	0.82	884	3.45
8H-3, 140–150	90.10	50	8.10	17.53	34.7	43.15	13.42	566.5	10.3	11.7	8.3	1.07	926	3.22
9H-3, 115–125	99.55	45	8.06	17.35	34.5	42.86	13.43	565.0	10.3	10.3	7.4	1.03	909	3.19
13X-3, 115–125	132.75	65	7.78	18.35	35.0	40.25	14.01	566.0	6.5	10.2	5.4	1.10	1055	2.87
16X-4, 115–125	163.15		7.74	17.74	34.8	39.35	14.48	570.0	6.2	11.9	4.8	1.00	1129	2.71
19X-3, 115–125	190.75	45	7.84	14.00	32.4	38.29	14.76	568.5	5.3	9.3	5.2	0.92	1117	2.59
22X-2, 115–125	218.15	60	7.99	13.77	34.2	35.99	14.87	569.0	5.0	8.7	5.8	1.11	1021	2.42
26X-2, 115–125	256.85	35	7.89	11.08	34.8	35.12	16.27	556.5	5.9	7.4	4.3	0.87	1020	2.16
29X-2, 115–125	285.95	40	7.93	11.57	34.6	35.71	16.21	571.5	4.7	7.7	2.8	0.83	1040	2.20
31X-2, 140–150	305.50	35	8.27	10.07	34.8	32.44	17.89	566.5	7.0	6.9	2.9	1.07	968	1.81

that the rates of the reactions removing ammonia (mainly adsorption and ion exchange processes, Berner, 1974) are low, i.e., there is very low bacterial generation in this interval. Ammonia level is high compared with other Leg 113 sites.

Calcium and Magnesium

Calcium and magnesium data are presented in Figures 27G and 27H, respectively. The concentration of calcium increases from close to seawater value (10.48 mmol/L) at 5.95 mbsf (Section 113-697A-1H-4) to 17.89 mmol/L in the deepest sample (Section 113-697B-31X-2). There is a strong correlation between calcium and magnesium ($n = 16$, $r = -.97$; Fig. 27I), but, magnesium decreases 2.6 times faster than calcium increases. Comparing the alkalinity and calcium profiles (Figs. 27C and 27G, respectively) suggests that in the lower parts the alkalinity is controlled by the concentration of calcium.

The concentration of magnesium increases from 51.68 mmol/L at 5.95 mbsf (Section 113-697A-1H-4) to 32.44 mmol/L at 305.5 mbsf (Section 113-697B-31X-2).

Potassium

The concentration profile for potassium is shown in Figure 27J. The concentration of potassium decreases linearly from 10.2 mmol/L in the shallower sample (Section 113-697A-1H-4) to 2.9 mmol/L in the deepest sample (Section 113-697B-31X-2). This is a more extensive depletion than observed at other Leg 113 sites. It is generally assumed (MacKenzie and Garrels, 1966; Manheim and Sayles, 1974) that potassium is removed from pore water by reversed weathering processes. Altered layers of volcanic glass are abundant at Site 697. The high value (14.8 mmol/L) at 60.65 mbsf (Section 113-697B-5H-3) shows that the seawater used for circulation during drilling has been contaminated, probably by drilling mud remaining in the system.

Dissolved Silica

The concentration of dissolved silica (Fig. 27K) varies between 162 and 1129 μmol/L (Sections 113-697B-5H and 113-697B-16X, respectively). The lower value is caused by dilution by seawater. For two replicate analyses the average difference amounts to 1.5%, thus the scatter observed in Figure 27K is not caused by random errors. It is not clear what causes the high silica level in the sample at 5.95 mbsf (Section 113-697A-1H-4). Since this sample is contaminated by phosphate, the same interpretation is made for silica. As at the other Leg 113 sites the concentration of silica falls between values predicted (with thermodynamic data provided by Stumm and Morgan, 1981) for saturation with respect to quartz and amorphous silica.

ORGANIC GEOCHEMISTRY

Light Hydrocarbons

Modest levels of methane were detected in the first sample, 5.95 mbsf, and persisted throughout the penetrated interval. Concentrations ranged from 21.2 to 117.8 μL of gas per liter of sediment, showing a steady increase to a maximum at 78.9 mbsf, and then declining with increasing depth, as shown in Figure 28. Data are given in Table 9. Although it is possible that the methane is biogenic, methane/ethane ratios are lower than would be expected, ranging from 8.8 to 107.1. Low ratios of methane to ethane have characterized the Cenozoic section at all locations in the Weddell Sea. It appears that in this instance, a modest increment of biogenic methane might have been added to the low-level methane-ethane mixture normally present. No hazard to drilling was evident.

The source of methane in this section is unknown, whether biogenic or thermogenic, although the question could probably be resolved by carbon isotopic measurement. At Sites 695 and 696 sulfate is reduced to very low levels (1–3 mmol/L) at those horizons where methane generation is prolific. At Site 697 sulfate decreases almost exponentially with depth, but only to 5 mmol/L at 285 mbsf. Sulfate concentrations are approximately 10 mmol/L at 70–100 mbsf, the depth region of the methane maximum and thus it is improbable that the methane is being generated at present. An alternative hypothesis would invoke a brief interlude of anoxia sometime during the deposition of the sediments at 50–100 mbsf (lower Pleistocene–upper Pliocene). A methane spike of this age might have subsequently diffused away from its source. However, the interstitial water chemistry no longer reflects such an event, nor do the analyzed kerogens.

Rock-Eval Analyses of Kerogens

Data are presented in Table 10, also in Figures 29 and 30. The figures indicate, by means of trend lines (Herbin et al., 1984), conventional interpretations of the analytical data. A prima facie interpretation of Figure 29 suggests that the Pliocene of Site 697 contains moderately mature terrestrial kerogens of Type III. Figure 30, however, shows that many are of low maturity, having maximum pyrolysis temperatures below 430°C, the equivalent of a vitrinite reflectance of 0.5%. A probable cause of these apparently conflicting interpretations is illustrated in Figure 31, representing earlier DSDP Site 535 (Herbin et al., 1984) The trend of the data in Figure 31 represents progressive oxidation of planktonic kerogen, ultimately yielding material with Type III pyrolysis characteristics. It is suspected that similar oxidized planktonic kerogens are present at Site 697. Confir-

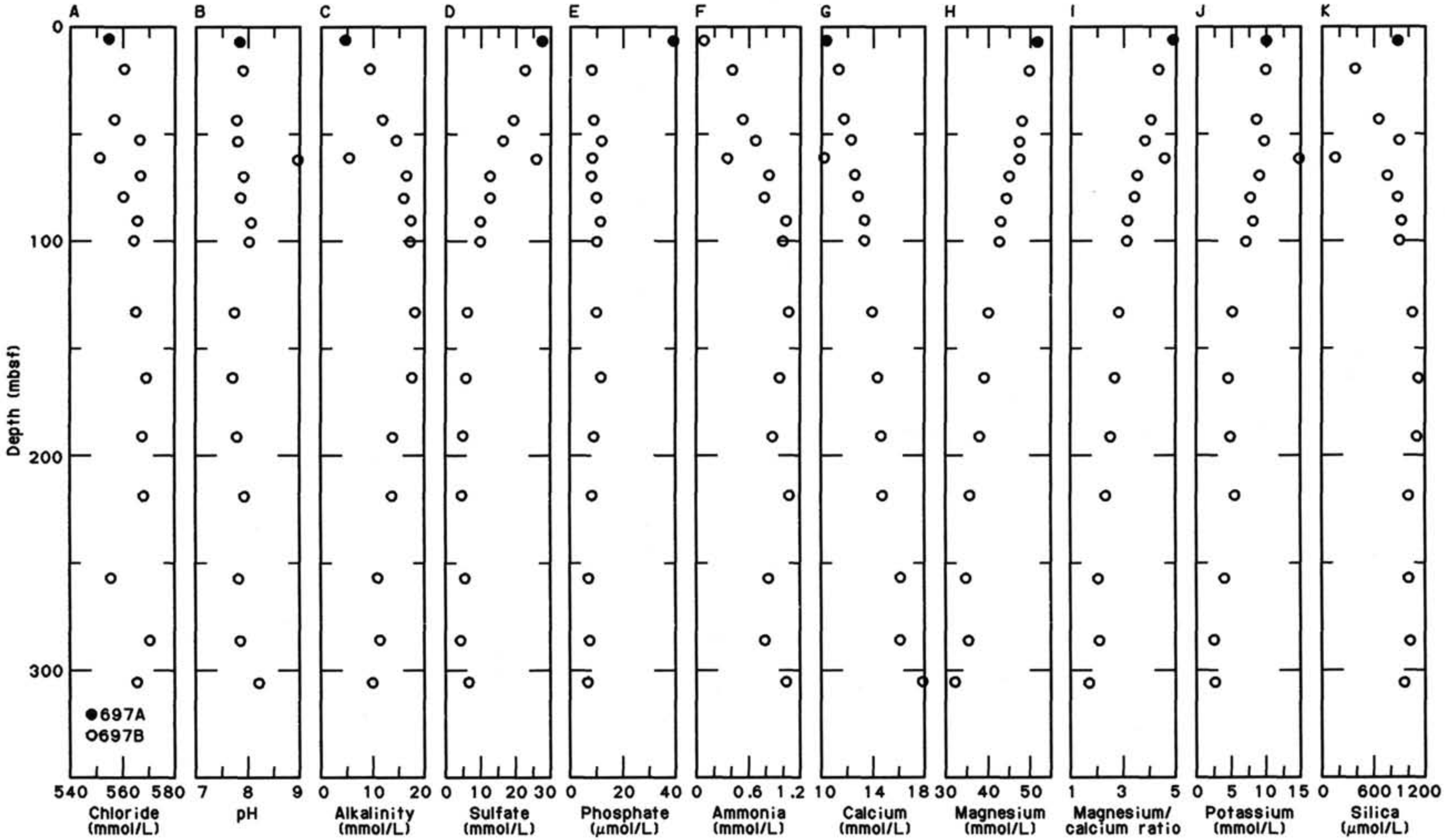

Figure 27. Concentrations vs. depth for Holes 697A and 697B. A. Chloride. B. pH. C. Alkalinity. D. Sulfate. E. Phosphate. F. Ammonia. G. Calcium. H. Magnesium. I. Magnesium/calcium ratio. J. Potassium. K. Silica. Data given in Table 8.

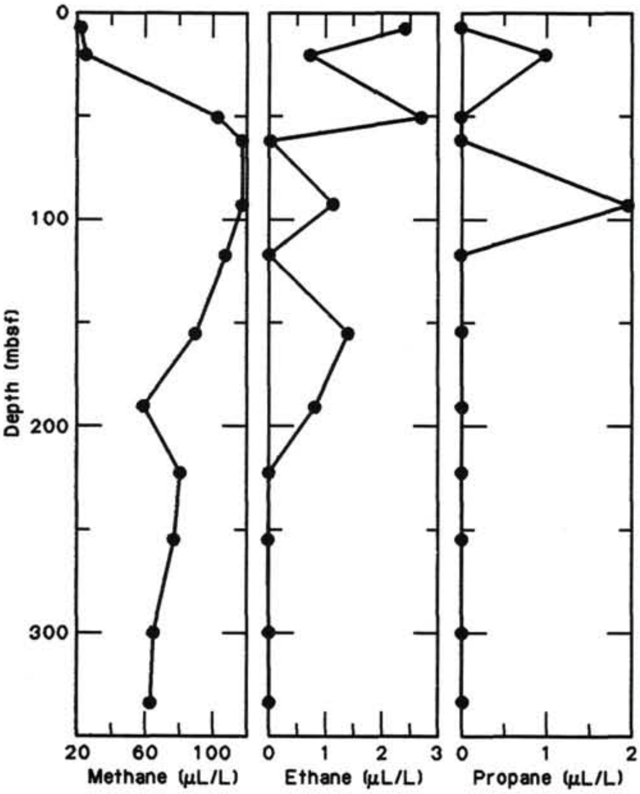

Figure 28. Light hydrocarbon data, Site 697. Data given in Table 9.

mation of this hypothesis will have to await further analyses. Recycled, mature kerogens of the type which dominated the section at Site 696 are present. The proportion of oxidized, first cycle kerogens approximately equals that of mature recycled kerogens, based on the limited number of samples analyzed.

DOWNHOLE MEASUREMENTS

No Downhole Measurements section was done for Site 697.

SUMMARY AND CONCLUSIONS

Site 697 was the deepest site of a three-site depth transect of the circum-Antarctic water masses on the northern margin of the Weddell Gyre. It lies in Jane Basin, at 61°48.63'S, 40° 17.74'W, at 3480 m water depth.

Jane Basin is a back-arc basin formed 25 to 30 Ma ago when Jane Bank, then an island arc actively subducting South American oceanic lithosphere, separated from the South Orkney microcontinent (SOM). Jane Basin sedimentation thus extends back to the upper Oligocene, but a prominent reflector at 550 ms (twt) at Site 697 separates a lower, probably turbiditic and volcaniclastic sequence of likely early Miocene age and older, from a mainly hemipelagic upper sequence. At present, Antarctic Bottom Water flows northward through Jane Basin, and the sediments should contain a record of bottom-water evolution. At Site 697 we planned, in the time remaining of Leg 113, to sample as much as possible of the upper sequence, which promised a high-resolution record of bottom-water production, circulation, and sediment transport, uncomplicated by terrigenous or volcaniclastic turbidites.

Two holes were drilled at Site 697 in 4 days, 2 hr, and 30 min from 3 to 7 March 1987. At Hole 697A we penetrated 20.9 mbsf and recovered 26.60 m (130%) in three APC cores. At Hole 697B we washed 18.0 m, then cored to 322.9 mbsf, recovering 188.27 m (62%) in 11 APC and 21 XCB cores. Drilling disturbance was generally minor, and severe in only a few cores. Hole 697A was abandoned when the APC corer could not be retracted, and Hole 697B when time ran out.

The sedimentary sequence at Site 697 is mainly of hemipelagic origin, with a minor siliceous biogenic component and numerous thin, altered volcanic ash layers. Ice-rafted detritus (IRD) is abundant near the base of the sequence only. Two lithologic units are recognized, the first divided into three subunits.

Unit I: 0–293.0 mbsf, includes silty and clayey mud, diatom-bearing silty and clayey mud, clay, and diatom clayey mud, and is Pliocene to Quaternary. Subunit IA, from 0 to 15.5 mbsf, is upper Quaternary silty mud and diatom-bearing silty mud. The diatom content fluctuates over a 2-m cycle. Subunit IB, from 15.5 to 85.7 mbsf, is upper Pliocene to Pleistocene clayey mud and clay with diatoms rare to absent but for one core. Subunit IC, from 85.7 to 293.0 mbsf, is mainly diatom-bearing clayey mud but ranges between clayey mud and diatom clayey mud. Diatoms are present in thin laminae and disseminated, and three thin turbidites occur near 161 mbsf. At the base, an ungraded, burrowed silt with dropstones may reflect an episode of stronger bottom currents.

Unit II: 293.0–322.9 mbsf, is lower Pliocene silty and clayey mud. It is coarser-grained than Unit I, with abundant IRD and very rare diatoms, and one possible thin silt turbidite.

Volcanic material occurs as dark gray and green fine-grained ash laminae altered to clay, as disseminated glass and in a few thin beds of coarse vitric ash. Dropstones are mostly sedimen-

Table 9. Headspace analyses of light hydrocarbons, Site 697.

Core, section interval (cm)	Depth (mbsf)	Methane	Ethane	Propane	n-C_4	n-C_5	n-C_6	Methane/ethane
		Microliters (gas)/liter (sediment)						
113-697A-								
1H-4, 145–150	5.95	21.2	2.4	0.9	—	—	—	8.8
3H-4, 125–129	17.05	24.0	0.7	1.6	0.2	—	0.7	34.3
113-697B-								
3H-4, 120–125	42.80	103.1	2.7	0.9	3.7	—	—	38.2
4H-4, 115–120	52.45	117.5	—	—	—	59.3	—	
7H-2, 140–150	78.90	117.8	1.1	2.9	1.5	—	28.4	107.1
9H-3, 140–150	99.80	108.1	—	—	—	—	12.7	—
13X-3, 115–125	132.75	90.1	1.4	—	—	—	35.7	64.4
16X-4, 115–120	163.15	58.2	0.8	—	1.1	—	36.9	72.8
19X-3, 115–120	190.75	80.9	—	—	2.1	—	15.9	—
22X-2, 115–120	218.15	77.0	—	—	1.1	—	19.4	—
26X-2, 115–120	256.85	64.6	—	—	—	—	—	—
29X-2, 125–129	287.55	62.8	—	—	—	—	15.4	—

Table 10. Rock-Eval data, Site 697.

Core, section interval (cm)	Depth (mbsf)	S_1 mg(HC)/g(rock)	S_2 mg(HC)/g(rock)	S_3 mg(CO_2)/ g(rock)	TOC (%)	HI mg(HC)/ g(C)	OI mg(CO_2)/ g(C)	T_{max} (°C)
113-697A-								
1H-4, 145-150	5.95	0.04	0.50	0.53	0.34	147	155	474
3H-4, 125-129	17.05	0.03	0.36	0.54	0.38	94	142	552
113-697B-								
1H-1, 145-150	19.45	0.03	0.56	0.53	0.38	147	139	554
3H-4, 120-125	42.80	0.05	0.39	0.64	0.43	90	148	555
4H-4, 115-125	52.45	0.03	0.23	0.51	0.37	62	137	511
6H-2, 115-125	68.85	0.03	0.15	0.64	0.41	36	156	463
7H-2, 140-150	78.90	0.05	0.09	1.15	0.40	22	287	411
9H-3, 115-125	99.55	0.06	0.29	0.45	0.33	87	136	390
13X-3, 115-125	132.75	0.05	0.42	0.27	0.42	100	64	432
16X-4, 115-125	163.15	0.03	0.29	0.28	0.32	90	87	398
19X-3, 115-125	190.75	0.03	0.33	0.25	0.43	76	58	369
22X-2, 115-125	218.15	0.06	0.41	0.40	0.29	141	137	427
26X-2, 115-125	256.85	0.05	0.48	0.13	0.30	160	43	530
29X-2, 115-125	287.55	0.00	0.26	0.32	0.37	70	86	400

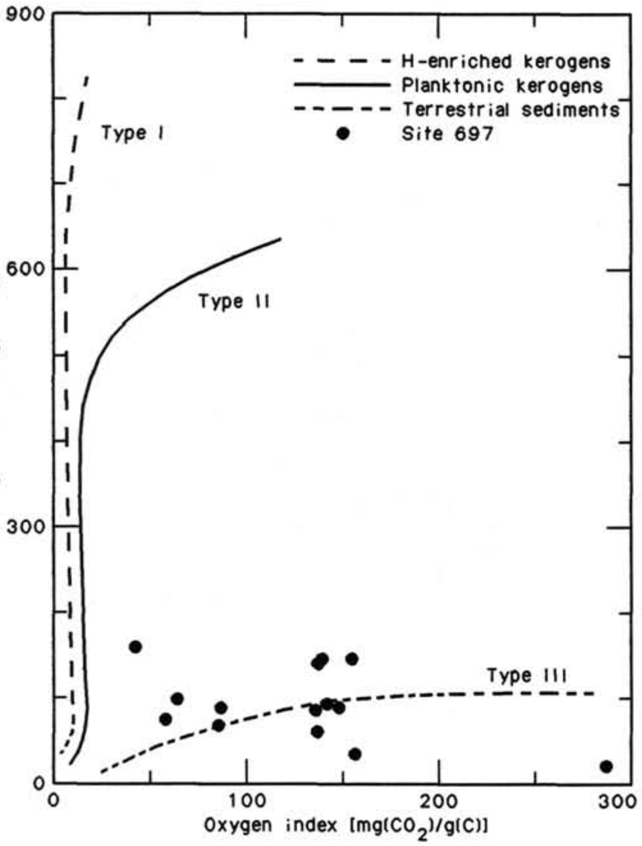

Figure 29. Rock-Eval data, Site 697: hydrogen index vs. oxygen index. Data given in Table 10.

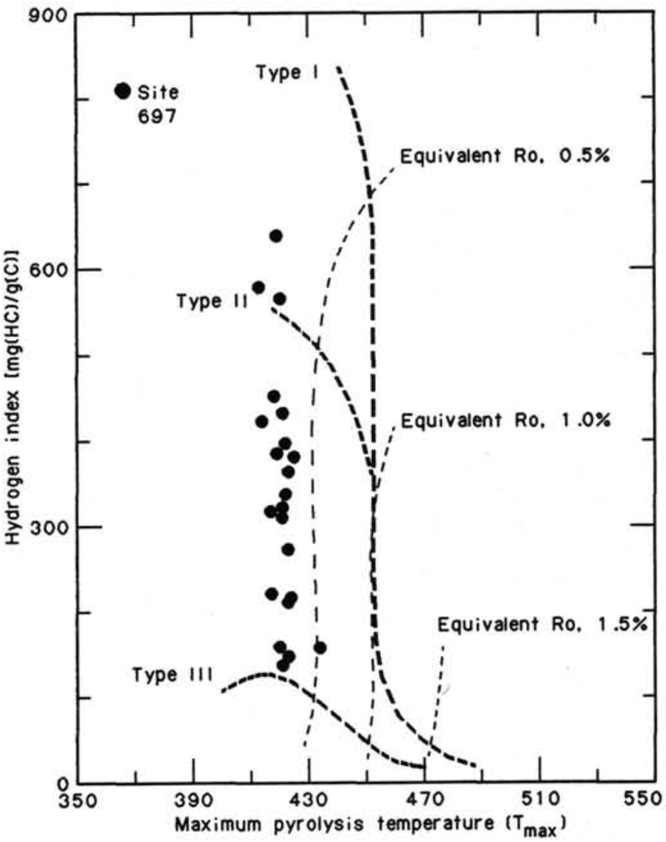

Figure 30. Hydrogen index vs. maximum pyrolysis temperature (T_{max}), and maturity levels of kerogens from Site 697. Ro = reflectance (isoreflectance curve).

tary, rounded or subrounded, and with a diameter of less than 2 cm. Bioturbation is minor. Authigenic minerals comprise fine-grained carbonates near 200 mbsf, common pyrite below 90 mbsf, and an unidentified mineral (?zeolite) occurring irregularly between 20 and 90 mbsf.

Illite is the dominant and most consistently abundant clay mineral, as at the other sites in the South Orkney transect (Sites 695 and 696). Chlorite is common to abundant, but less abundant than in coeval sediments at Site 696 or (mostly) 695. Kaolinite is rare to common, as at the other sites, and smectite quite variable, from absent to very abundant, probably reflecting fluctuations in the amount of altered fine-grained volcanic ash.

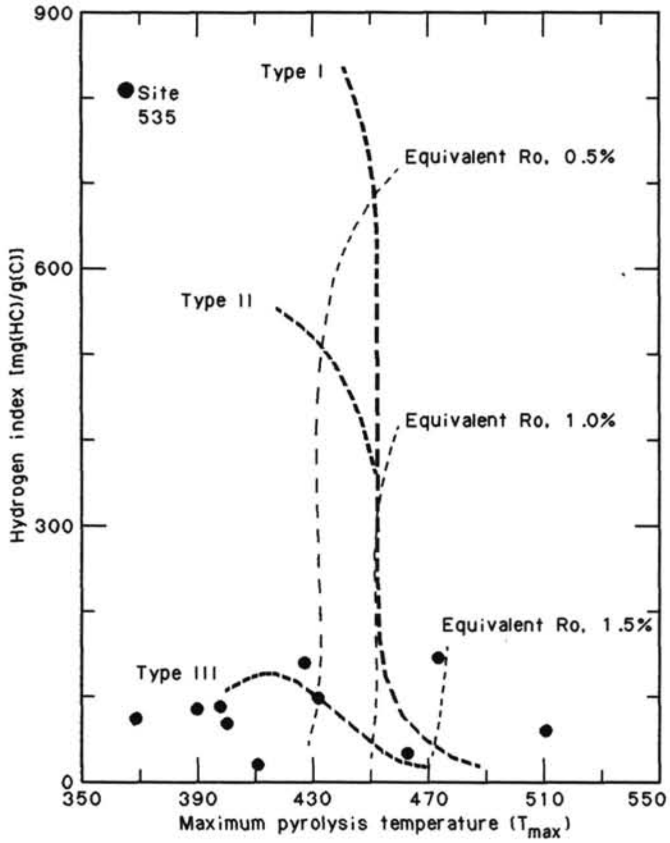

Figure 31. Rock-Eval data, Site 535 in the Florida Straits, showing continuous variability in degree of oxidation of Cretaceous planktonic kerogens (from Herbin et al., 1984). Ro = vitrinite reflectance (isoreflectance curve).

The biogenic component is completely siliceous, with diatoms dominant, minor radiolarians, and rare silicoflagellates and agglutinated benthic foraminifers. Diatoms fluctuate widely in abundance and preservation, from a few thin, pristine ooze interbeds to more generally rare to few, poorly to moderately preserved: diatoms are more abundant and better preserved (the thin oozes apart) in the Pliocene of Subunit IC than above or below. Radiolarians are rare in Pleistocene sediments but common and generally moderately to poorly preserved in the Pliocene. Silicoflagellates are sparse or absent above 250 mbsf, more common below. In general, siliceous abundance and preservation patterns follow those of other sites, but at lower levels. The three sets of siliceous biostratigraphic data are in general agreement.

Magnetostratigraphic zonation is reasonably precise; overprinting appears limited and correspondence to the geomagnetic polarity time scale is good, indicating high and smoothly-varying sedimentation rates. Rates range from 135–150 m/m.y. for the Gilbert to middle Gauss to 40 m/m.y. from then through the upper Brunhes. Quaternary rates are the highest of all Leg 113 sites, and the short-duration Blake event is provisionally identified near 4 mbsf, occurring as a doublet. The expanded section at Site 697 provides a high-fidelity magnetostratigraphic record with opportunities for calibration with siliceous biostratigraphic data and for high-resolution paleoceanographic studies. Whole-core susceptibility measurements show a short-wavelength variability which may reflect orbitally-induced changes in sediment composition.

A more detailed study of pore-water chemistry than at other sites (except 695) showed a steep alkalinity increase and sulfate decrease in the uppermost 70 m, indicating vigorous bacterial oxidation of organic matter by sulfate reduction. Modest levels of methane, peaking at about 80 mbsf, are probably biogenic, a reflection of the high rates of sedimentation and of biosiliceous productivity in the surface waters around the South Orkney microcontinent, particularly during the Pliocene.

The increase in abundance of coarse-grained, ice-rafted detritus towards the base of Hole 697B reflects partly the lesser dilution by hemipelagic and siliceous biogenic sediment in the period before the late early Pliocene. The near-absence of turbidites confirms the original interpretation of the reflection profiles and the unimportance of Jane Bank and the SOM as direct sources of sediment since the early Pliocene. There is an abundance of potential sources of air-fall volcanic ash including, to the west, Deception Island in Bransfield Strait, James Ross and other islands on the eastern margin of the Antarctic Peninsula, and in the east the South Sandwich island arc. During the Pliocene and Pleistocene these sources changed their geographic location relative to the South Orkney microcontinent (Bransfield Strait probably did not exist at 5 Ma, and the South Sandwich arc was probably only half as far away) but Sites 695, 696, and 697 are sufficiently close to each other that ash beds are a potential means of stratigraphic correlation between them, where core recovery permits. This could be particularly valuable for high-resolution studies.

Quaternary sedimentation rates at Site 697 are at least five times as high as at any other Leg 113 site. Since these high rates are mainly for fine-grained hemipelagic rather than pelagic biogenic or ice-rafted sediments, they are a reflection of the amount of sediment being transported in a nepheloid layer at the northern edge of the Weddell Gyre. This origin is confirmed by the uniformity of the clay mineral content (volcanogenic smectite apart), compared with adjacent, shallow sites. From the scour at the western margin of Jane Basin, it seems clear that the uppermost 500 m of sediment in the basin has been laid down under bottom-current control.

The main control over long-term sedimentation rates in this lithology will probably have been the supply of sediment to the nepheloid layer. In this respect, it is difficult to reconcile the high Quaternary rates of deposition at Site 697 with the results of drilling at the other sites. The Jane Basin hemipelagics could be the suspended fines of turbidites from West Antarctica or the Antarctic Peninsula, except that Site 694, characterized as a representative destination of such turbidites during the earliest Pliocene, is without major Quaternary turbidites. Is East Antarctica a potential source? Hemipelagic sedimentation from East Antarctica at Site 693 decreased markedly in the late Pliocene, which we explained in terms of a more intense Quaternary glaciation with an ice-cap grounded to the shelf edge all or most of the time. The SOM itself is equally unpromising, either as a direct turbidite source (Site 697) or as having an enhanced Quaternary sediment transport across the shelf to the southern margin (Sites 695 and 696). One possibility is that the source is the winnowed fine fraction of West Antarctic and Antarctic Peninsula turbidites, but that the distribution of unstable sediment at the shelf edge has changed with the changing state of glaciation. For example, it may be that turbidites are now more numerous but that individual turbidites are smaller and do not reach the more distal regions around Site 694 following the major earliest Pliocene erosional event recorded at Site 694.

The absence of calcareous microfossils, including a layer containing abundant *Neogloboquadrina pachyderma* (see Sites 689, 690, 692, 693, 695, 696) in the Quaternary sediments at Site 697 demonstrates that, however deep the carbonate compensation depth became in circum-Antarctic waters (it reached below 3000 m on Maud Rise and 2400 m on the Dronning Maud Land margin), it did not extend to 3500 m in Jane Basin. This calcareous layer, which in most places will be within reach of piston corers, provides a potentially useful paleoceanographic indicator within the Antarctic water mass.

REFERENCES

Barker, P. F., Barber, P. L., and King, E. C., 1984. An early Miocene ridge crest-trench collision on the South Scotia Ridge near 36°W. *Tectonophysics*, 102:315–322.

Barron, J. A., 1985. Miocene to Holocene planktic doatoms. *In* Bolli, H. M., Saunders, J. B., Perch-Nielsen, K. (Eds.) *Plankton Stratigraphy*: New York (Cambridge Univ. Press), 763–810.

Berggren, W. A., Kent, D. V., Flynn, J. J., and VanCouvering, J. A., 1985. Cenozoic geochronology, *Geol. Soc. Am. Bull.*, 96:1407–1418.

Berner, R. A., 1974. Kinetic models for the early diagenesis of nitrogen, sulfur, phosphorus, and silicon in anoxic marine sediments. *In* Goldberg, E.D. (Ed.), *The Sea* (Vol. 5): New York (Wiley), 5:527–568.

Carlson, R. L., Gangi, A. F., and Snow, K.R., 1986. Empirical reflection travel time versus depth and velocity versus depth functions for the deep sea sediment column. *J. Geophys Res.*, 91:8249–8266.

Ciesielski, P. F., 1975. Biostratigraphy and paleoecology of Neogene and Oligocene silicoflagellates from cores recovered during Antarctic Leg 28, Deep Sea Drilling Project. *In* Hayes, D. E., Frakes, L. A., et al., *Init. Repts. DSDP*, 28: Washington (U.S. Govt. Printing Office), 625–691.

_______, 1983. The Neogene diatom biostratigraphy DSDP Leg 71, subantarctic sediments. *In* Ludwig, W. J., Krasheninnikov, V. A., et al., *Init. Repts. DSDP*, 71: Washington (U.S. Govt. Printing Office), 635–665.

Creer, K. M., Readman, P. W., and Jacobs, A. M., 1980. Palaeomagnetic and palaeontological dating of a section at Gioia Tauro, Italy: identification of the Blake event. *Earth Planet. Sci. Lett.* 50:289–300.

Echols, R. J., 1971. Distribution of Foraminifera in sediments of the Scotia Sea area, Antarctic waters. *Antarct. Res. Ser.*, Am. Geophys. Union, 15:93–168.

Fenner, J., 1984. Eocene-Oligocene planktic diatom stratigraphy in the low latitudes and the high southern latitudes. *Micropaleontology*, 30:319–342.

Foster, T. D., and Middleton, J. H., 1979. Variability in the bottom water of the Weddell Sea. *Deep-Sea Res.*, 26A:743–762.

_______, 1980. Bottom water formation in the western Weddell Sea. *Deep-Sea Res.*, 27A:367–381.

Gardner, J. V., Nelson, C. S., and Baker, P. A., 1985. Distribution and character of pale green laminae in sediment from Lord Howe Rise: a probable late Neogene and Quaternary tephrostratigraphic record. *In* Kennett, J. P., Von der Borch, C., et al., *Init. Repts. DSDP*, 90: Washington (U.S. Govt. Printing Office), 1145–1159.

Goldhaber, M. B., and Kaplan, I. R., 1974. The sulfur cycle. *In* Goldberg, E. D. (Ed.), *The Sea* (Vol. 5): New York (John Wiley and Sons), 569–655.

Gombos, A. M., 1977. Paleogene and Neogene diatoms from the Falkland Plateau and Malvinas Outer Basin: Leg 36, Deep Sea Drilling Project. *In* Barker, P. F., Dalziel, I. W. D., et al., *Init. Repts. DSDP*, 36: Washington (U.S. Govt. Printing Office), 575–690.

Gombos, A., and Ciesielski, P. F., 1983. Late Eocene to early Miocene diatoms from the Southwest Atlantic Ocean. *In* Ludwig, W. J., Krasheninnikov, V. A., et al., *Init. Repts. DSDP*, 71: Washington (U.S. Govt. Printing Office), 583–634.

Grobe, H., 1986. Sedimentation processes on the Antarctic continental margin at Kapp Norvegia, during the late Pleistocene. *Geol. Rundschau*, 75:97–104.

Herbin, J. P., Deroo, G., and Roucaché, J., 1984. Organic Geochemistry of Lower Cretaceous sediments from Site 535, Leg 77, Florida Straits. *In* Buffler, R. T., Schlager, W., et al., *Init. Repts. DSDP*, 77: Washington (U.S. Govt. Printing Office), 459–475.

King, E. C., and Barker, P. F., 1988. The margins of the South Orkney Microcontinent. *J. Geol. Soc. (Lond.)*, 145:317–331.

Lawver, L. A., Della Vedova, B., and Von Herzen, R. P., 1986. Heat flow in Jane Basin, a small back-arc basin, Northern Weddell Sea. *Antarct. J. U.S.*, 19:87–88.

Ledbetter, M. T., and Ciesielski, P. F., 1982. Bottom-current erosion along a traverse in the south Atlantic sector of the southern ocean. *Mar. Geol.*, 46:329–341.

MacKenzie, F.T, and Garrels, R.M., 1966. Chemical mass balance between rivers and oceans. *Am. J. Sci.*, 264:507–525.

Manheim, F. T., and Sayles, F. L., 1974. Composition and origin of interstitial waters of marine sediments. *In* Goldberg, E. D. (Ed.), *The Sea* (Vol. 5): New York (Wiley), 527–568.

Pudsey, C. J., Barker, P. F., and Hamilton, N., in press. Weddell Sea abyssal sediments: a record of Antarctic Bottom Water flow. *Mar. Geol.*

Robert, C., and Maillot, H., 1983. Paleoenvironmental significance of clay mineralogical and geochemical data, Southwest Atlantic, DSDP Legs 36 and 71. *In* Ludwig, W. I., Krasheninnikov, V., et al., *Init. Repts. DSDP*, 71: Washington (U.S. Govt. Printing Office), 317–343.

Schrader, H. J., 1976. Cenozoic planktonic diatom biostratigraphy of the Southern Pacific Ocean. *In* Hollister, C. D., Craddock, C., et al., *Init. Repts. DSDP*, 35: Washington (U.S. Govt. Printing Office), 605–671.

Stumm, W., and Morgan, J. J., (Eds.), 1981. *Aquatic Chemistry* (2nd Ed.): New York (Wiley).

Stumm, W., and Leckie, Z. O., 1970. Phosphate exchange with sediments, its role in the productivity of surface waters. *Advances In Water Pollution Research* (Vol. 2): New York (Pergamon Press), III: 26/1–26/16.

Von Herzen, R. P., and Maxwell, A. E., 1959. The measurement of thermal conductivity of deep-sea sediments by a needle probe method. *J. Geophys. Res.*, 65:1535–1541.

Weaver, F. M., and Gombos, A. M., 1981. Southern high-latitude diatom biostratigraphy. *Soc. Econ. Paleontol. Mineral. Spec. Publ.*, 32:445–470.

Ms 113A/113

SITE 697 HOLE A CORE 1H CORED INTERVAL 3480.5-3489.4 mbsl; 0-8.9 mbsf

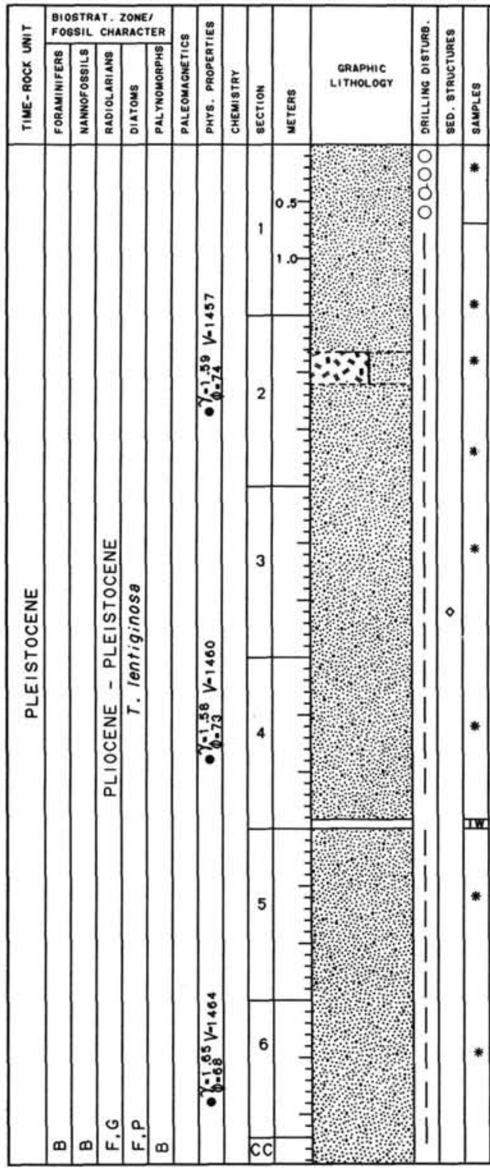

LITHOLOGIC DESCRIPTION

SILTY MUD

Major lithology: Silty mud with minor color changes from top to bottom of core. Section 1, 0-55 cm, light brownish gray (2.5Y 6/2); Section 1, 55-110 cm, light olive gray (5Y 6/1, 6/2); Section 1, 110 cm, to Section 3, 34 cm, gray (5Y 5/1); Section 3, 34-105 cm, greenish gray (5GY 5/1); Section 3, 105-150 cm, gray (5Y 5/1); Section 4, 0-150 cm, greenish gray (5BG 5/1); Section 5, 0-35 cm, greenish gray (5G 5/1); Section 5, 35-120 cm, bluish gray (5B 5/1); and Section 5, 120-CC, greenish gray (5G 5/1).

Minor lithologies: Altered vocanic ash, greenish gray (5Y 5/1), in Section 1, 54-55 cm. Glass-bearing silty mud, very dark grayish brown (2.5Y 3/2), interbedded with silty mud, greenish gray (5G 5/1), in Section 2, 32-60 cm.

Dropstone, rounded, metamorphic, 1.5 cm in diameter, in Section 3, 100 cm.

SMEAR SLIDE SUMMARY (%):

	1, 22 M	1, 140 D	2, 36 M	2, 125 D	3, 58 M	4, 60 D
TEXTURE:						
Sand	—	—	2	2	2	2
Silt	60	70	67	58	60	68
Clay	40	30	31	40	38	30
COMPOSITION:						
Quartz	35	38	15	30	6	40
Feldspar	—	1	2	—	1	—
Mica	4	2	2	6	—	4
Clay	40	30	31	40	—	30
Volcanic glass	5	11	20	10	83	12
Calcite/dolomite	—	—	Tr	—	—	—
Accessory minerals	4	7	3	2	3	—
Zeolites	—	1	—	—	—	1
Opaque minerals	12	4	17	5	1	6
Diatoms	—	6	10	6	6	6
Radiolarians	—	—	—	Tr	—	1
Sponge spicules	—	—	Tr	1	—	—

	D	D
TEXTURE:		
Silt	60	50
Clay	40	50
COMPOSITION:		
Quartz	25	30
Feldspar	2	1
Mica	4	6
Clay	40	50
Volcanic glass	12	5
Accessory minerals	8	4
Opaque minerals	6	4
Diatoms	3	Tr

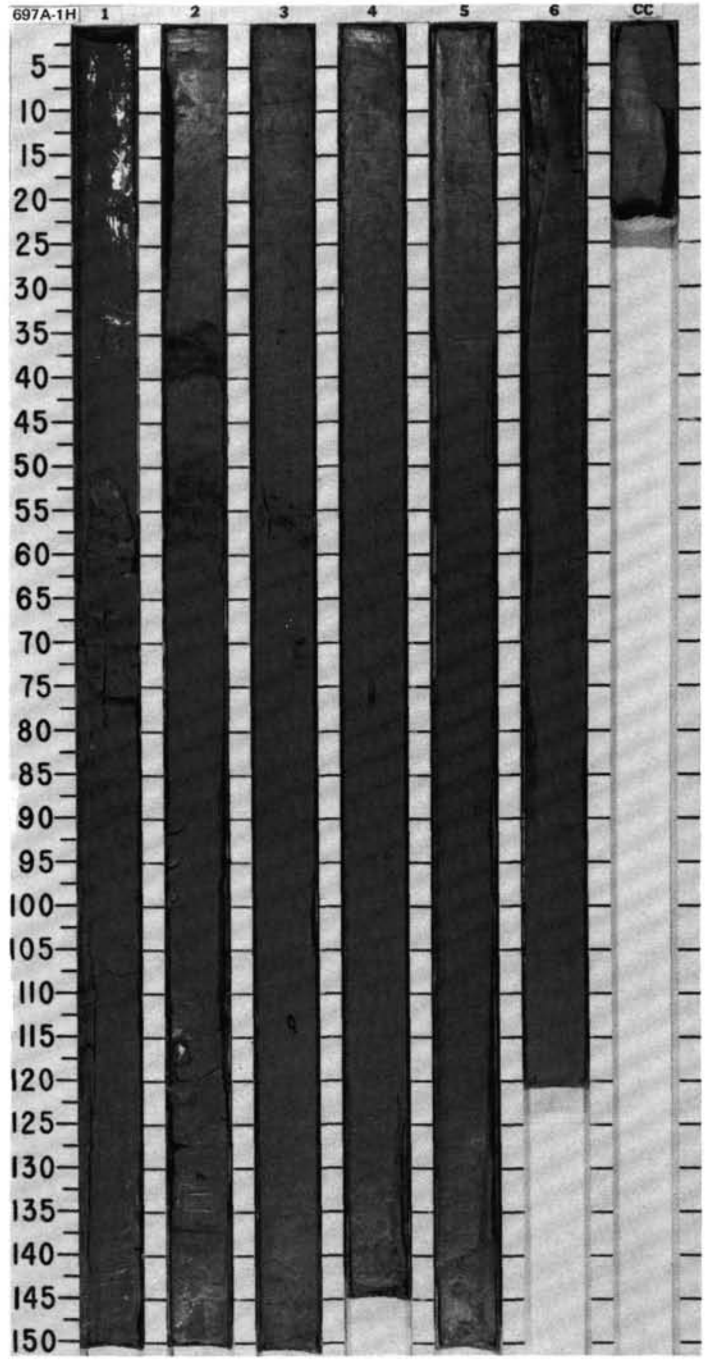

SITE 697 HOLE A CORE 2H CORED INTERVAL 3485.8-3495.4 mbsl; 5.3-14.9 mbsf

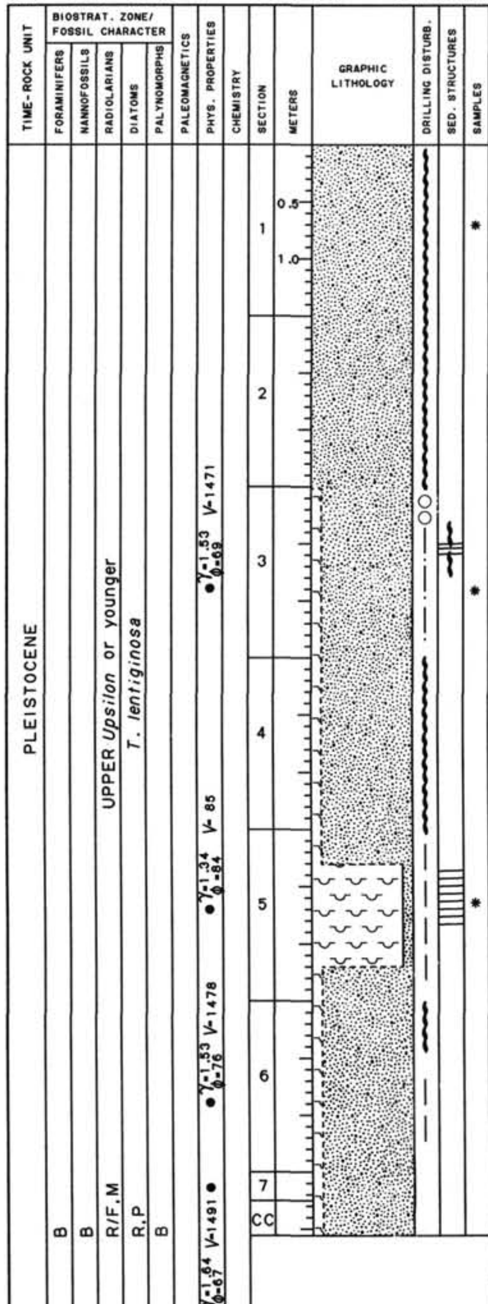

LITHOLOGIC DESCRIPTION

SILTY MUD and DIATOM-BEARING SILTY MUD

Major lithologies: Silty mud, greenish gray (5GY 5/1), very disturbed by drilling. Diatom-bearing silty mud in Section 3 and Section 5-CC, dark greenish gray (5G 4/1; 5GY 5/1, 5/2). Section 4, gray (5Y 5/1), contains layers of altered volcanic ash.

Minor lithology: Altered volcanic ash(?), thin layers, grayish green (5G 5/2) and greenish bluish (no Munsell Color Chart number) in Section 3, 51, 53, and 58 cm(?); greenish gray (5G 5/2) in Section 5, 33-35 cm; gray (N 4/0) in Section 5, 38 cm; grayish green (5G 5/2) in Section 6, 29, 31, 34, 37,70-71, and 107-108 cm; and gray (N 4/0) in Section 6, 109-129 cm. Diatom ooze in Section 5, 30-80 cm, greenish gray (5G5/1), contains lamination, sharp basal contacts. Predominantly formed by*Corethron*.

No dropstones.

SMEAR SLIDE SUMMARY (%):

	1, 40 D	3, 90 D	5, 65 M
TEXTURE:			
Silt	45	60	—
Clay	55	40	—
COMPOSITION:			
Quartz	18	30	—
Feldspar	2	4	—
Mica	Tr	3	—
Clay	55	40	8
Volcanic glass	8	15	—
Accessory minerals	7	4	—
Opaque minerals	4	2	2
Diatoms	6	12	90
Radiolarians	—	Tr	—

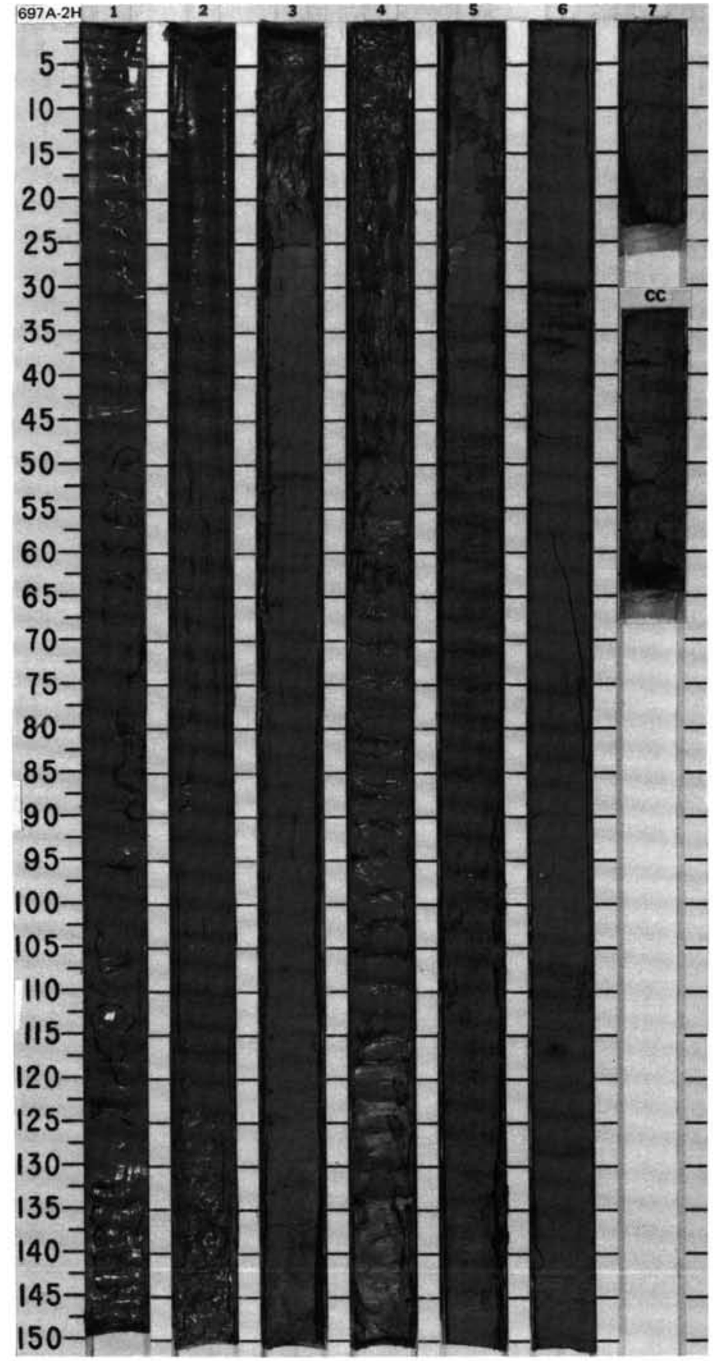

SITE 697 HOLE A CORE 3H CORED INTERVAL 3491.8-3501.4 mbsl; 11.3-20.9 mbsf

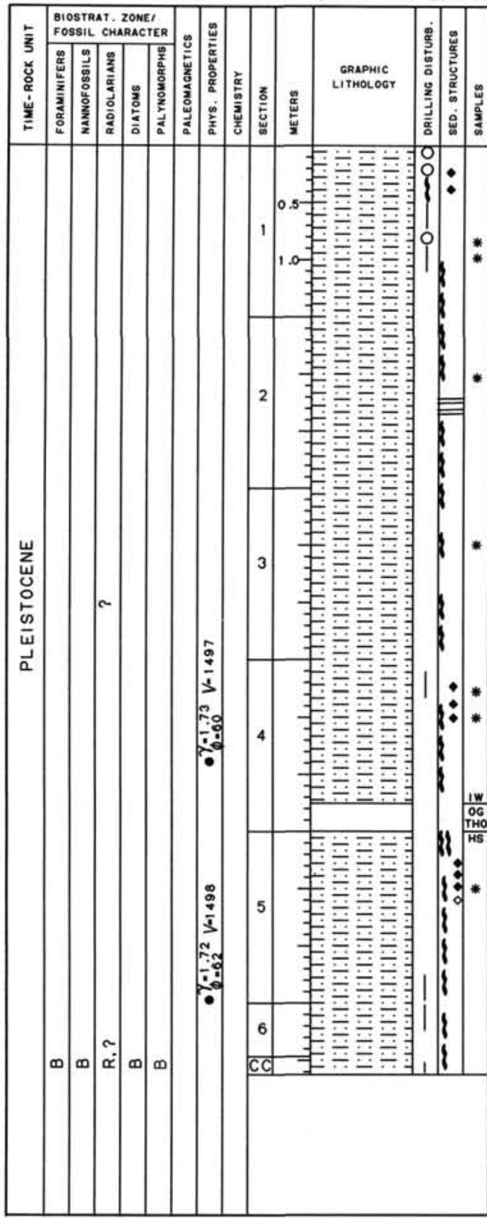

LITHOLOGIC DESCRIPTION

CLAYEY MUD

Major lithology: Clayey mud, dark gray (N 4/0) to dark greenish gray (5G 4/1, 5GY 4/1, 5BG 4/1); color changes are gradational and difficult to see. Laminated interval in Section 2, 68–83 cm, contains greenish gray (5GY 5/1), dark gray (N 4/0), dark greenish gray (5G 4/1, 5GY 4/1), and olive gray (5Y 4/1) laminae.

Minor lithologies: Diatom ooze, dark greenish gray (5GY 4/1), occurs as 2–3 cm clasts within soupy/very disturbed layer in Section 1, 0–45 cm. This resembles the diatom ooze (*Corethron*) layer in 113-697A-2H-5. Clay and clayey mud, dark greenish gray (5G 4/1), very dark gray (N 3/0), and dark gray N 4/0), occurs as laminae (continuous, burrowed, or disturbed during coring) in all sections, and forms about 2% of sedimentary sequence of at least 38 laminae. Silty mud, light gray (5Y 6/1), occurs as tiny (1–2 mm) clasts in Section 4, 23–52 cm, and Section 5, 22–49 cm.

Dropstone, subrounded mudstone, 0.6 cm long, in Section 5, 59 cm. Minor bioturbation.

SMEAR SLIDE SUMMARY (%):

	1, 84 M	1, 100 D	2, 50 D	3, 50 D	4, 27 M	4, 50 D	5, 50 D
TEXTURE:							
Sand	—	—	1	Tr	—	—	—
Silt	27	41	39	38	11	26	39
Clay	63	59	60	62	89	74	61
COMPOSITION:							
Quartz	12	18	14	14	6	14	24
Feldspar	—	1	Tr	1	1	1	2
Rock fragments	—	—	—	—	Tr	—	—
Mica	10	9	7	5	2	4	3
Clay	63	59	60	62	89	74	61
Volcanic glass	—	—	1	1	—	1	—
Accessory minerals:							
Heavy minerals	4	2	2	4	Tr	1	2
Amphibole	—	1	2	2	—	1	1
Opaque minerals	3	2	3	3	1	3	2
Glauconite	—	Tr	1	Tr	—	—	Tr
Diatoms	8	8	9	8	1	1	5
Radiolarians	Tr	Tr	Tr	Tr	—	Tr	Tr
Sponge spicules	Tr	Tr	1	Tr	—	—	—

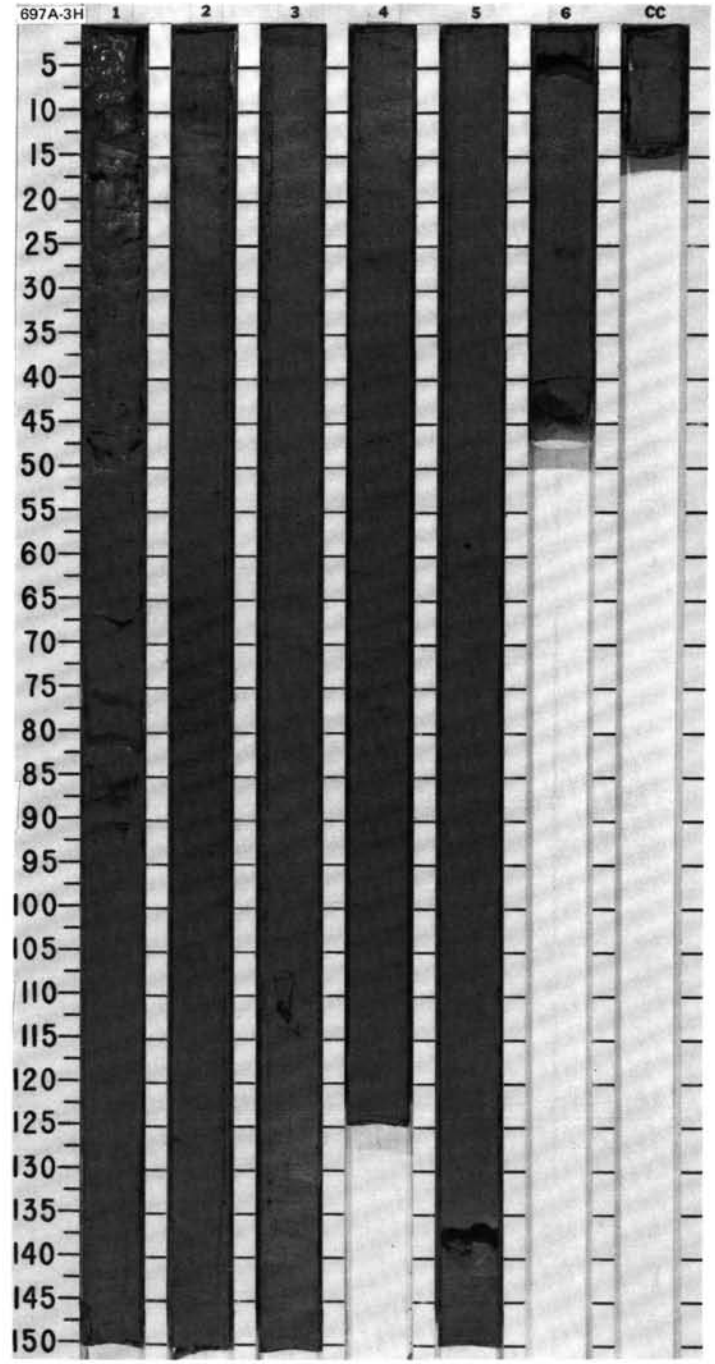

SITE 697 HOLE B CORE 1H CORED INTERVAL 3498.5-3508.0 mbsl; 18.0-27.5 mbsf

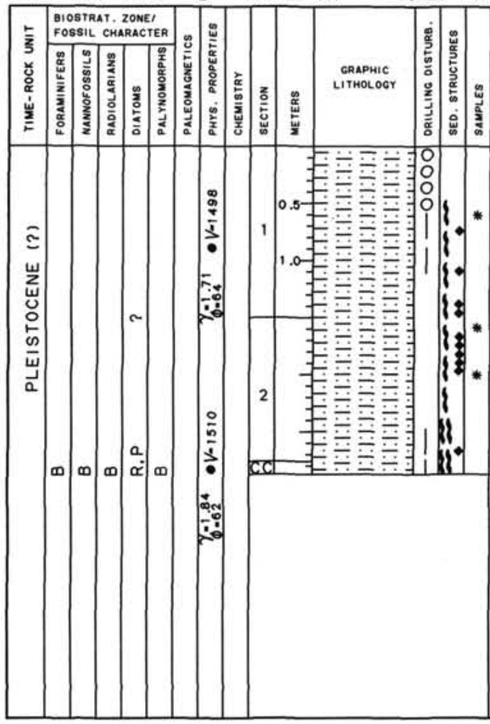

LITHOLOGIC DESCRIPTION

CLAYEY MUD

Major lithology: Clayey mud, dark gray (N 4/0) to dark greenish gray (5G 4/1, 5GY 4/1, 5BG 4/1); color changes subtle and gradational.

Minor lithologies: Clay, dark bluish gray (5B 4/1) or dark greenish gray (5BG 4/1), occurs as fuzzy laminae in Section 1, 63, 64, and 80 cm. Probably altered ash layers. Silt, gray (N 5/0), occurs as 1-2 mm clasts in both sections. particularly Section 2, 23-59 cm. Fecal pellets(?). Core contains 10-12% of a clay/fine silt-sized high relief mineral, round to rhombic, high relief and birefringence, Zeolite(?), dolomite(?). Silt clasts present throughout core.

Minor to moderate bioturbation.

SMEAR SLIDE SUMMARY (%):

	1, 60 D	2, 7 M	2, 50 D
TEXTURE:			
Silt	36	29	32
Clay	64	71	68
COMPOSITION:			
Quartz	25	18	23
Feldspar	2	2	2
Mica	—	1	1
Clay	52	59	58
Volcanic glass(?)	1	1	1
Accessory minerals:			
Glauconite	—	1	—
Zeolites(?)	12	12	10
Amphibole	2	1	1
Opaque minerals	3	2	2
Heavy minerals	1	3	2
Diatoms	2	Tr	Tr
Sponge spicules	Tr	—	—

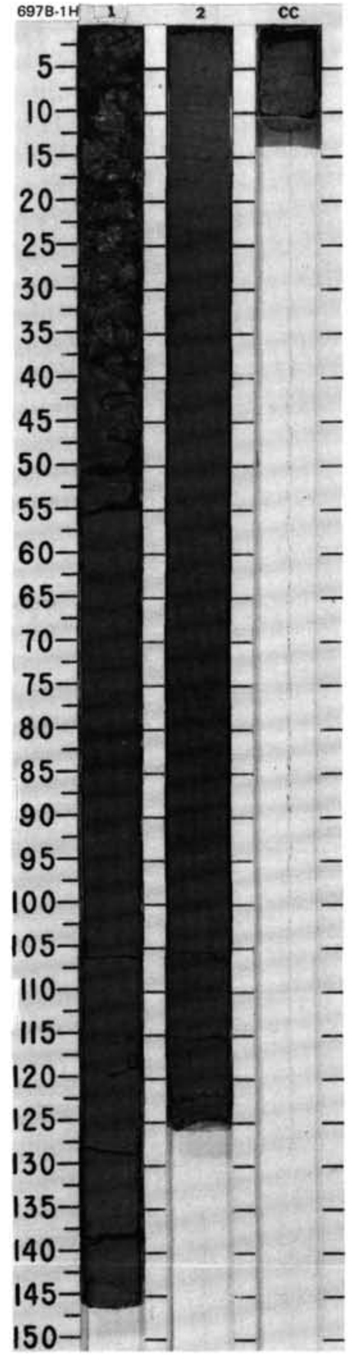

SITE 697 HOLE B CORE 2H CORED INTERVAL 3508.0-3517.6 mbsl; 27.5-37.1 mbsf

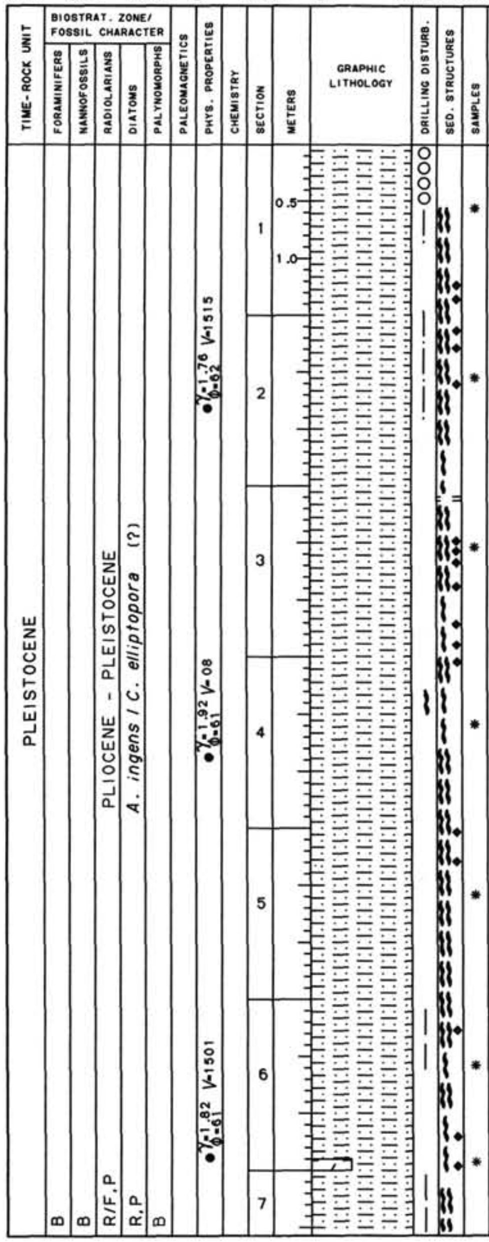

LITHOLOGIC DESCRIPTION

CLAYEY MUD

Major lithology: Clayey mud, mainly dark gray (N 4/0), shading to dark greenish gray (5G 4/1, 5GY 4/1) in Sections 1-3 and the base of Section 4. Cracks in Sections 3-7 attributed to coring disturbance during rough weather.

Minor lithologies: Clay, very dark gray (N 3/0) or dark greenish gray (5G 4/1), occurs as fuzzy laminae commonly 5 mm thick (many are disseminated by burrows), in Section 1, 63 cm; Section 2, 6, 20, 46, 62, 72, 135, and 137 cm; Section 3, 4, 5, 13, 36, 71, 96, and 135 cm; Section 4, 6, 50, 58, 60, 101, and 105 cm; and Section 6, 6, 10, 35, 47, 53, 66, 97, 116, and 134 cm. In Section 4 there is disseminated ash from 88-93 cm. Silt, gray (N 5/0), occurs as tiny (1 mm) clasts in all sections, concentrated in Section 2, 15-34 cm, and Section 3, 45-88 cm. Dolomite(?) silt, olive gray (5Y 5/3), occurs as rounded clasts 1-3 cm across, and in disturbed bed at the base of Section 6.

Moderate to minor bioturbation, includes halo burrows.

SMEAR SLIDE SUMMARY (%):

	1, 50 D	2, 60 D	3, 60 D	4, 60 D	5, 60 D	6, 60 D	6, 143 M
TEXTURE:							
Sand	—	—	—	1	—	—	—
Silt	26	24	43	34	39	38	100
Clay	74	76	57	65	61	62	—
COMPOSITION:							
Quartz	19	18	37	28	34	31	2
Feldspar	1	1	2	2	1	1	—
Mica	2	1	1	—	1	Tr	—
Clay	62	61	55	53	59	52	—
Volcanic glass	1	1	1	—	—	1	—
Calcite/dolomite(?)	—	—	—	—	—	—	98
Accessory minerals	12	15	2	12	2	10	—
Glauconite	—	—	Tr	—	—	1	—
Heavy minerals	2	2	1	3	1	3	—
Amphibole	Tr	Tr	—	—	Tr	—	—
Opaque minerals	1	1	1	2	2	Tr	—
Diatoms	Tr	—	Tr	Tr	—	1	—
Radiolarians	—	—	—	Tr	—	Tr	—

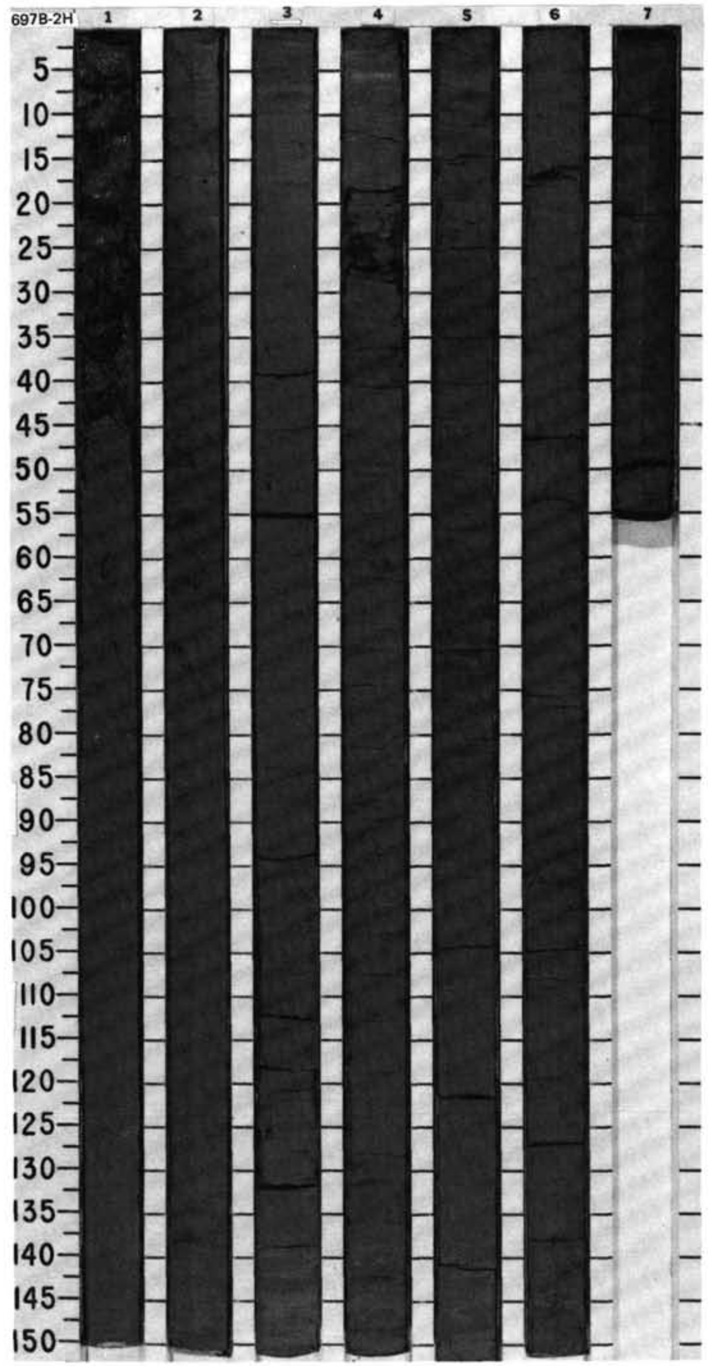

SITE 697 HOLE B CORE 3H CORED INTERVAL 3517.6-3527.3 mbsl; 37.1-46.8 mbsf

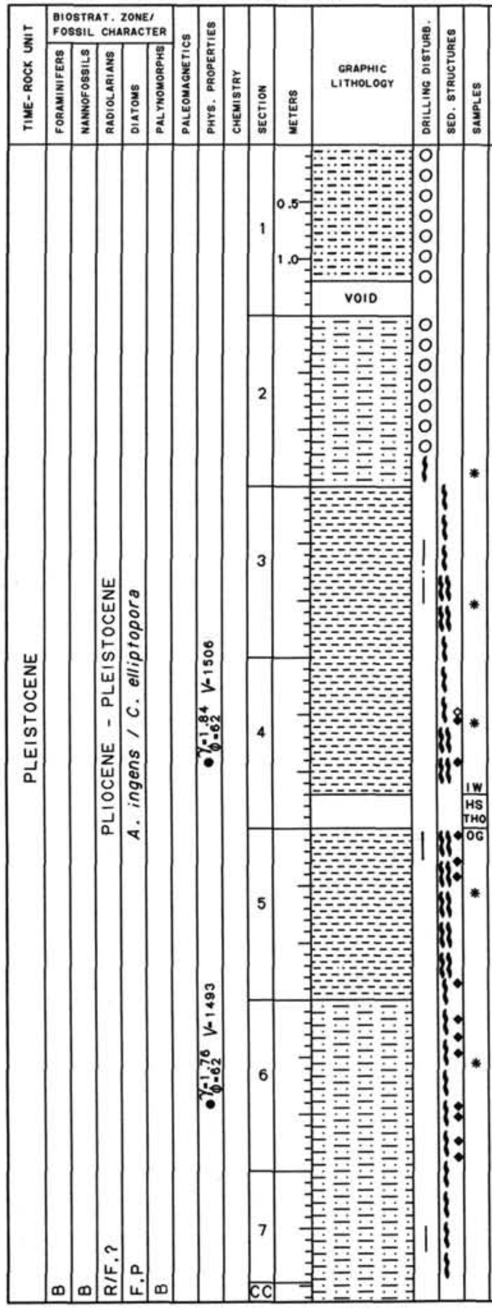

LITHOLOGIC DESCRIPTION

CLAY and CLAYEY MUD

Major lithologies: Clay and clayey mud (79-91% clay), dark gray (N 4/0). Sections 1 and 2, gassy and soupy to very disturbed; cracks in Sections 5 and 7 attributed to coring disturbance during rough weather.

Minor lithologies: Clay, very dark gray (N 3/0), altered ash(?), occurs as laminae and burrow fills in Section 4, 85 and 96–105 cm; Section 5, 80, 125, 133, 139, and 141 cm; and Section 6, 6, 37, and 90 cm. Silt, gray (N 5/0), occurs as tiny (1 mm) clasts in Section 4, 48 and 92 cm, Section 5, 0–38 and 131–136 cm, and throughout Section 6.

Minor to moderate bioturbation. Dropstone in Section 4, 44 cm (1.5 cm in size), chlorite-biotite schist, subangular.

SMEAR SLIDE SUMMARY (%):

	2, 140 D	3, 100 D	4, 60 D	5, 60 D	6, 60 D
TEXTURE:					
Sand	—	1	1	—	1
Silt	23	19	17	9	20
Clay	77	80	82	91	79
COMPOSITION:					
Quartz	15	15	15	7	10
Feldspar	—	Tr	—	—	Tr
Clay	77	80	76	88	59
Accessory minerals	3	2	7	3	20
Heavy minerals	—	1	Tr	1	—
Opaque minerals	2	2	2	1	3
Amphibole	—	Tr	Tr	Tr	—
Diatoms	2	—	—	—	7
Sponge spicules	—	—	—	—	1

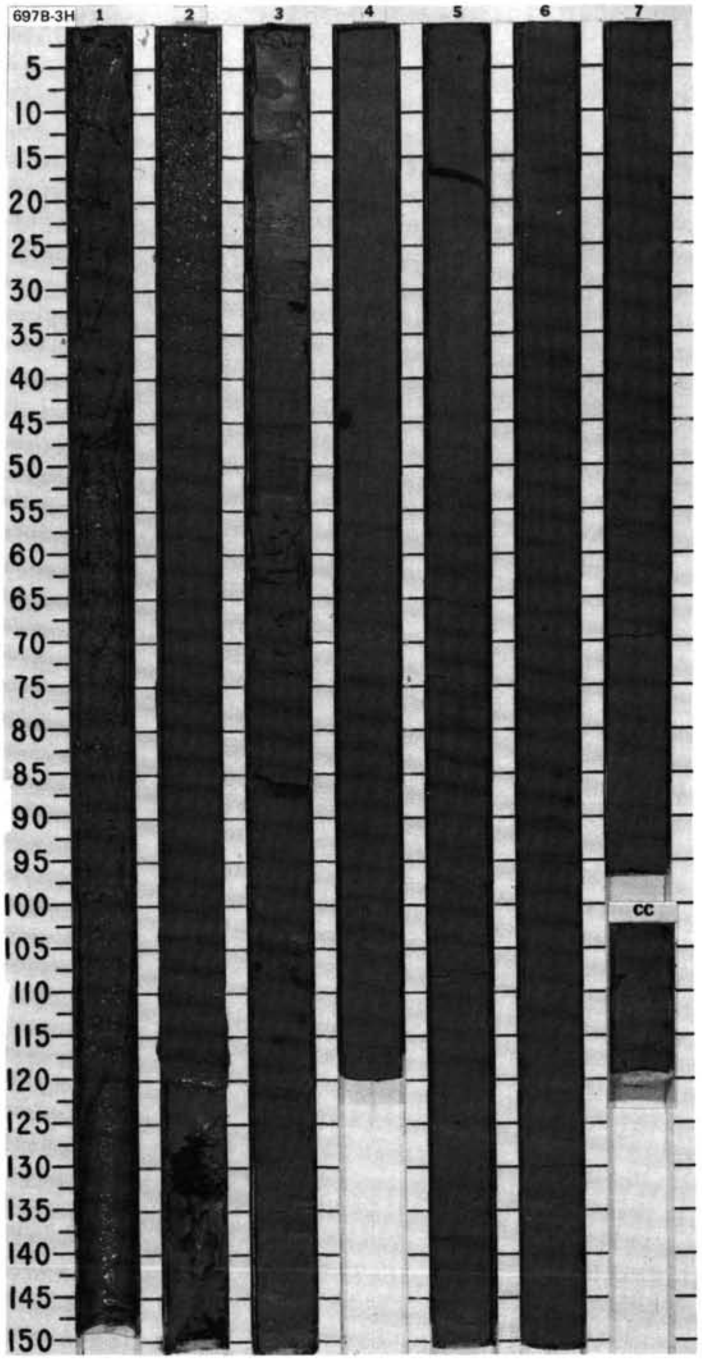

SITE 697 HOLE B CORE 4H CORED INTERVAL 3527.3-3537.0 mbsl; 46.8-56.5 mbsf

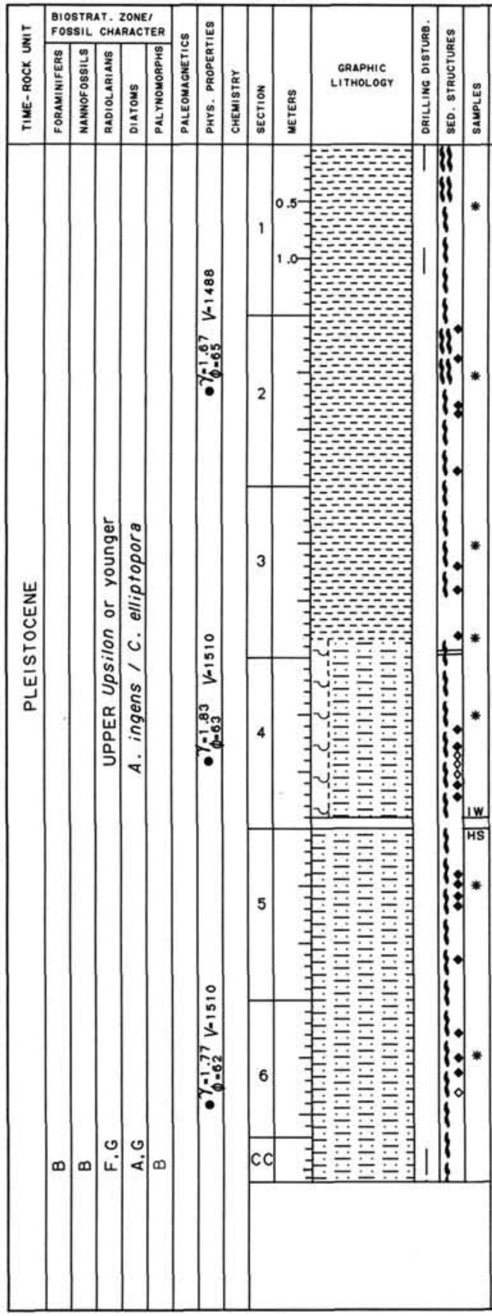

LITHOLOGIC DESCRIPTION

CLAY, CLAYEY MUD, and DIATOM-BEARING CLAYEY MUD

Major lithologies: Clay in Sections 1 through 3, grading to diatom-bearing clayey mud in Section 4; and clayey mud in Section 5 through CC, dark gray (N4/0).

Minor lithologies: Clay, very dark gray (N 3/0), occurs as laminae in Section 1, 61 and 94 cm; Section 2, 95 cm; Section 3, 7, 88, 130, 136, 141, 142, and 143 cm; Section 5, 49, 55, 62, and 66 cm; Section 6, 84, 101, and 105 cm; and CC, 1, 14, and 26 cm. Additionally occurs as scattered burrow fills in Sections 1, 4, and 5. Clay, very dark greenish gray (5G 3/1), occurs as laminae in Section 3, 85 cm. These two minor lithologies are interpreted as altered ashes. Diatom ooze, gray (N 5/0, 5Y 5/1), occurs as thin laminae in Section 3, 141 cm; Section 4, 8 and 12 cm; and CC, 28 and 35 cm; and as clasts (broken-up beds?) 2–5 mm thick, in Section 4, 23–25 and 93–96 cm. Silt, gray (N5/0), occurs as tiny (1–2 mm) clasts in all sections.

Minor to moderate bioturbation. Dropstones in Section 4, 83, 100, and 101 cm, black siltstone, rounded, 0.5 cm each in size. Dropstone in Section 6, 84 cm, black siltstone, subrounded, 1.1 cm in size.

SMEAR SLIDE SUMMARY (%):

	1, 50 D	2, 50 D	3, 50 D	3, 130 M	4, 50 D	5, 50 D	6, 50 D
TEXTURE:							
Sand	1	1	—	1	1	1	1
Silt	18	20	14	34	26	29	28
Clay	81	79	86	65	73	70	71
COMPOSITION:							
Quartz	15	25	7	10	10	20	15
Feldspar	—	Tr	—	—	—	—	—
Mica	—	Tr	1	Tr	1	1	2
Clay	71	77	83	58	68	69	64
Accessory minerals	10	2	3	7	5	1	7
Amphibole	Tr	1	—	Tr	Tr	Tr	1
Opaque minerals	3	2	3	3	3	2	2
Heavy minerals	—	1	2	—	1	2	2
Garnet	—	Tr	—	—	—	—	—
Diatoms	1	2	1	20	10	5	7
Radiolarians	Tr	Tr	Tr	2	2	Tr	Tr
Sponge spicules	Tr	—	Tr	—	Tr	Tr	—

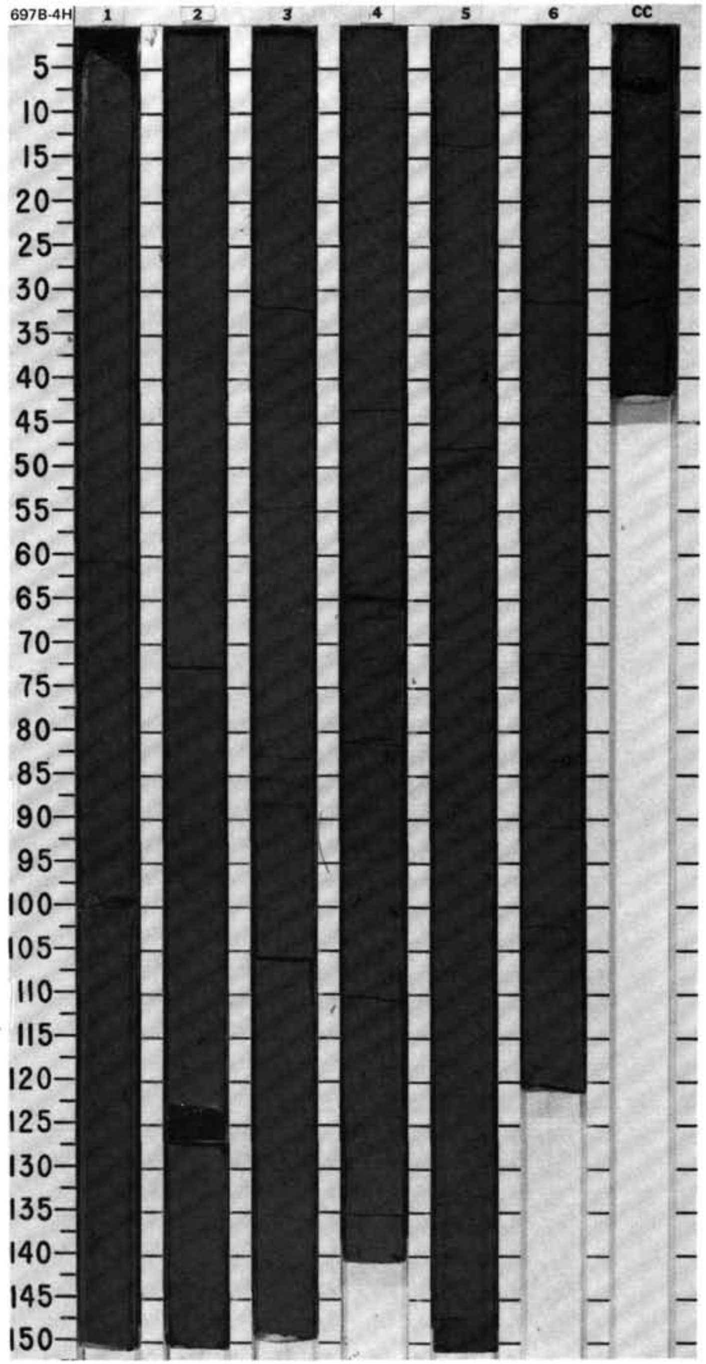

SITE 697 HOLE B CORE 5H CORED INTERVAL 3537.0-3546.7 mbsl; 56.5-66.2 mbsf

TIME-ROCK UNIT	BIOSTRAT. ZONE/ FOSSIL CHARACTER: FORAMINIFERS	NANNOFOSSILS	RADIOLARIANS	DIATOMS	PALYNOMORPHS	PALEOMAGNETICS	PHYS. PROPERTIES	CHEMISTRY	SECTION	METERS	GRAPHIC LITHOLOGY	DRILLING DISTURB.	SED. STRUCTURES	SAMPLES
UPPER PLIOCENE - PLEISTOCENE (?)	B	B	Chi or Phi; R,P	?; R,P	B				1, 2, 3, 4, 5, CC	0.5, 1.0				*

LITHOLOGIC DESCRIPTION

CLAY and CLAYEY MUD

Major lithologies: Clay and clayey mud, dark gray (N 4/0), probably mixed with drilling mud, soupy to very disturbed core. No primary structures. A few spots of pipe grease.

SMEAR SLIDE SUMMARY (%):

	1, 36 D	5, 40 D
TEXTURE:		
Silt	15	22
Clay	85	78
COMPOSITION:		
Quartz	10	10
Mica	—	1
Clay	84	77
Accessory minerals	1	1
Opaque minerals	2	2
Heavy minerals	Tr	1
Diatoms	3	7
Sponge spicules	Tr	1

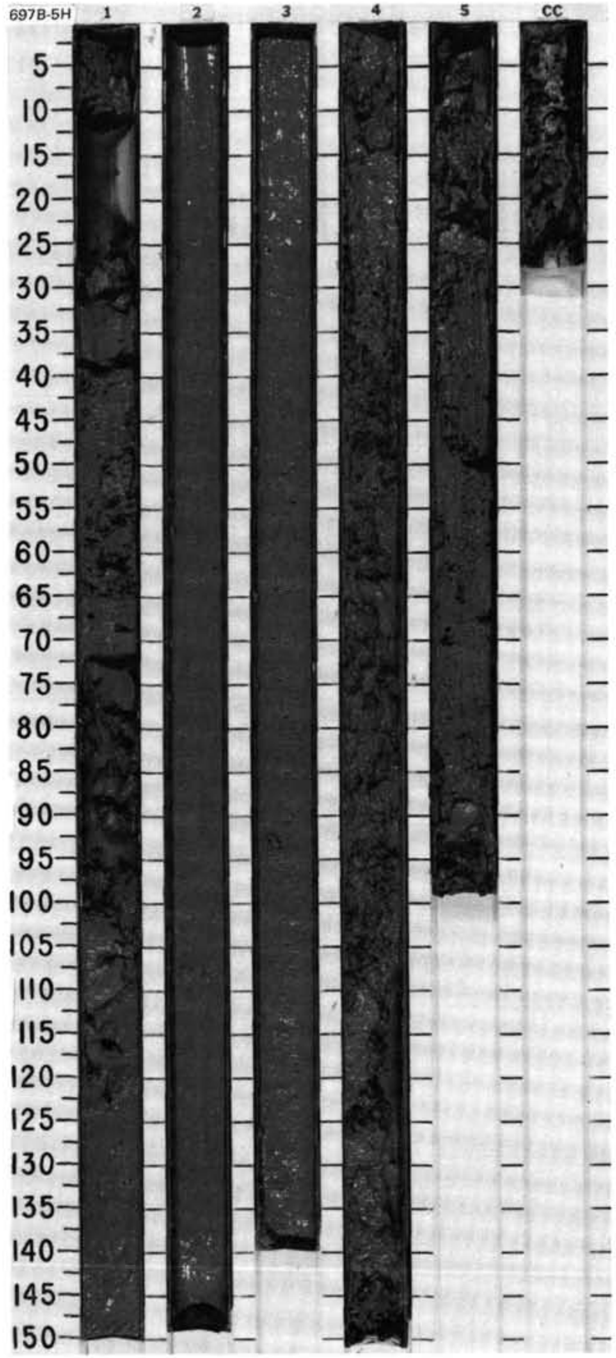

SITE 697 HOLE B CORE 6H CORED INTERVAL 3546.7-3556.5 mbsl; 66.2-76.0 mbsf

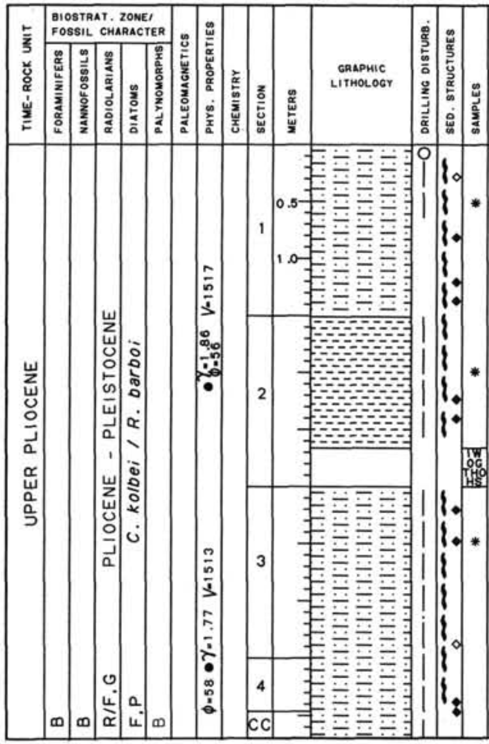

LITHOLOGIC DESCRIPTION

CLAY and CLAYEY MUD

Major lithologies: Clay and clayey mud (74-89% clay), dark gray (N 4/0), faint minor bioturbation.

Minor lithologies: Clay (altered volcanic ash?), very dark gray (N 3/0), occurs as laminae in Section 1, 51, 89, and 123 cm; Section 2, 34, 47, and 92 cm; and Section 3, 7, 50, 56, 71, and 122 cm. Clay (altered volcanic ash?), dark greenish gray (5G 4/1) laminae in Section 1, 83-85 and 122 cm. Silt, gray (N 5/0), occurs sparsely as tiny (1-2 mm) clasts in Sections 1 through 3, and in Section 4, 33-44 cm.

Dropstones in Section 1, 27 cm (0.8 cm long). In Section 3, 137 cm, very angular tubular object, 2 cm long, like pyritized burrow.

SMEAR SLIDE SUMMARY (%):

	1, 50 D	2, 50 D	3, 50 D
TEXTURE:			
Silt	22	11	26
Clay	78	89	74
COMPOSITION:			
Quartz	14	9	16
Feldspar	Tr	1	1
Mica	Tr	—	—
Clay	75	79	69
Volcanic glass	2	—	1
Accessory minerals	3	10	5
Heavy minerals	Tr	—	1
Glauconite	1	—	—
Opaque minerals	-3	1	3
Amphibole	2	—	1
Foraminifers	—	—	Tr
Diatoms	—	—	3
Sponge spicules	—	—	Tr

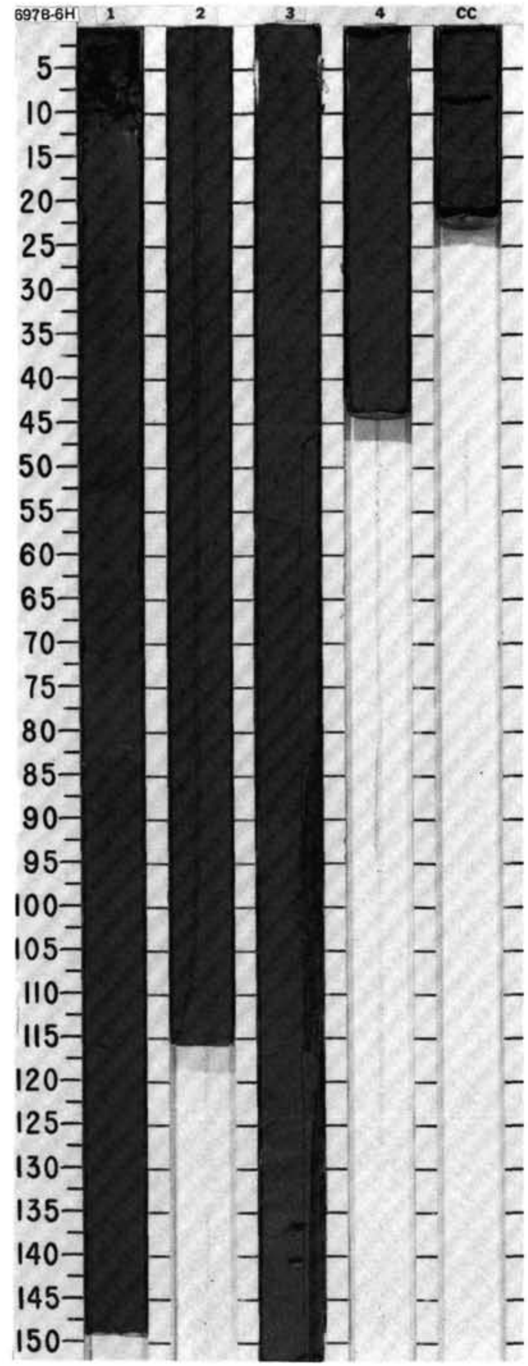

SITE 697 HOLE B CORE 7H CORED INTERVAL 3556.5-3566.2 mbsl; 76.0-85.7 mbsf

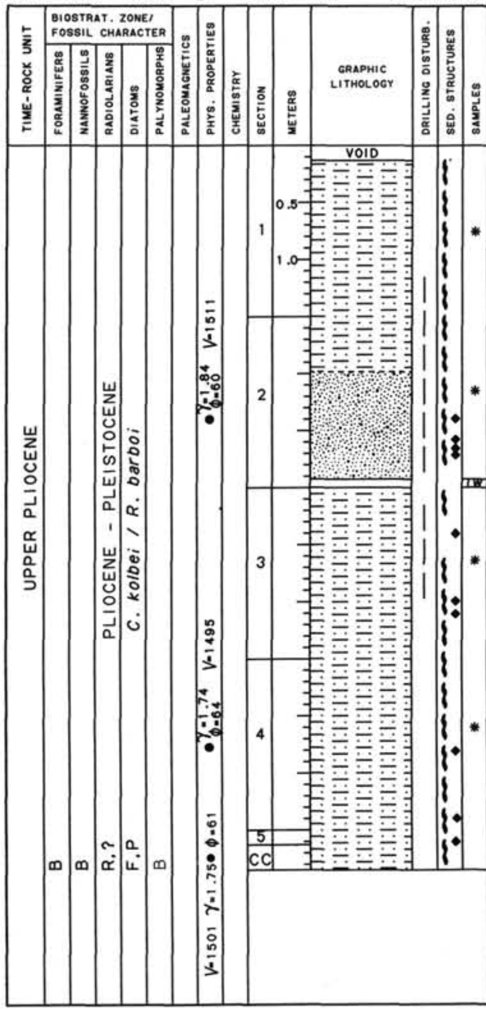

LITHOLOGIC DESCRIPTION

CLAYEY MUD and SILTY MUD

Major lithology: Clayey mud and silty mud, greenish gray (5BG 5/1), with dark gray (N 5/0) layers in Section 2, 58 and 110 cm.

Minor lithologies: Several volcanic ash laminae, dark greenish gray (5BG 5/1), in Section 1, 118 cm; Section 2, 103 and 105 cm; and Section 3, 60 and 63 cm. Silt clasts, white, mm-sized, are most abundant in Section 2. Their location is shown in the sedimentary structures column.

No dropstones. Minor bioturbation.

SMEAR SLIDE SUMMARY (%):

	1, 70 D	2, 70 D	3, 70 D	4, 70 D
TEXTURE:				
Silt	30	55	45	35
Clay	70	45	55	65
COMPOSITION:				
Quartz	22	38	33	25
Feldspar	1	2	1	2
Rock fragments	—	—	—	1
Mica	—	1	Tr	Tr
Clay	70	45	55	65
Volcanic glass	4	6	4	4
Accessory minerals	1	4	3	—
Opaque minerals	2	4	4	3
Glauconite	Tr	Tr	Tr	Tr
Unidentified white spheres	Tr	Tr	—	Tr
Amphibole	—	Tr	Tr	—
Diatoms	Tr	—	—	—

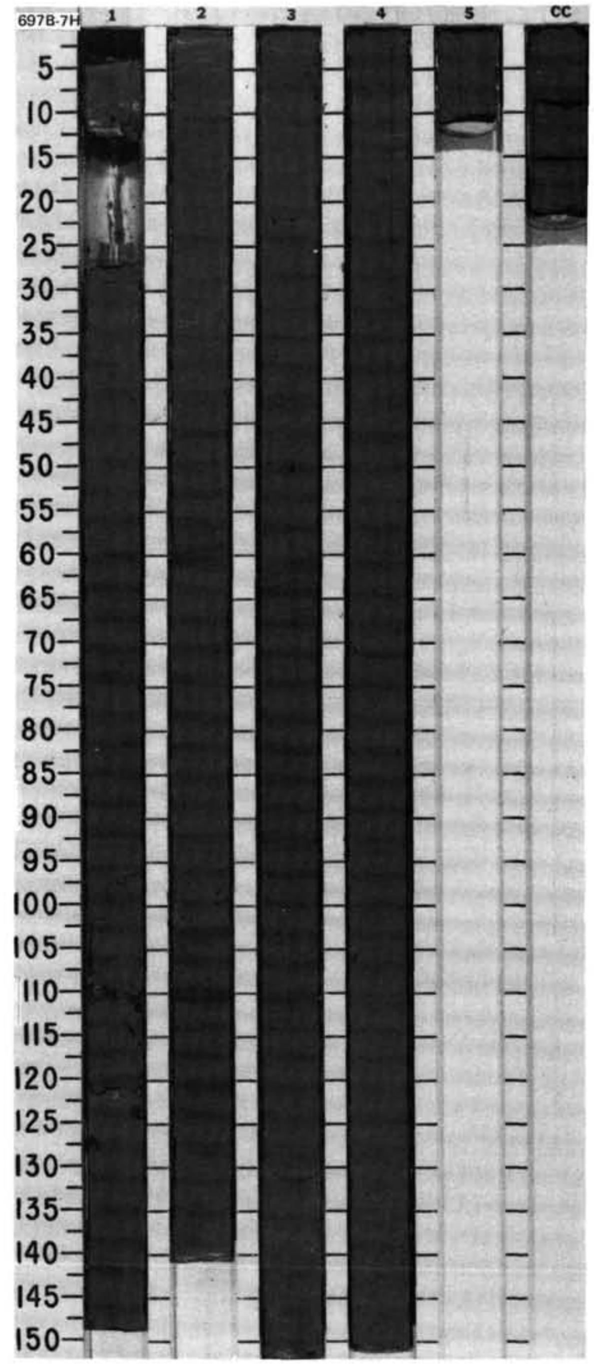

SITE 697 HOLE B CORE 8H CORED INTERVAL 3566.2-3575.9 mbsl; 85.7-95.4 mbsf

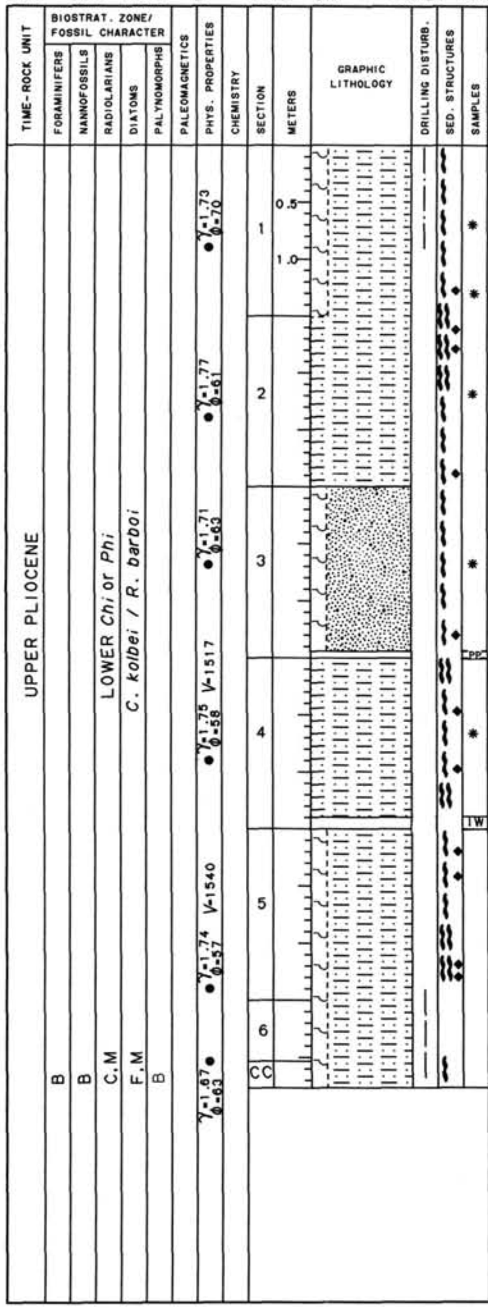

LITHOLOGIC DESCRIPTION

DIATOM-BEARING CLAYEY MUD, DIATOM-BEARING SILTY MUD, and CLAYEY MUD

Major lithologies: Diatom-bearing clayey mud, diatom-bearing silty mud, and clayey mud, predominantly dark greenish gray (5G 4/1), with minor layers of greenish gray (5G 5/1) and dark gray (N 4/0). The greenish gray (5G 5/1) layers appear to immediately overlie the dark gray (N 4/0) layers, and have a gradational contact with the overlying material.

Minor lithologies: Altered volcanic ash layers, grayish green (5G 5/1), difficult to see in this section because of "blending" with the rest of the sediment. These layers are most detectable when adjacent to the dark gray (N 4/0) layers, which they commonly overlie. Silt, in white clasts, mm size and as patches in Section 1, 134-140 cm.

Bioturbation is minor to moderate throughout with halo burrows and *Planolites*.

SMEAR SLIDE SUMMARY (%):

	1, 70 D	1, 135 M	2, 70 D	3, 70 D	4, 70 D	5, 60 D
TEXTURE:						
Sand	—	—	—	Tr	—	—
Silt	40	90	30	60	25	40
Clay	60	10	70	40	75	60
COMPOSITION:						
Quartz	17	3	16	33	18	21
Feldspar	Tr	—	Tr	2	Tr	—
Mica	Tr	—	1	1	—	1
Clay	60	10	70	40	75	60
Volcanic glass	2	—	4	4	3	2
Accessory minerals	—	82	—	—	—	—
Unidentified white spheres	2	—	1	1	Tr	3
Opaque minerals	4	2	3	4	2	2
Amphiboles	Tr	—	—	Tr	—	—
Diatoms	15	3	5	15	2	11
Sponge spicules	—	—	—	—	—	Tr

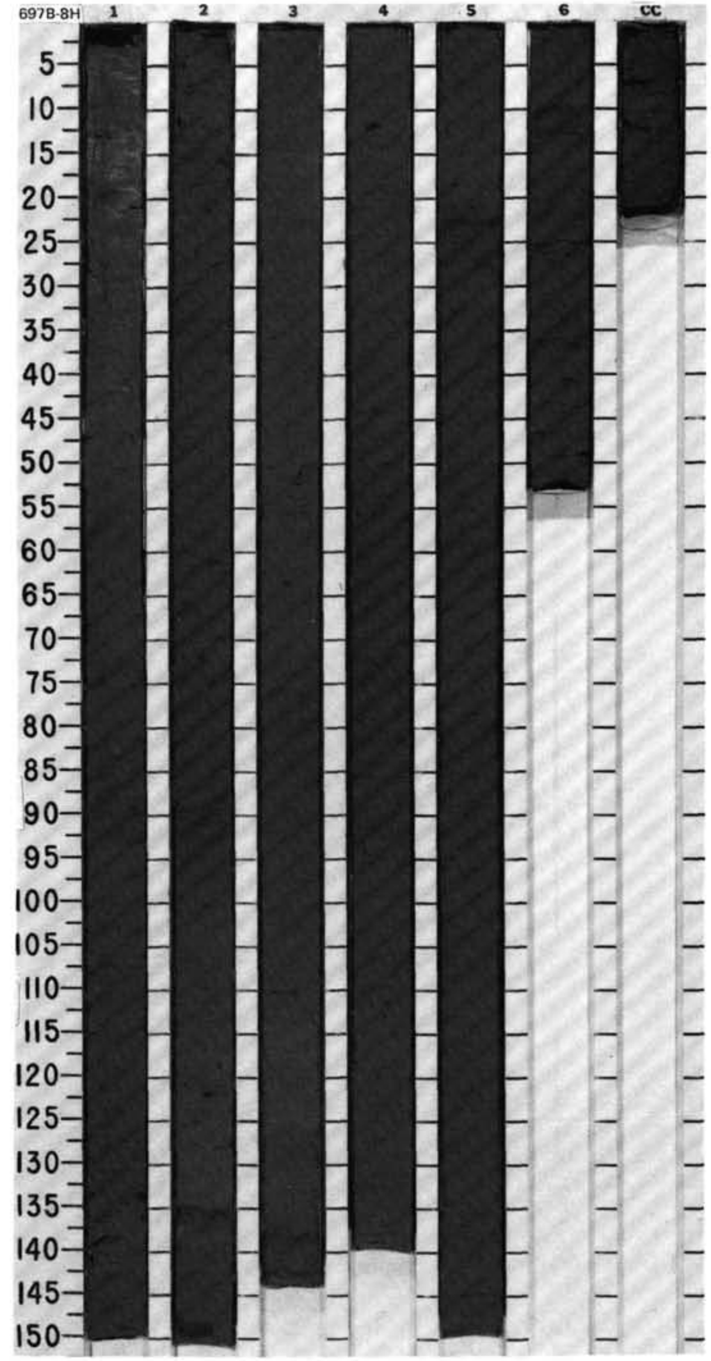

SITE 697 HOLE B CORE 9H CORED INTERVAL 3575.9-3585.2 mbsl; 95.4-104.7 mbsf

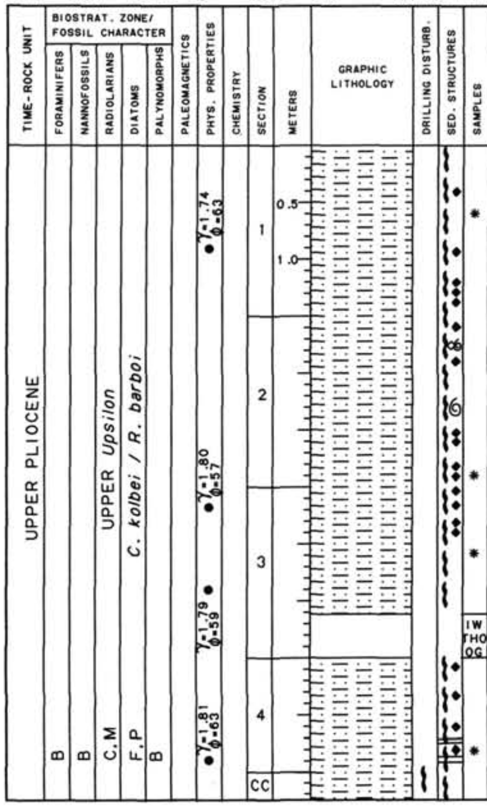

LITHOLOGIC DESCRIPTION

CLAYEY MUD

Major lithology: Clayey mud, dark bluish gray (5B 4/1) and bluish gray (5B 5/1) in Section 1, dark bluish gray (5BG 4/1 to 5G 4/1) in Sections 2 and 3, and dark gray (N 4/0) in Section 4.

Minor lithologies: Diatom-bearing clayey mud, grayish green (5G 4/2), thin layer in Section 2, 140–142 cm. Pyritized-diatom ooze laminae in Section 4, 75–79 cm. Altered volcanic ash layers, dark gray, in Section 2, 60 and 140 cm, and Section 4, 7 cm. Indurated calcareous structures in Section 2, 70 cm, interpreted to be of unknown biological origin, are termed fossil "fish eggs" because of egg-shaped cohesive sructure, although they may be burrow fills or fecal material. Individual structures are 1–2 mm long.

Bioturbation, minor throughout, includes halo burrows. Dropstones occur in Section 2, 10 cm (2 cm in size), igneous rounded; Section 2, 18 cm (2 cm), pyrite concretion; Section 3, 11 cm (0.3 cm), sedimentary, subangular; and Section 4, 80 cm (3 mm), igneous angular. Silt clasts are common.

SMEAR SLIDE SUMMARY (%):

	1, 56 D	1, 142 M	3, 56 D	4, 78 M
TEXTURE:				
Silt	35	48	36	—
Clay	65	52	64	—
COMPOSITION:				
Quartz	20	23	27	5
Feldspar	1	—	2	—
Rock fragments	—	1	Tr	—
Mica	—	3	—	—
Clay	65	52	64	—
Volcanic glass	3	3	1	Tr
Accessory minerals	2	2	3	Tr
Opaque minerals	1	1	1	—
Zeolites	Tr	—	—	—
Glauconite	Tr	—	—	—
Pyrite	—	—	—	35
Diatoms	8	15	2	60
Silicoflagellates	—	Tr	—	—

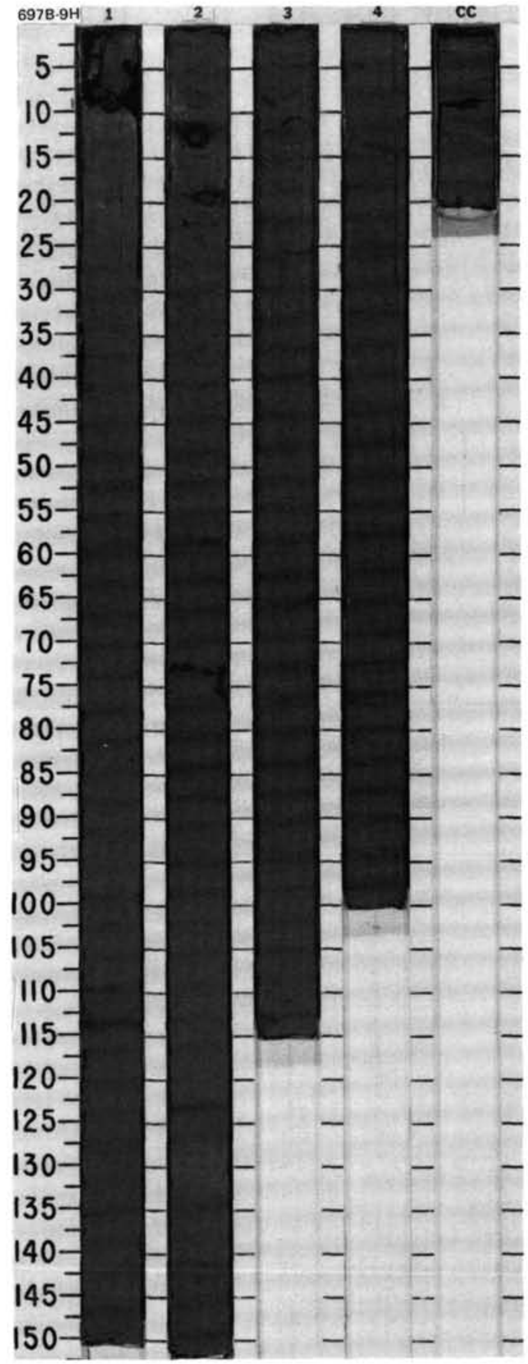

SITE 697 HOLE B CORE 10H CORED INTERVAL 3585.2-3594.8 mbsl; 104.7-114.3 mbsf

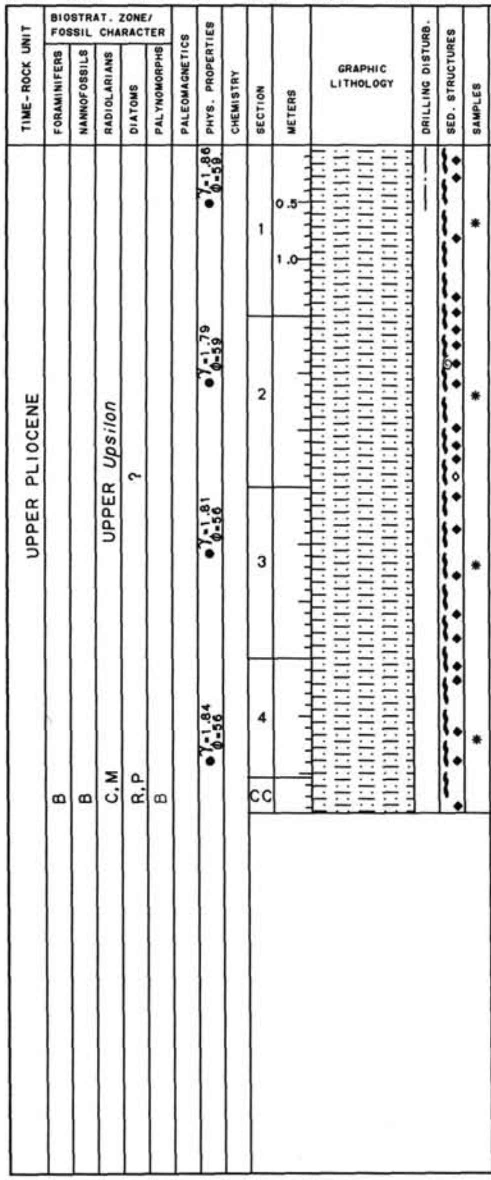

LITHOLOGIC DESCRIPTION

CLAYEY MUD

Major lithology: Clayey mud, dark greenish gray (5G 4/1).

Minor lithologies: Altered volcanic ash(?), diffuse, 0.5–30 mm thick, grayish green (5G 5/2) and dark gray (N 4/0) layers, particularly concentrated in Section 3 (6 layers). Silt, as light colored mm-sized clasts composed mainly of silt-sized quartz. Clasts are evenly distributed (20–30 per section) throughout. Calcareous indurated layer, fossil "fish eggs" in Section 2, 43 cm, cohesive; individual structures are 1–2 mm long.

Dropstone, Section 2, 135 cm, igneous, 0.8 cm long. Moderate to slight drilling disturbance at top of Section 1 and below Section 3. Minor bioturbation.

SMEAR SLIDE SUMMARY (%):

	1, 70 D	2, 70 D	3, 70 D	4, 70 D
TEXTURE:				
Silt	25	25	30	30
Clay	75	75	70	70
COMPOSITION:				
Quartz	12	14	17	19
Feldspar	—	—	2	2
Rock fragments	—	—	1	1
Mica	—	Tr	—	1
Clay	75	75	70	70
Volcanic glass	4	2	2	3
Accessory minerals	3	3	2	2
Opaque minerals	4	2	3	—
Unidentified white spheres	—	—	1	Tr
Diatoms	2	4	2	2

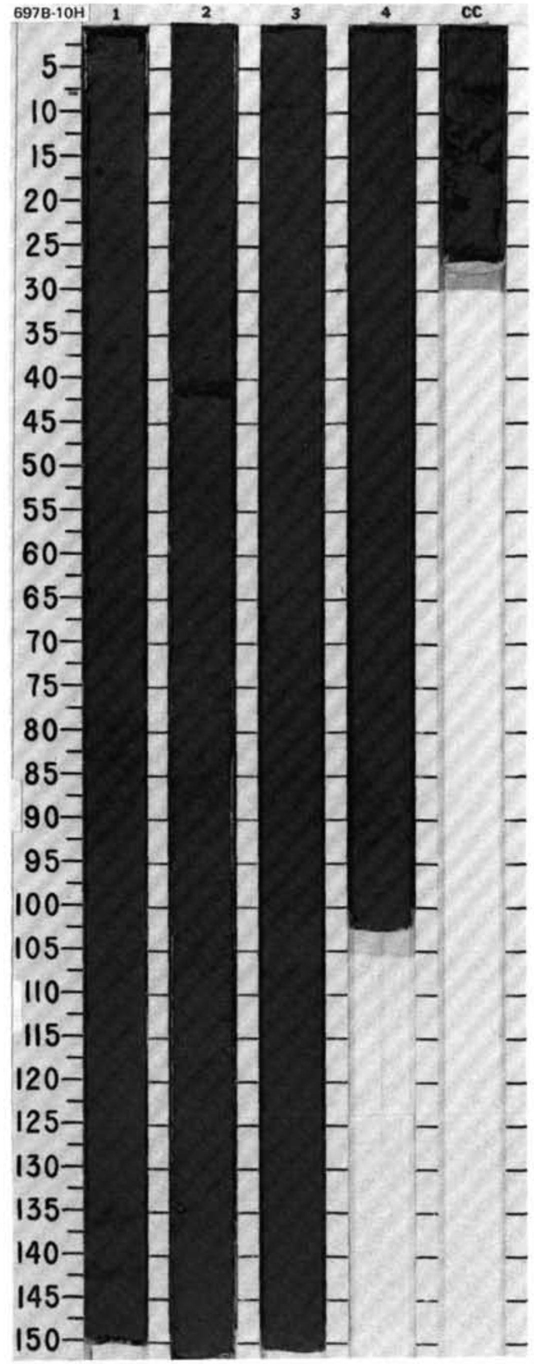

SITE 697 HOLE B CORE 11H CORED INTERVAL 3594.8-3600.3 mbsl; 114.3-119.8 mbsf

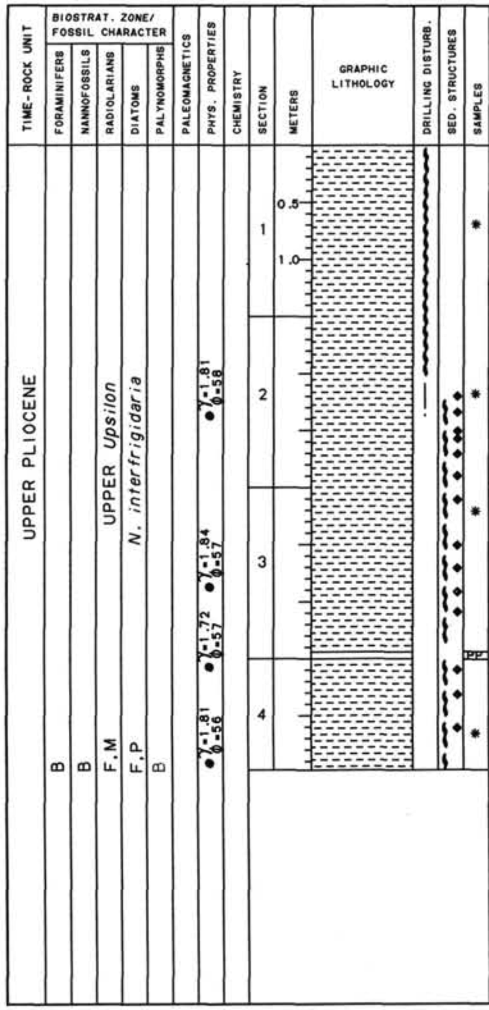

LITHOLOGIC DESCRIPTION

CLAY

Major lithology: Clay, dark greenish gray (5G 4/1), in Section 1 and upper 50 cm of Section 2, is strongly disturbed by drilling.

Minor lithologies: Altered volcanic ash layers, four grayish green (5G 5/2), tilted, diffuse layers in upper half of Section 4. Silt clasts, small (mm-sized), composed of silt-sized quartz, are scattered throughout undisturbed areas.

Bioturbation (as estimated from occurrence of dark gray (N 4/0) mottles) is minor.

SMEAR SLIDE SUMMARY (%):

	1, 70 D	2, 70 D	3, 70 D	4, 70 D
TEXTURE:				
Silt	20	15	15	20
Clay	80	85	85	80
COMPOSITION:				
Quartz	9	9	4	6
Mica	Tr	—	—	—
Clay	80	85	85	80
Volcanic glass	4	2	4	4
Accessory minerals	Tr	—	3	2
Opaque minerals	2	2	2	2
Unidentified white spheres	—	Tr	—	—
Diatoms	5	2	2	6

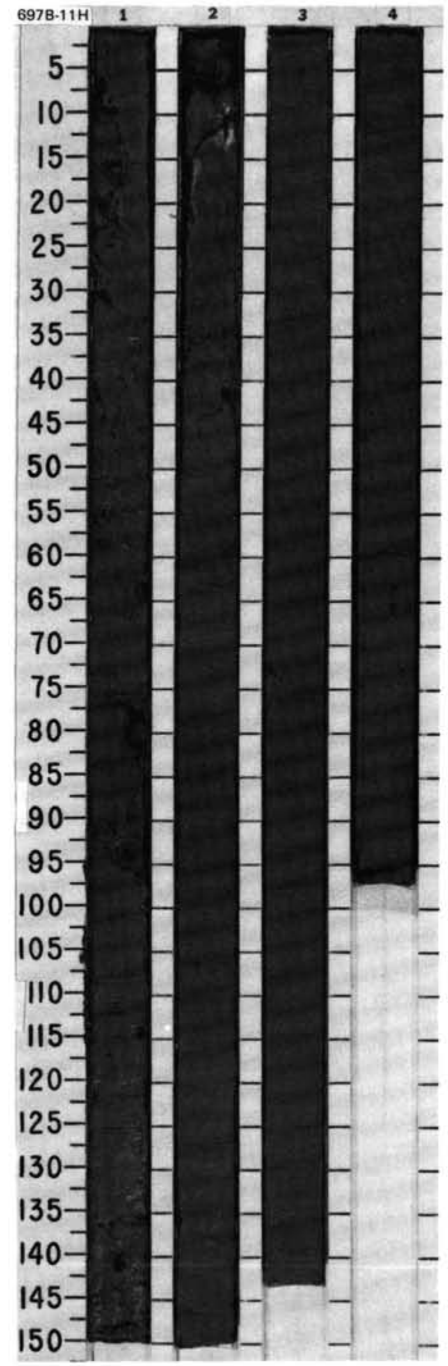

SITE 697 HOLE B CORE 12X CORED INTERVAL 3600.3-3609.1 mbsl; 119.8-128.6 mbsf

TIME-ROCK UNIT	BIOSTRAT. ZONE/FOSSIL CHARACTER: FORAMINIFERS	NANNOFOSSILS	RADIOLARIANS	DIATOMS	PALYNOMORPHS	PALEOMAGNETICS	PHYS. PROPERTIES	CHEMISTRY	SECTION	METERS	GRAPHIC LITHOLOGY	DRILLING DISTURB.	SED. STRUCTURES	SAMPLES
UPPER PLIOCENE	B	B	UPPER *Upsilon* F,M	*N. interfrigidaria* F,P	B				1	0.5, 1.0				*
									2		VOID			
									3					*
									CC		VOID			

LITHOLOGIC DESCRIPTION

DIATOM-BEARING CLAYEY MUD

Major lithology: Diatom-bearing clayey mud, dark greenish gray (5G 4/1). Silt clasts are present, but the core is too disturbed to determine their pre-coring location.

SMEAR SLIDE SUMMARY (%):

	1, 70 D	3, 70 D
TEXTURE:		
Silt	48	50
Clay	52	50
COMPOSITION:		
Quartz	20	20
Feldspar	4	4
Rock fragments	—	4
Mica	3	1
Clay	52	50
Volcanic glass	5	—
Accessory minerals	3	4
Opaque minerals	2	2
Glauconite	Tr	—
Diatoms	11	15
Radiolarians	—	Tr

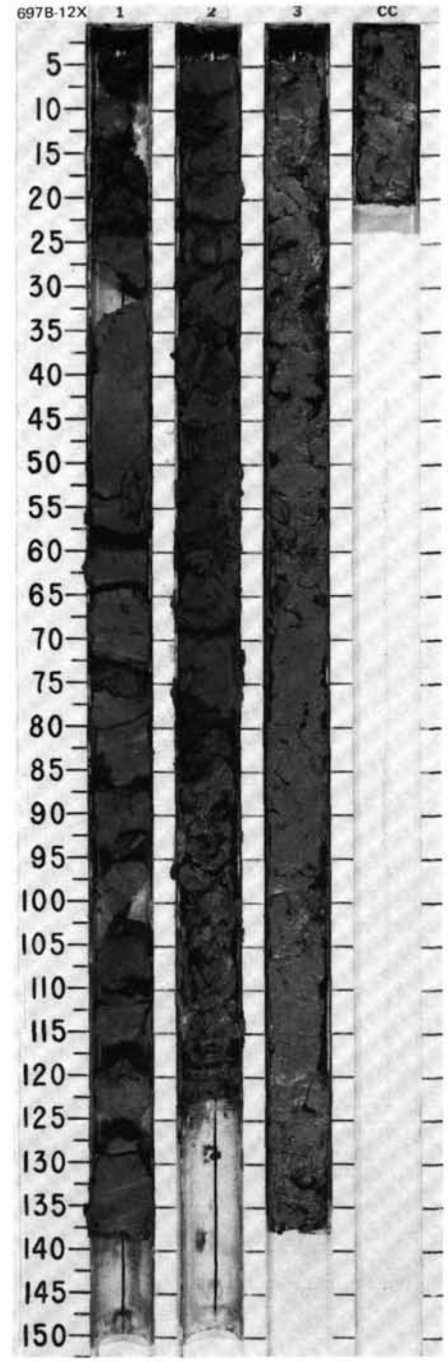

SITE 697 HOLE B CORE 13X CORED INTERVAL 3609.1-3618.7 mbsl; 128.6-138.2 mbsf

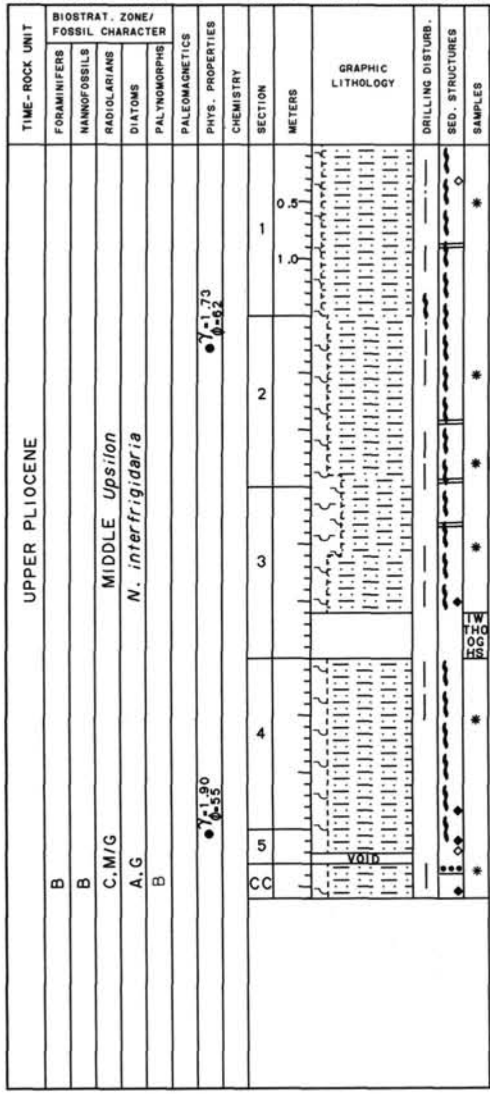

LITHOLOGIC DESCRIPTION

DIATOM-BEARING CLAYEY MUD

Major lithology: Diatom-bearing clayey mud, dark gray (N 4/0) to dark greenish gray (5G 4/1).

Minor lithology: Clay, very dark gray (N 3/0), occurs as laminae in Section 1, 19, 22, 49, 78, and 80 cm; Section 2, 20, 44, 79, 103, 122, and 127 cm; and as small burrow fills throughout Sections 1, 2, and 4. Silicoflagellate-bearing diatom ooze, light olive gray (5Y 6/2), occurs as thin laminae in Section 2, 140, 142, and 150 cm, and Section 3, 0, 15, 23, 28, 31, 32, and 51 cm. Mud-bearing diatom ooze, gray (5Y 5/1), occurs as graded bed in CC, 14-16 cm. Silt clasts, gray, in Section 1, 19 cm, Section 2, 106 cm, Section 3, 98 cm, Section 4, 143 cm, and CC, 17 cm.

Dropstone in Section 1, 132 cm, biotite schist, subangular, 7 cm in size (broken). Scattered sand grains in Section 4, 120-140 cm. Minor bioturbation.

SMEAR SLIDE SUMMARY (%):

	1, 50 D	2, 60 D	2, 143 M	3, 50 D	4, 50 D	CC, 16 M
TEXTURE:						
Sand	1	Tr	—	—	1	—
Silt	25	36	—	37	30	—
Clay	74	64	—	63	69	—
COMPOSITION:						
Quartz	10	15	1	11	14	5
Feldspar	Tr	—	—	1	1	—
Mica	1	1	—	2	—	—
Clay	74	61	5	63	69	13
Volcanic glass	—	—	—	2	1	2
Accessory minerals:						
Micronodules	—	—	Tr	—	—	—
Opaque minerals	3	3	1	2	2	Tr
Heavy minerals	1	2	—	1	1	—
Amphibole	Tr	Tr	—	Tr	Tr	—
Unidentified white spheres	—	3	—	—	—	5
Glauconite	—	—	Tr	—	—	—
Diatoms	11	15	79	17	12	69
Radiolarians	Tr	—	1	—	—	—
Sponge spicules	Tr	Tr	1	Tr	—	Tr
Silicoflagellates	—	—	12	1	—	8

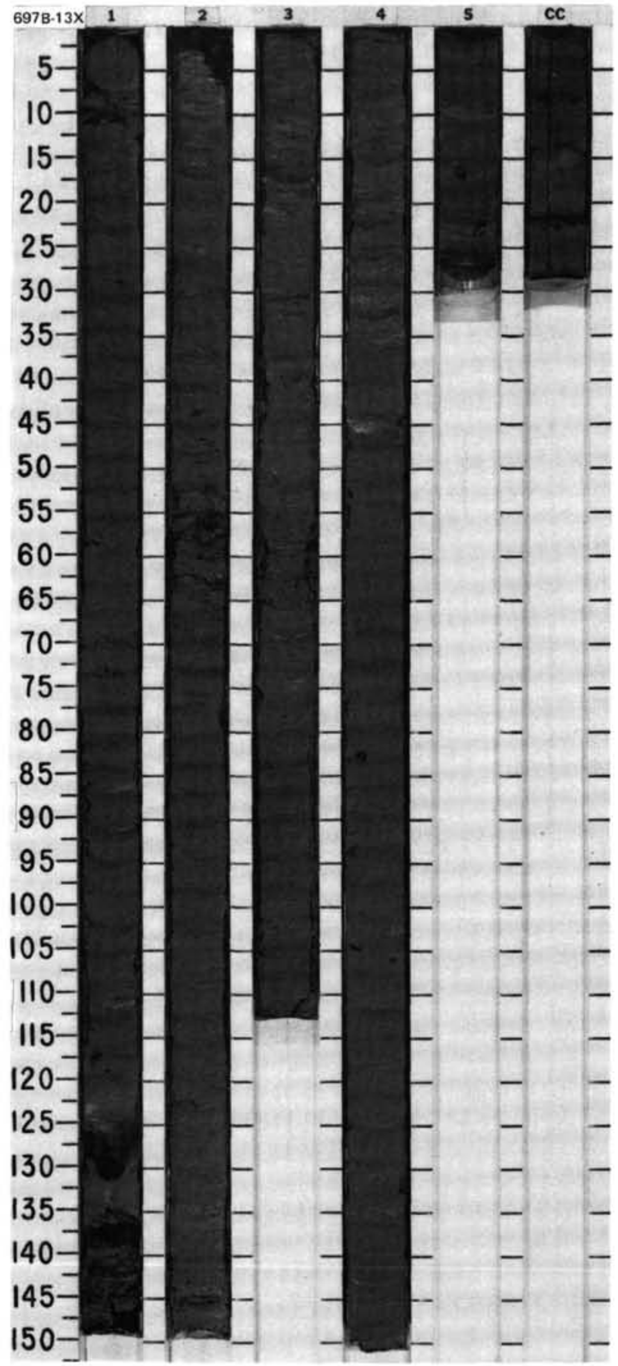

SITE 697 HOLE B CORE 14X CORED INTERVAL 3618.7-3628.4 mbsl; 138.2-147.9 mbsf

TIME-ROCK UNIT	FORAMINIFERS	NANNOFOSSILS	RADIOLARIANS	DIATOMS	PALYNOMORPHS	PALEOMAGNETICS	PHYS. PROPERTIES	CHEMISTRY	SECTION	METERS
UPPER PLIOCENE	B	B	MIDDLE *Upsilon* C, G	? *N. interfrigidaria* R, P	B		• γ=1.77 φ=63 (Section 2); • γ=1.76 φ=62 (Section 3); • γ=1.73 φ=60 (Section 5)		1, 2, 3, 4, 5, 6, 7, CC	0.5, 1.0

BIOSTRAT. ZONE/ FOSSIL CHARACTER

GRAPHIC LITHOLOGY | DRILLING DISTURB. | SED. STRUCTURES | SAMPLES

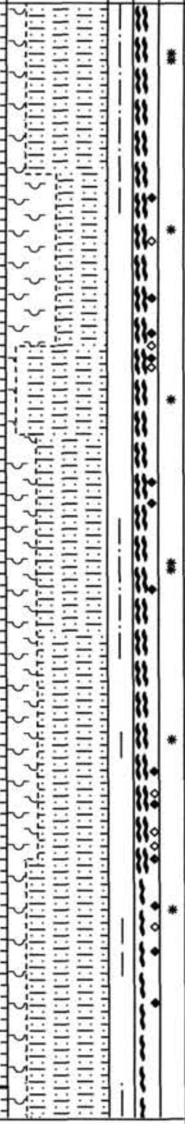

LITHOLOGIC DESCRIPTION

DIATOM-BEARING CLAYEY MUD, CLAYEY MUD, and MUDDY DIATOM OOZE

Major lithologies: Diatom-bearing clayey mud, dominant lithology grading to muddy diatom ooze in Section 2, clayey mud in Section 3, 0(?)–78 cm, and diatom clayey mud in Section 3, 78 cm, to Section 6, dark gray (N 4/0). Burrow fills of clay, very dark gray (N 3/0), throughout core; these decrease from about 5% of sediment surface area in Section 1 to 1% in Section 5.

Minor lithologies: Vitric ash, very dark grayish brown (2.5Y 3/2), occurs as burrowed and disturbed laminae in Section 1, 41, 81, and 111 cm. Clay, dark greenish gray (5GY 4/1), occurs as faint laminae/very thin beds in Sections 1 through 4; 22 layers totalling 31 cm. Diatom ooze, gray (N 5/0), occurs as thin burrowed laminae in Section 1, 67, 110, and 117 cm, and Section 2, 21, 50, 79, 83, 86, 90, 94, and 121 cm. Silt, gray (N 5/0), occurs as tiny clasts in Sections 2 through 6.

Moderate bioturbation, minor in Sections 6 and 7 because of lack of color contrast. Dropstones in Section 2, 141 cm (4 cm long), quartz-biotite-garnet schist, angular; Section 3, 17 cm (1.5 cm long), quartz, angular; and Section 6, 57 cm (1 cm long), mudstone, rounded. Pyritized burrows in Section 2, 60 cm, and Section 5, 128 and 140 cm.

SMEAR SLIDE SUMMARY (%):

	1, 42 M	1, 50 D	2, 55 D	3, 50 D	4, 42 M	4, 50 D
TEXTURE:						
Sand	—	2	—	—	—	3
Silt	97	39	—	22	85	38
Clay	3	59	—	78	15	59
COMPOSITION:						
Quartz	1	11	7	10	3	10
Feldspar	—	Tr	1	—	—	—
Mica	—	2	2	—	—	—
Clay	3	59	37	78	15	59
Volcanic glass	93	3	—	—	—	—
Calcite/dolomite(?)	—	—	—	—	71	—
Accessory minerals:						
Amphibole	—	—	—	Tr	—	Tr
Glauconite	—	Tr	Tr	Tr	—	—
Heavy minerals	Tr	2	1	1	—	Tr
Opaque minerals	—	1	—	2	1	1
Diatoms	3	20	50	7	10	30
Radiolarians	—	—	—	—	—	Tr
Sponge spicules	—	Tr	—	2	—	Tr
Silicoflagellates	—	2	2	—	—	Tr

	5, 50 D	6, 50 D
TEXTURE:		
Sand	1	2
Silt	42	35
Clay	57	63
COMPOSITION:		
Quartz	7	15
Feldspar	—	Tr
Mica	Tr	Tr
Clay	57	63
Volcanic glass	Tr	—
Accessory minerals	1	—
Amphibole	—	Tr
Heavy minerals	1	Tr
Opaque minerals	2	1
Diatoms	30	20
Radiolarians	1	1
Sponge spicules	Tr	—
Silicoflagellates	1	—

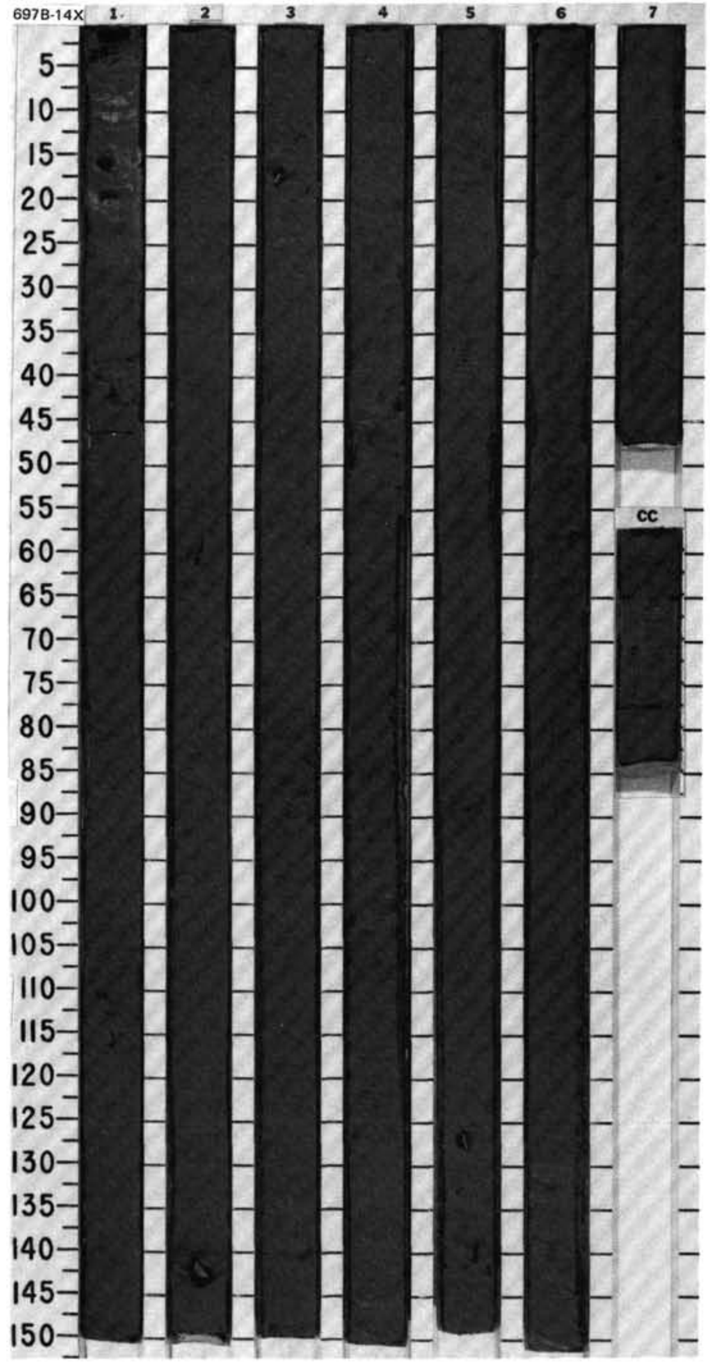

SITE 697 HOLE B CORE 15X CORED INTERVAL 3628.4-3638.0 mbsl; 147.9-157.5 mbsf

TIME-ROCK UNIT	FORAMINIFERS	NANNOFOSSILS	RADIOLARIANS	DIATOMS	PALYNOMORPHS	PALEOMAGNETICS	PHYS. PROPERTIES	CHEMISTRY	SECTION	METERS
LOWER PLIOCENE	B	B	MIDDLE *Upsilon* C/A,G	*N. interfrigidaria* C,M	B		● γ=1.91 φ=55; ● γ=1.81 φ=61; ● γ=1.73 φ=61		1, 2, 3, 4, 5, 6, 7, CC	0.5, 1.0

BIOSTRAT. ZONE/FOSSIL CHARACTER

GRAPHIC LITHOLOGY | DRILLING DISTURB. | SED. STRUCTURES | SAMPLES

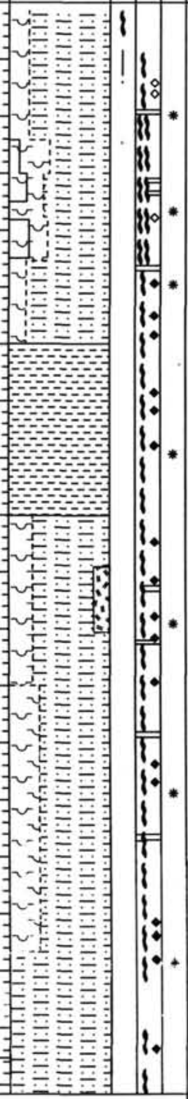

LITHOLOGIC DESCRIPTION

DIATOM-BEARING CLAYEY MUD, CLAY, DIATOM CLAYEY MUD, and CLAYEY MUD

Major lithologies: Diatom-bearing clayey mud in Sections 1, 2, and 4; grading to clay in Section 3; to diatom clayey mud in Section 5 and in Section 6, 0-82 cm; and to clayey mud in Section 6, 82 cm, to CC; dark gray (N 4/0).

Minor lithologies: Diatom ooze, gray (5Y 6/1), occurs as laminae and burrow fills from Section 1, 103 cm, to Section 2, 27 cm, and in Section 2, 39-76 cm, forming 10-20% of the sediment. Also isolated laminae in Section 2, 83 cm; Section 4, 53 and 85 cm; and Section 5, 33, 53, 55, 84, 89, 100, 111, 116, and 123 cm. Muddy diatom ooze, gray (N 5/0), in Section 5, 137-144 cm. Clay, very dark gray (N 3/0), occurs as laminae and thin beds in Section 1,93-96 cm; Section 2, 14, 34, 48, 53, and 55 cm; Section 4, 61, 74,102, 106, 110, and 121 cm; Section 5, 130 cm; and Section 6, 11, 62-65, 82, and 106 cm. Clay, dark greenish gray (5G 4/1), occurs as very thin beds in Section 1, 92-93 cm; Section 4, ten 1-cm beds from 45 to 112 cm; and Section 5, 53, 86, 106, 113, and 130 cm. Silt, gray (N 5/0), occurs as tiny clasts in Sections 2 through 7.

Moderate to minor bioturbation. Dropstone, in Section 1, 89 cm (6 mm in size), siltstone, rounded; pyritized burrow in Section 3, 61 cm(1 cm).

SMEAR SLIDE SUMMARY (%):

	1, 100 D	2, 31 M	2, 100 D	3, 100 D	4, 100 D	5, 100 D	6, 100 D
TEXTURE:							
Sand	Tr	2	Tr	—	2	2	Tr
Silt	28	78	25	16	44	40	34
Clay	72	20	75	84	54	58	66
COMPOSITION:							
Quartz	7	1	7	10	20	10	25
Feldspar	—	—	Tr	—	Tr	—	Tr
Mica	—	—	1	—	—	Tr	Tr
Clay	72	20	75	84	54	58	66
Volcanic glass	—	5	—	—	—	—	—
Calcite/dolomite(?)	—	43	—	—	—	—	—
Accessory minerals:							
Glauconite	—	—	—	—	—	—	Tr
Amphibole	—	—	—	—	Tr	Tr	Tr
Garnet	—	—	—	—	—	—	Tr
Opaque minerals	1	—	1	1	1	1	2
Heavy minerals	Tr	—	Tr	Tr	Tr	Tr	Tr
Zeolites(?)	—	1	—	—	—	—	—
Diatoms	20	30	15	5	25	30	7
Radiolarians	Tr	—	1	—	Tr	1	Tr
Sponge spicules	—	—	Tr	Tr	—	Tr	Tr
Silicoflagellates	—	—	—	—	—	Tr	Tr

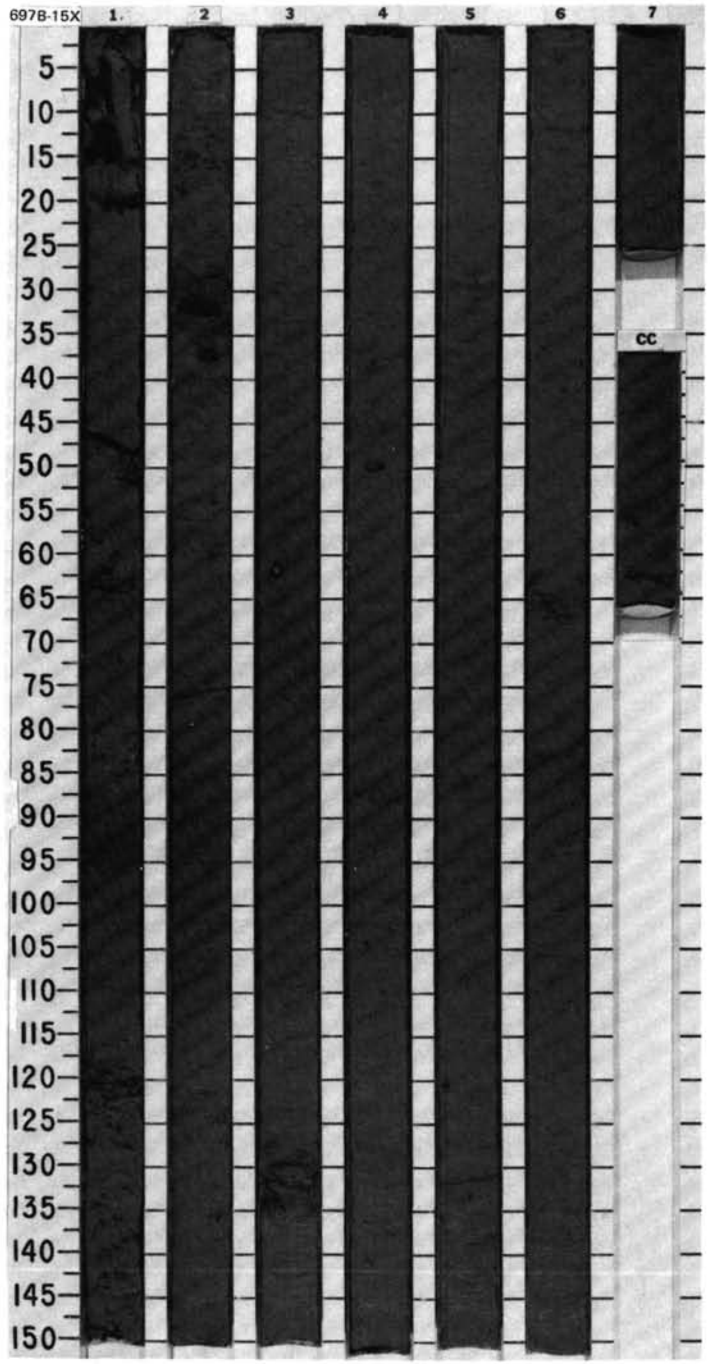

SITE 697 HOLE B CORE 16X CORED INTERVAL 3638.0-3647.7 mbsl; 157.5-167.2 mbsf

TIME-ROCK UNIT: LOWER PLIOCENE

BIOSTRAT. ZONE/FOSSIL CHARACTER: FORAMINIFERS B; NANNOFOSSILS B; RADIOLARIANS MIDDLE *Upsilon* C,M/G; DIATOMS *N. angulata – N. reinholdii* F,M; PALYNOMORPHS B

PALEOMAGNETICS | PHYS. PROPERTIES | CHEMISTRY | SECTION | METERS | GRAPHIC LITHOLOGY | DRILLING DISTURB. | SED. STRUCTURES | SAMPLES

PHYS. PROPERTIES: γ=1.96 φ=57 V=1577; γ=1.79 φ=58 V=1530; γ=1.89 φ=53

SECTION: 1, 2, 3, 4, 5, 6, CC

METERS: 0.5, 1.0

SAMPLES: IW OG

LITHOLOGIC DESCRIPTION

DIATOM-BEARING CLAYEY MUD and CLAYEY MUD

Major lithologies: Diatom-bearing clayey mud, dark greenish gray (5GY 4/1). Clayey mud, dark greenish gray (5GY 4/1, grading to 5G 4/1).

Minor lithology: Silt, as white clasts throughout the core. Silty mud, dark grayish brown (2.5Y 4/2) layer and patch, Section 5, 107 and 140 cm. Silty mud to clayey mud turbidite, Section 3, 45–80 cm, consists of 3 graded units. Pale green laminae, sometimes associated with dark gray (N 4/0) laminae, in Sections 5 and 6. Dark gray (N 4/0) streaks throughout the core.

Dropstone, in Section 6, 35 cm (2 cm in size), mudstone, rounded.

SMEAR SLIDE SUMMARY (%):

	1, 50 D	2, 50 D	3, 50 D	3, 72 M	4, 50 D	5, 50 D	6, 50 D
TEXTURE:							
Sand	Tr	1	2	15	—	—	Tr
Silt	35	45	48	46	22	26	23
Clay	65	54	50	39	78	74	77
COMPOSITION:							
Quartz	12	12	17	41	10	12	8
Feldspar	1	1	—	3	1	Tr	1
Mica	1	—	1	—	—	—	1
Clay	62	54	49	39	77	72	73
Volcanic glass	3	2	3	4	1	1	1
Accessory minerals	3	—	1	—	1	2	4
Amphibole	—	—	—	1	1	—	1
Glauconite	1	1	1	1	—	1	—
Heavy minerals	2	3	1	2	2	1	1
Opaque minerals	2	2	2	5	2	4	2
Micronodules	—	—	—	1	—	—	—
Diatoms	11	20	23	3	5	7	8
Radiolarians	—	Tr	—	—	—	—	—
Sponge spicules	Tr	1	Tr	—	Tr	Tr	Tr
Silicoflagellates	2	4	2	—	—	—	—

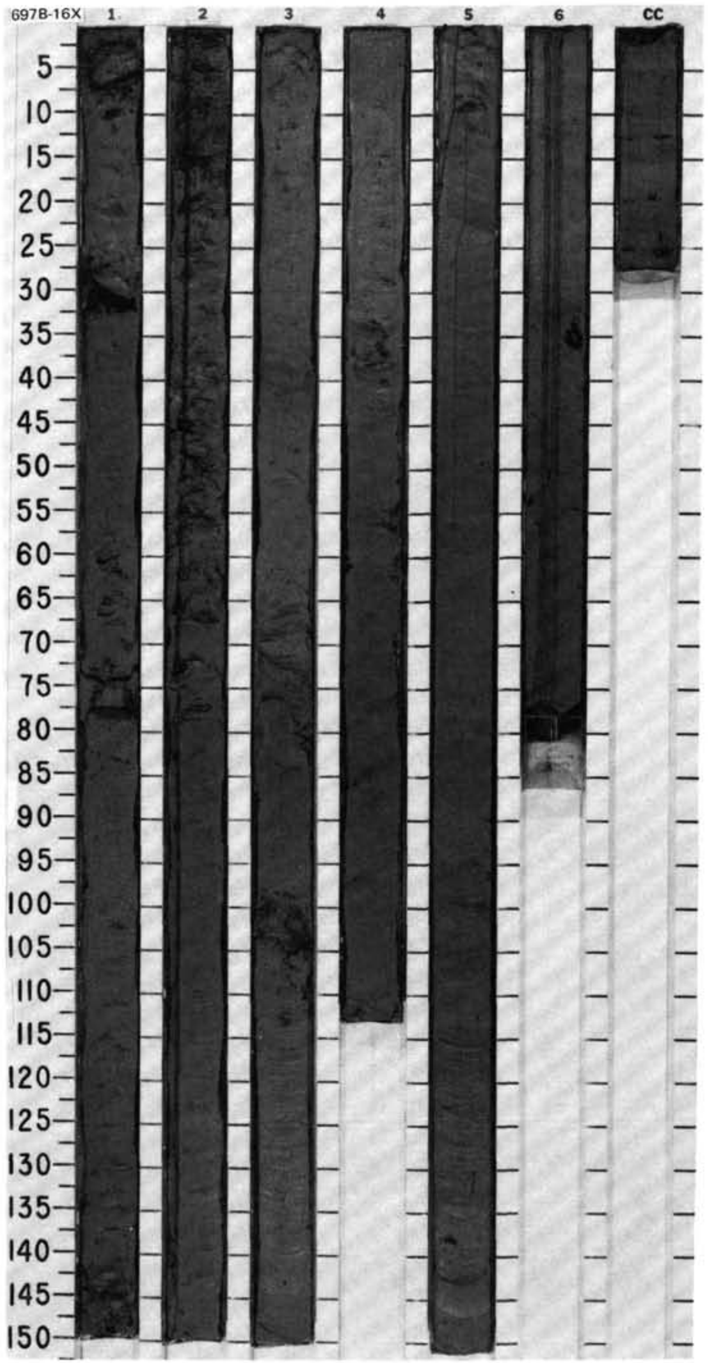

SITE 697 HOLE B CORE 17X CORED INTERVAL 3647.7-3657.4 mbsl; 167.2-176.9 mbsf

TIME-ROCK UNIT	FORAMINIFERS	NANNOFOSSILS	RADIOLARIANS	DIATOMS	PALYNOMORPHS	PALEOMAGNETICS	PHYS. PROPERTIES	CHEMISTRY	SECTION	METERS	GRAPHIC LITHOLOGY	DRILLING DISTURB.	SED. STRUCTURES	SAMPLES
LOWER PLIOCENE	B	B	C,M	R,P MIDDLE *Upsilon* *N. angulata – N. reinholdii*	B		●γ=1.96 φ=50 V=1569 ●γ=1.97 φ=57 V=1581 ●γ=1.89 φ=52 V=1610		1 2 3 4 5 6 7 CC	0.5 1.0				*

LITHOLOGIC DESCRIPTION

CLAY, CLAYEY MUD, and DIATOM-BEARING CLAYEY MUD

Major lithologies: Clay (Sections 1-2), grading to clayey mud (Sections 3-4),and and diatom-bearing clayey mud (Sections 5 through CC), dark gray (N4/0). Burrow fills are very dark gray (N 3/0) clay.

Minor lithologies: Clay, very dark gray (N 3/0), occurs as laminae in Section 2, 57, 59, 73, and 97 cm; Section 3, 17, 40, 72, 80, and 114 cm; and Section 5, 20 and 21 cm. Clay, dark greenish gray (5GY 4/1), occurs as faint fuzzy layers in Section 2, 140-141 cm; Section 3, 12-14, 119-120, and 124-125 cm; Section 5, 12-13, 25-26, 47-48, 53-54, 97-98, and 122-123 cm; and Section 6, 30-32 and 44-45 cm. Silt, gray (N 6/0), occurs as tiny (1-2 mm) clasts in all sections, particularly Sections 3 and 6.

Minor bioturbation throughout. Dropstones in Section 4, 20 cm; Section 4, 38 cm (1.5 cm in size), granite, rounded; and Section 5, 108 cm. Pyritized burrow in Section 4, 93 cm.

SMEAR SLIDE SUMMARY (%):

	1, 50 D	2, 50 D	3, 50 D	4, 50 D	5, 50 D	6, 50 D
TEXTURE:						
Sand	—	3	10	12	2	4
Silt	16	13	23	10	30	30
Clay	84	84	67	78	68	66
COMPOSITION:						
Quartz	5	10	25	7	15	15
Feldspar	Tr	Tr	Tr	—	Tr	—
Mica	Tr	2	Tr	Tr	—	Tr
Clay	84	84	67	78	68	66
Accessory minerals	—	—	—	10	—	2
Glauconite	—	Tr	Tr	—	—	Tr
Amphibole	Tr	Tr	1	Tr	Tr	Tr
Garnet	—	Tr	Tr	—	Tr	—
Opaque minerals	2	1	2	2	2	2
Heavy minerals	Tr	—	Tr	Tr	Tr	Tr
Diatoms	8	3	5	3	15	15
Radiolarians	1	—	—	—	—	Tr
Sponge spicules	—	Tr	Tr	Tr	Tr	—

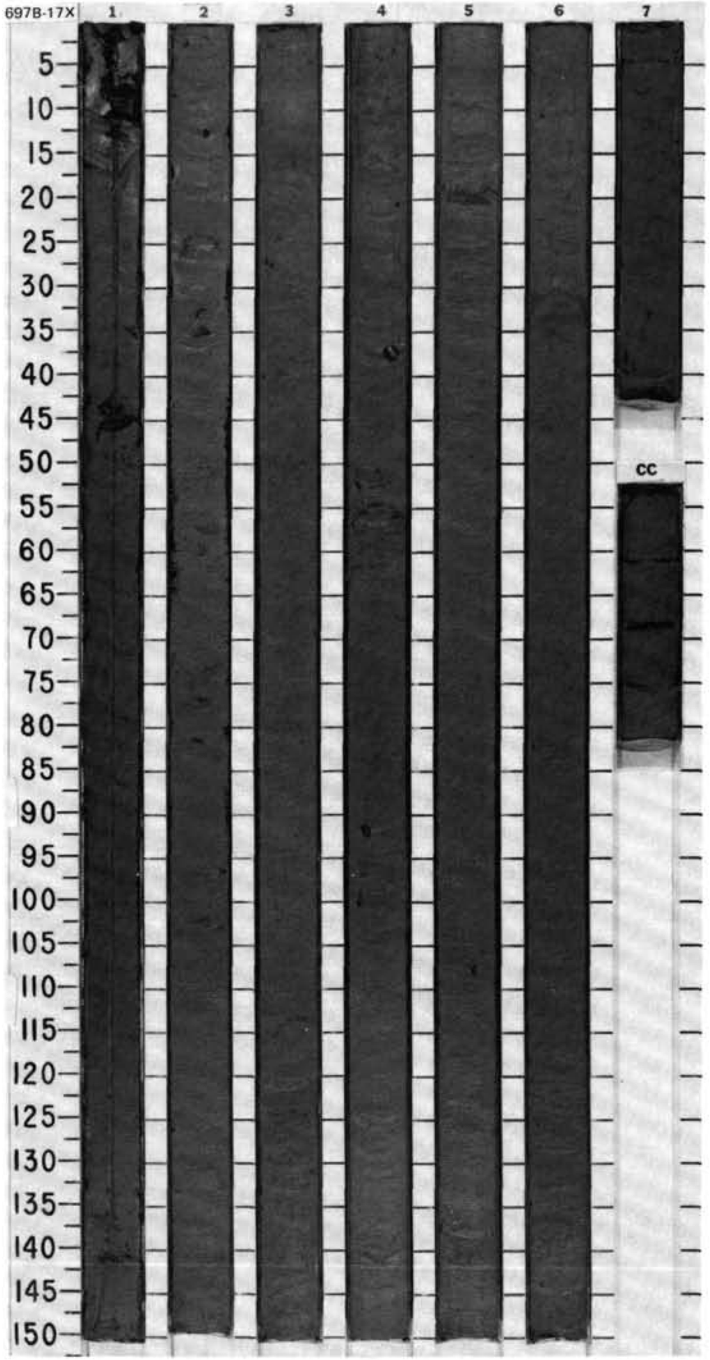

SITE 697 HOLE B CORE 18X CORED INTERVAL 3657.4-3667.1 mbsl; 176.9-186.6 mbsf

TIME-ROCK UNIT	FORAMINIFERS	NANNOFOSSILS	RADIOLARIANS	DIATOMS	PALYNOMORPHS	PALEOMAGNETICS	PHYS. PROPERTIES	CHEMISTRY	SECTION	METERS	GRAPHIC LITHOLOGY	DRILLING DISTURB.	SED. STRUCTURES	SAMPLES	LITHOLOGIC DESCRIPTION
LOWER PLIOCENE	B	B	C,G MIDDLE *Upsilon*	C,M *N. angulata – N. reinholdii*	B				CC					*	CLAYEY MUD

(BIOSTRAT. ZONE/FOSSIL CHARACTER: FORAMINIFERS, NANNOFOSSILS, RADIOLARIANS, DIATOMS, PALYNOMORPHS)

CLAYEY MUD

Major lithology: Clayey mud, dark greenish gray (5G 4/1). Smear slide contains many grains with a clay coating; by size and shape they appear to be quartz.

Minor lithology: Carbonate-cemented, partially indurated layer in CC, 11-14 cm, has a clumpy texture. Altered volcanic ash(?), greenish gray (5G 5/1), in CC, 35-38 cm, and a bluish green lamina at CC, 31 cm. Contains two white silt clasts.

SMEAR SLIDE SUMMARY (%):

	CC, 20 D
TEXTURE:	
Sand	Tr
Silt	30
Clay	70
COMPOSITION:	
Quartz	20
Feldspar	2
Mica	1
Clay	70
Volcanic glass	1
Accessory minerals	2
Glauconite	Tr
Opaque minerals	3
Diatoms	1

SITE 697 HOLE B CORE 19X CORED INTERVAL 3667.1-3676.7 mbsl; 186.6-196.2 mbsf

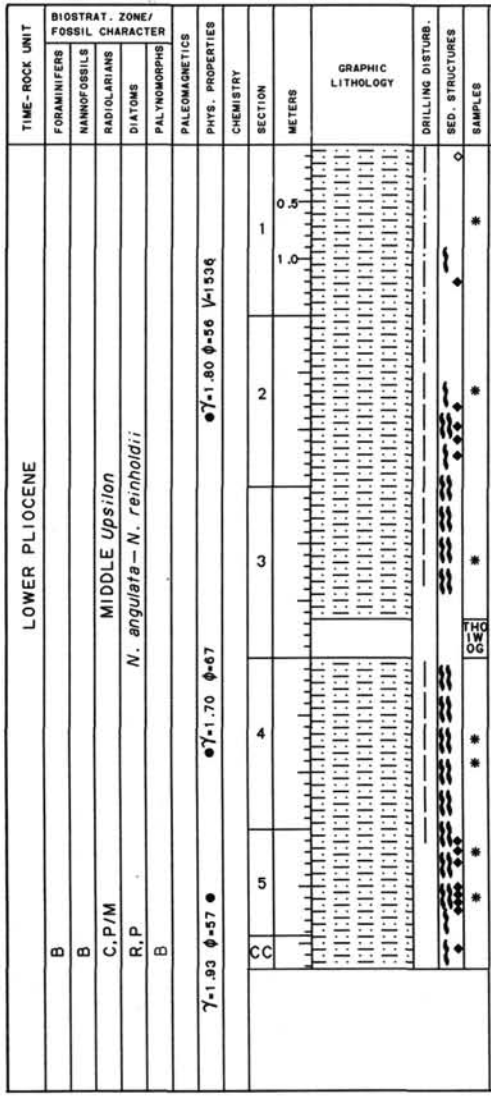

LITHOLOGIC DESCRIPTION

CLAYEY MUD

Major lithology: Clayey mud, dark greenish gray (5GY 4/1, 5Y 4/2), Section 5, 54–67 cm. The olive gray layer is slightly more carbonate rich.

Minor lithologies: Pyritized diatom ooze, Section 4, 91–94 cm, with a "net veined" surface texture, black (N 4/0) and dark greenish gray (5G 4/1). Muddy diatom ooze in Section 5, 12–17 cm, black (5Y 2.5/2). Altered volcanic ash, greenish gray (5G 4/1), poorly defined layers in Section 3, 34, 54, and 88(?) cm, and Section 4, 49–51 and 131 cm. Silt clasts are minor. The highest abundance is in Section 5, 30–45 cm, where 12 are present.

Bioturbation is minor to moderate and is a major factor in diffusing the boundaries. Two dropstones, Section 1, 4 cm (2.5 cm in size), subangular, quartzite; and in Section 5, (2.5 cm in size), subangular, very weathered igneous. Coring disturbance is high in Sections 1 and 2 and low in the remainder of the core.

SMEAR SLIDE SUMMARY (%):

	1, 70 D	2, 70 D	3, 70 D	4, 70 D	4, 91 M	5, 17 M	5, 60 D
TEXTURE:							
Silt	25	30	30	30	—	—	35
Clay	75	70	70	70	—	—	65
COMPOSITION:							
Quartz	10	14	14	15	8	9	16
Mica	—	—	—	—	—	—	1
Clay	75	70	70	70	30	20	65
Volcanic glass	4	4	4	3	2	1	2
Calcite/dolomite	—	—	—	—	—	—	8
Accessory minerals	4	6	3	2	—	—	4
Opaque minerals	3	2	2	1	—	—	—
Amphibole	—	Tr	—	—	—	—	—
Unidentified white spheres	—	—	Tr	—	Tr	Tr	2
Diatoms	4	4	7	9	60	70	2

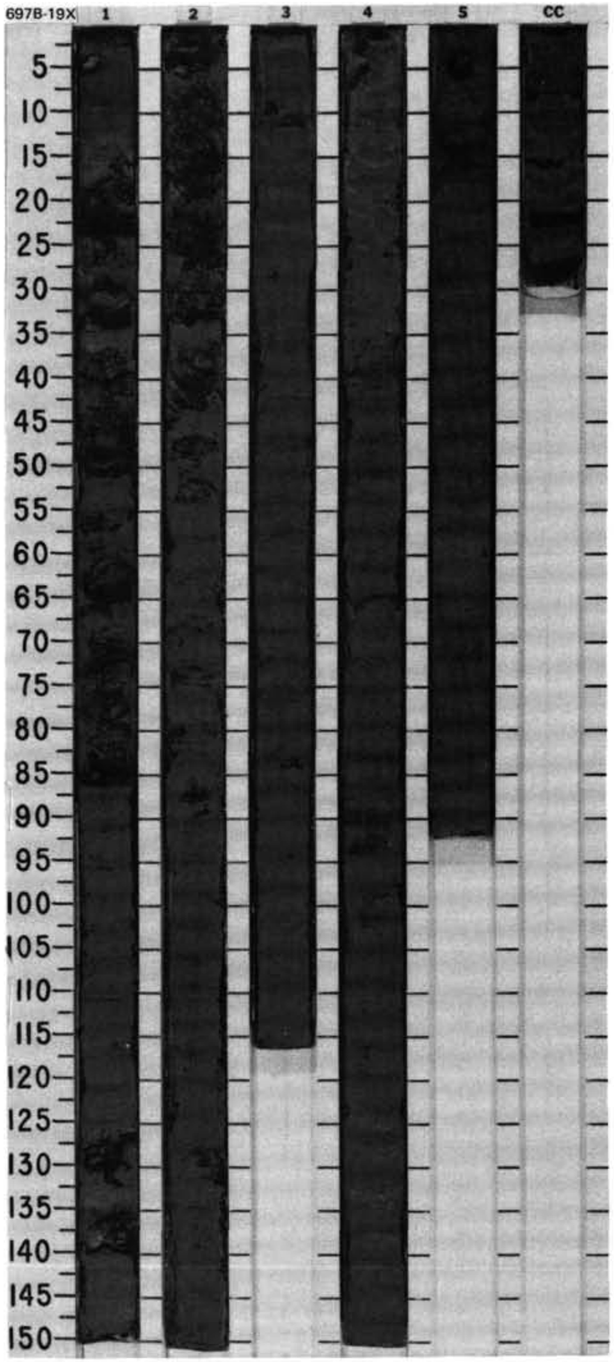

SITE 697 HOLE B CORE 20X CORED INTERVAL 3676.7-3686.4 mbsl; 196.2-205.9 mbsf

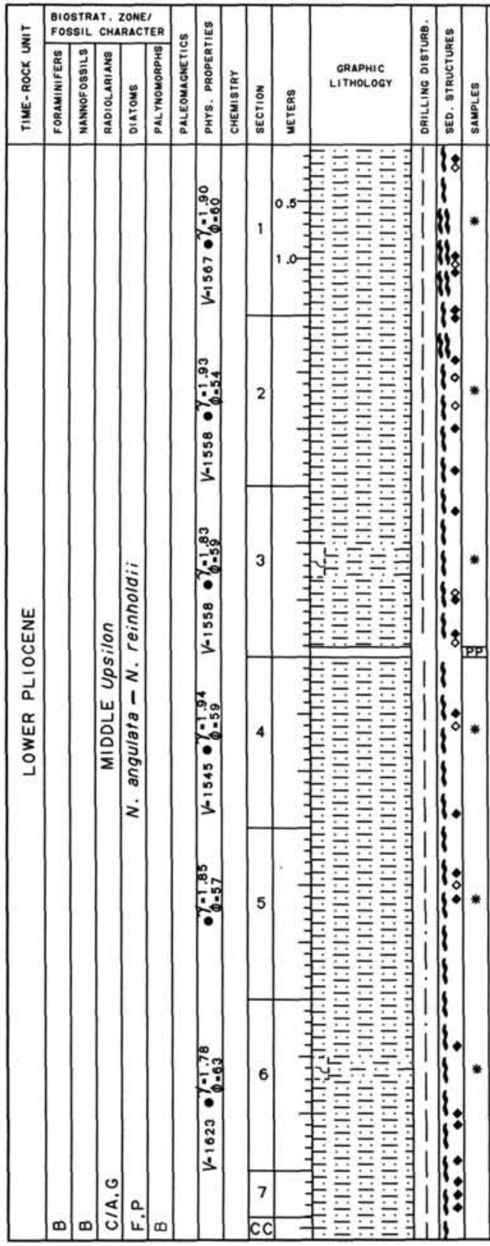

LITHOLOGIC DESCRIPTION

CLAYEY MUD

Major lithology: Clayey mud, dark gray (N 4/0), dark bluish gray (5B 4/1), and dark greenish gray (5G 4/1). Color transitions are gradual.

Minor lithologies: Diatom-bearing clayey mud in Section 3, 50-80 cm, and Section 6, 50-70 cm, dark greenish gray (5G 4/1) and dark bluish gray (5B 4/1); coincides with the more indurated layers. Altered volcanic ash, grayish green (5G 4/2), common in Section 2, 3, and 6. Carbonate cemented burrow in Section 1, 149 cm; light brown burrow filling contains mainly dolomite. White silt clasts are common.

Bioturbation is minor to moderate. Dropstones are present in Section 1, 4 cm (10 cm in size), subrounded sandstone; Section 1, 100 cm (0.3 cm), rounded, igneous; Section 2, 100 cm (0.5 cm), rounded, sedimentary; Section 2, 140 cm (0.5 cm), shale; Section 4, 75 cm (0.4 cm), shale; and Section 5, (0.8 cm in size), rounded, igneous.

SMEAR SLIDE SUMMARY (%):

	1, 70 D	2, 70 D	3, 70 D	4, 70 D	5, 70 D	6, 70 M
TEXTURE:						
Sand	—	—	—	—	1	—
Silt	43	27	51	36	45	50
Clay	57	73	49	64	54	50
COMPOSITION:						
Quartz	20	15	20	10	26	25
Feldspar	3	2	—	1	—	3
Rock fragments	—	1	—	—	—	—
Mica	—	—	—	1	—	—
Clay	47	59	49	64	54	50
Volcanic glass	2	2	3	1	2	—
Calcite/dolomite	20	14	10	—	—	5
Accessory minerals	—	1	—	2	2	1
Zeolites	1	1	1	—	—	—
Opaque minerals	2	3	2	4	2	1
Clay-covered grains	—	—	—	15	10	—
Diatoms	5	2	15	2	4	15
Silicoflagellates	—	—	—	—	—	Tr

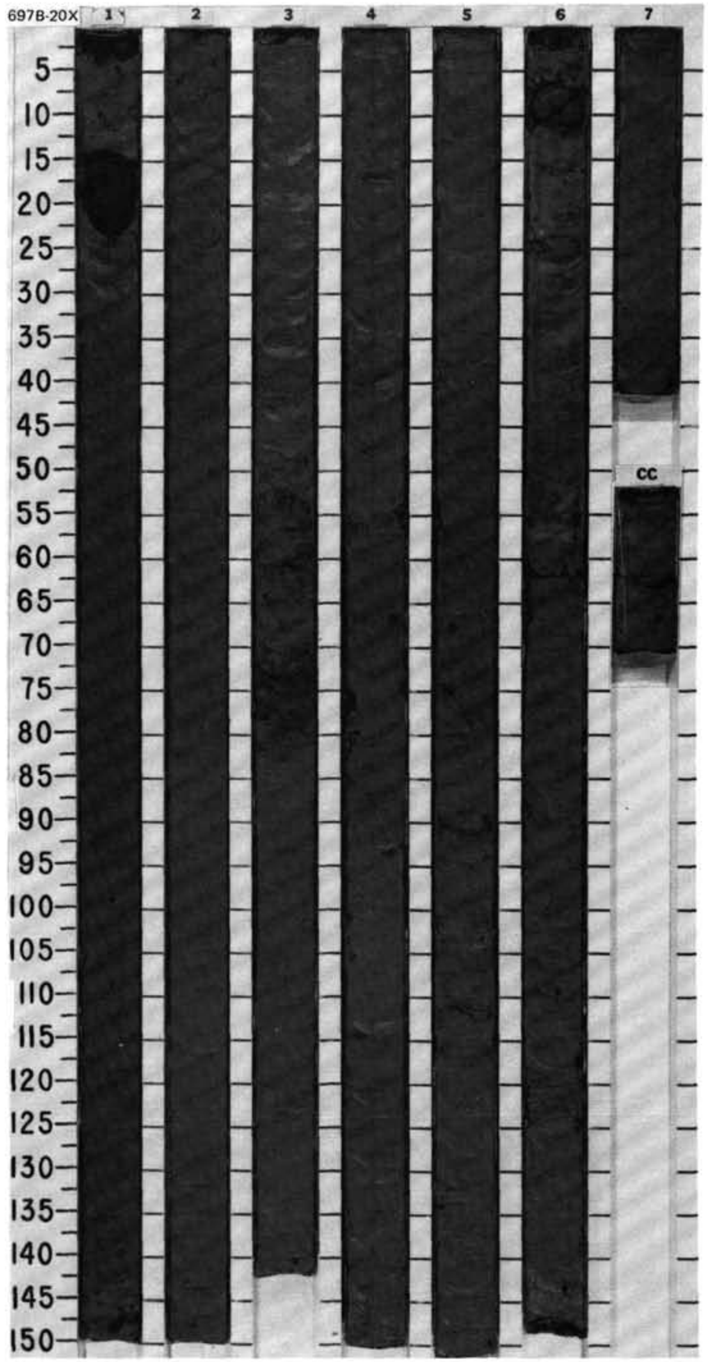

SITE 697 HOLE B CORE 21X CORED INTERVAL 3686.4-3696.0 mbsl; 205.9-215.5 mbsf

TIME-ROCK UNIT	FORAMINIFERS	NANNOFOSSILS	RADIOLARIANS	DIATOMS	PALYNOMORPHS	PALEOMAGNETICS	PHYS. PROPERTIES	CHEMISTRY	SECTION	METERS	GRAPHIC LITHOLOGY	DRILLING DISTURB.	SED. STRUCTURES	SAMPLES
LOWER PLIOCENE	B	B	C,P/M MIDDLE *Upsilon*	F,P *N. angulata — N. reinholdii*	B		●γ=1.83 ϕ=57 V=1590		1, 2, CC	0.5, 1.0				* * *

CLAYEY MUD

Major lithology: Clayey mud, dark greenish gray (5G 4/1). *Pyrite concretions* observed at Section 1, 148 cm. Drilling disturbance varies from very strong to moderate.

Minor lithology: Muddy diatom ooze, olive gray (5Y 5/2), at Section 2, 15-17 cm. Altered volcanic ash, grayish green (5G 4/2), Section 2, 102 cm. Silt clasts occur at base of Section 1 and from 70-120 cm in Section 2.

Bioturbation is minor.

SMEAR SLIDE SUMMARY (%):

	1, 130 D	2, 16 M	2, 80 D
TEXTURE:			
Silt	40	—	30
Clay	60	—	70
COMPOSITION:			
Quartz	12	10	14
Feldspar	2	—	1
Mica	Tr	—	—
Clay	60	15	70
Volcanic glass	6	—	2
Accessory minerals	5	5	2
Opaque minerals	4	—	3
Zeolites	Tr	—	Tr
Clay-covered grains	6	—	—
Diatoms	5	70	8
Radiolarians	Tr	—	—

SITE 697 HOLE B CORE 22X CORED INTERVAL 3696.0-3705.7 mbsl; 215.5-225.2 mbsf

TIME-ROCK UNIT	FORAMINIFERS	NANNOFOSSILS	RADIOLARIANS	DIATOMS	PALYNOMORPHS	PALEOMAGNETICS	PHYS. PROPERTIES	CHEMISTRY	SECTION	METERS	GRAPHIC LITHOLOGY	DRILLING DISTURB.	SED. STRUCTURES	SAMPLES
LOWER PLIOCENE	B	B	C,M MIDDLE *Upsilon*	R,P ?	B		V=1639 ●γ=1.88 ϕ=58; V=1550 ●γ=1.84 ϕ=57		1, 2, 3, CC	0.5, 1.0				* * IW OG THO HS

CLAYEY MUD

Major lithology: Clayey mud, dark greenish gray (5G 4/1), strongly disturbed in upper part of Section 1, otherwise moderately to slightly disturbed.

Minor lithology: Altered volcanic ash(?), grayish green (5G 5/2), in Section 2, 7, 38, 69, and 72 cm; and Section 3, 17 and 22 cm.

Igneous dropstones at top of Section 1 and at base of CC. Pyrite concretion at top of Section 3. Bioturbation is minor.

SMEAR SLIDE SUMMARY (%):

	1, 80 D	2, 80 D
TEXTURE:		
Silt	25	30
Clay	75	70
COMPOSITION:		
Quartz	9	13
Clay	75	70
Volcanic glass	3	2
Accessory minerals	2	3
Opaque minerals	3	2
Diatoms	8	10
Radiolarians	—	Tr
Silicoflagellates	—	Tr

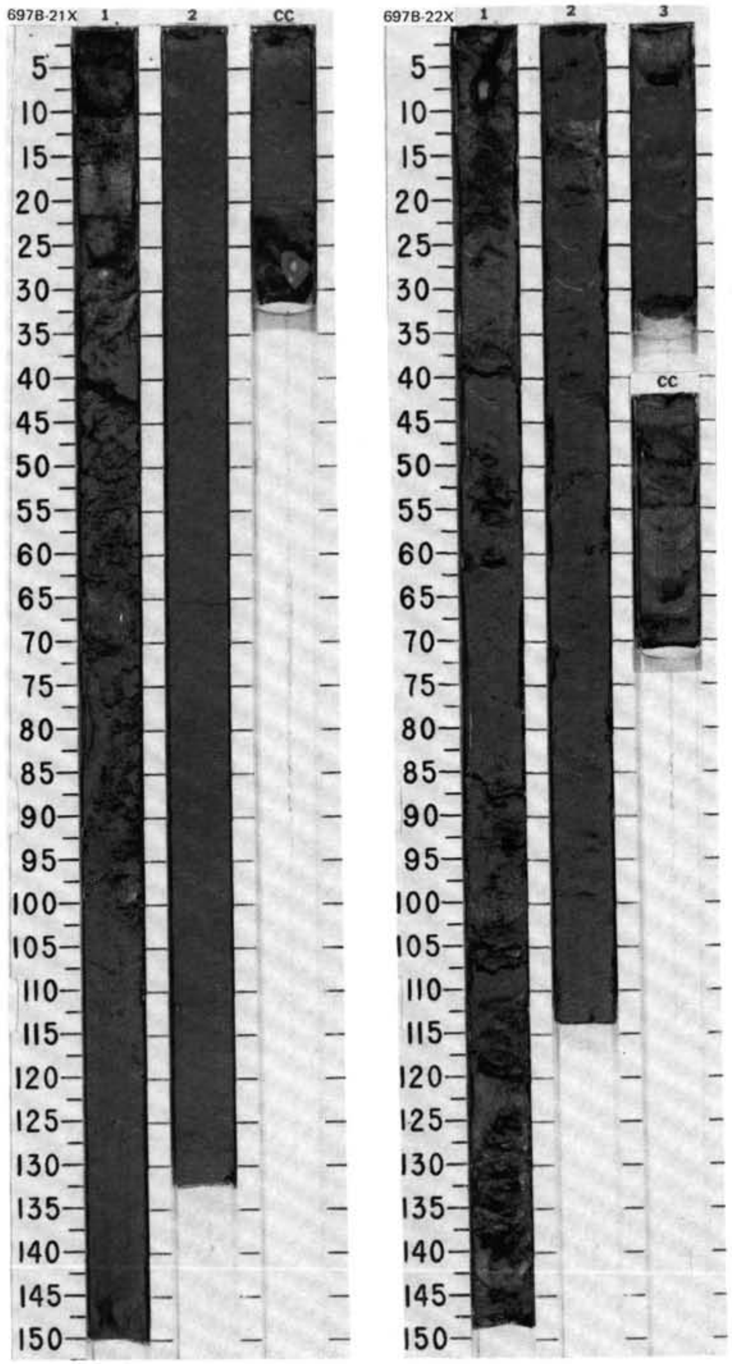

SITE 697 HOLE B CORE 23X CORED INTERVAL 3705.7-3715.3 mbsl; 225.2-234.8 mbsf

TIME-ROCK UNIT	FORAMINIFERS	NANNOFOSSILS	RADIOLARIANS	DIATOMS	PALYNOMORPHS	PALEOMAGNETICS	PHYS. PROPERTIES	CHEMISTRY	SECTION	METERS	GRAPHIC LITHOLOGY	DRILLING DISTURB.	SED. STRUCTURES	SAMPLES
LOWER PLIOCENE	B	B	MIDDLE *Upsilon* C,M	*N. angulata* — *N. reinholdii* R,P	B				1	0.5				*
										1.0				
									CC					

BIOSTRAT. ZONE/FOSSIL CHARACTER

LITHOLOGIC DESCRIPTION

DIATOM-BEARING CLAYEY MUD

Major lithology: Diatom-bearing clayey mud, dark greenish gray (5G 4/1), very strongly disturbed by drilling.

SMEAR SLIDE SUMMARY (%):

	1, 70
	D
TEXTURE:	
Silt	30
Clay	70
COMPOSITION:	
Quartz	6
Clay	70
Volcanic glass	2
Accessory minerals	5
Opaque minerals	2
Diatoms	15

SITE 697 HOLE B CORE 24X CORED INTERVAL 3715.3-3725.0 mbsl; 234.8-244.5 mbsf

TIME-ROCK UNIT	FORAMINIFERS	NANNOFOSSILS	RADIOLARIANS	DIATOMS	PALYNOMORPHS	PALEOMAGNETICS	PHYS. PROPERTIES	CHEMISTRY	SECTION	METERS	GRAPHIC LITHOLOGY	DRILLING DISTURB.	SED. STRUCTURES	SAMPLES
LOWER PLIOCENE	B	B	LOWER *Upsilon* / UPPER *Tau* C,M/P	? *N. angulata* – *N. reinholdii* R,P	B		γ=1.93 φ=58 V=1580 ●		1	0.5				*
									CC	1.0				

BIOSTRAT. ZONE/FOSSIL CHARACTER

LITHOLOGIC DESCRIPTION

CLAYEY MUD

Major lithology: Clayey mud, dark gray (N 4/0); faint minor bioturbation, with burrow fills of very dark gray (N 3/0) clay. Most of the core is too disturbed to see any primary structures.

SMEAR SLIDE SUMMARY (%):

	1, 50
	D
TEXTURE:	
Silt	22
Clay	78
COMPOSITION:	
Quartz	10
Clay	78
Accessory minerals:	
Heavy minerals	1
Opaque minerals	2
Zeolites(?)	1
Diatoms	7
Sponge spicules	1

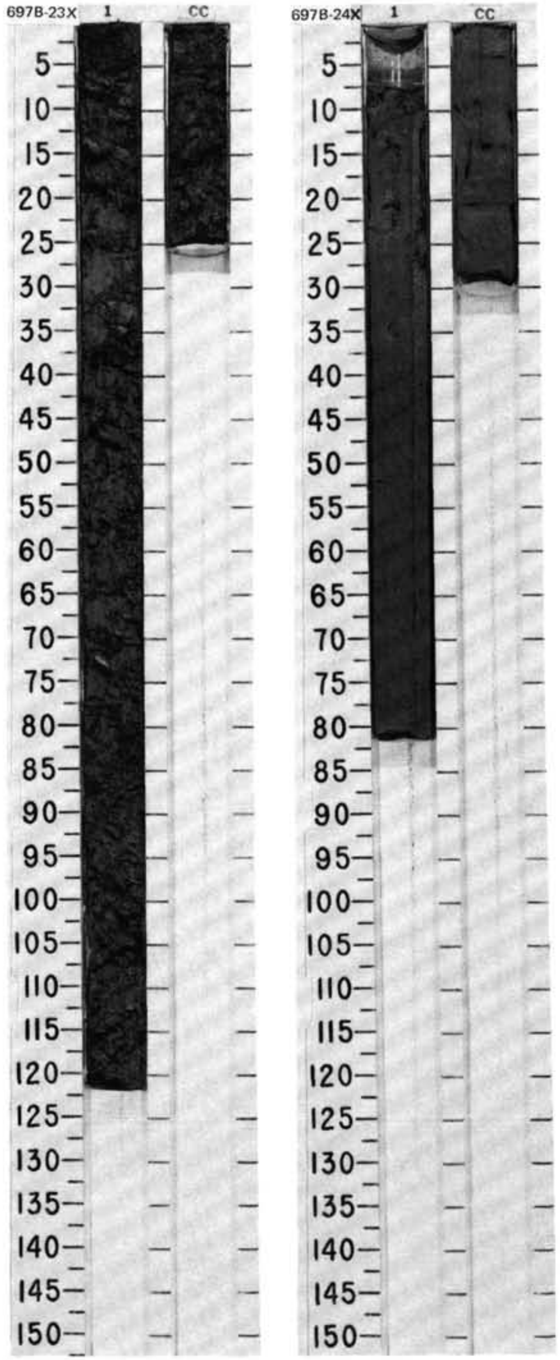

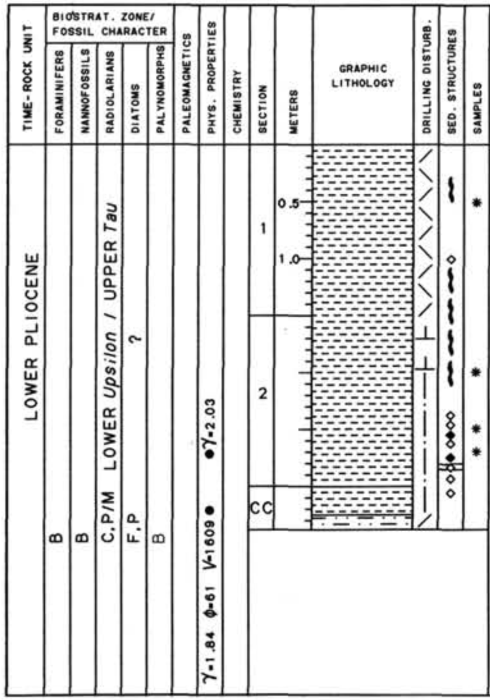

LITHOLOGIC DESCRIPTION

CLAY

Major lithology: Clay, dark greenish gray (5BG 4/1 to 5GY 4/1), faint minor bioturbation where not too disturbed. Section 1 contains drilling biscuits.

Minor lithologies: Clayey mud, gray (5Y 5/1), in Section 2, 117-120 cm, and CC, 24-37 cm. Clay, dark gray (N 4/0), in Section 2, 122-132 and 135-138 cm, probably altered ash layers.

Dropstones in Section 1, 102 cm (1 cm in size), quartzite, subrounded; Section 2, 86 cm (6 cm), amphibolite with granite vein, subangular; Section 2, 88 cm (1 cm), biotite schist, subangular; Section 2, 114 cm (1 cm), siltstone, subrounded; Section 2, 131 cm (1 cm), siltstone, rounded; Section 2, 135 cm (1 cm), quartzite, subangular; and CC, 4 cm (3 cm), diorite, rounded.

SMEAR SLIDE SUMMARY (%):

	1, 50 D	2, 50 D	2, 109 M	2, 127 D
TEXTURE:				
Silt	17	15	19	18
Clay	83	85	81	82
COMPOSITION:				
Quartz	10	7	8	9
Feldspar	—	—	1	—
Mica	Tr	1	1	1
Clay	83	85	81	82
Volcanic glass	Tr	Tr	—	2
Accessory minerals:				
Heavy minerals	2	3	3	1
Opaque minerals	2	1	2	2
Foraminifers	3	3	4	3
Nannofossils	—	—	Tr	—

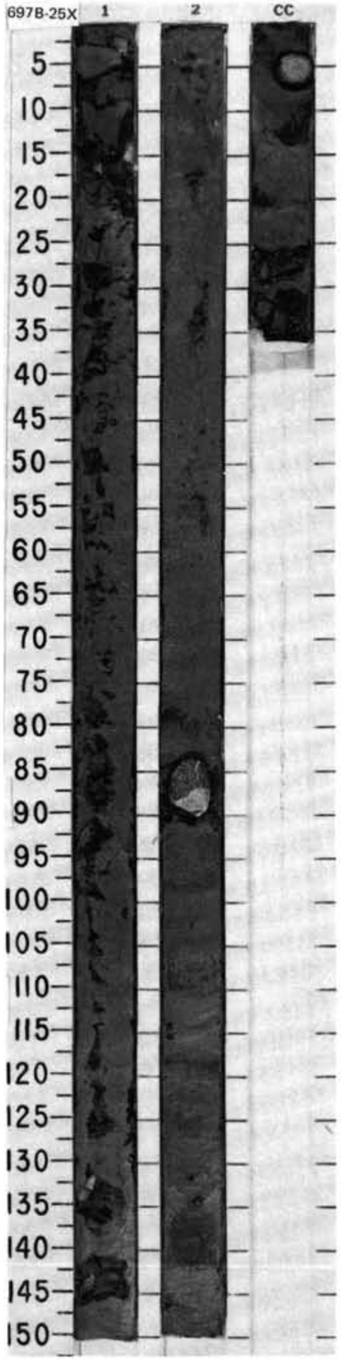

SITE 697 HOLE B CORE 26X CORED INTERVAL 3734.7-3744.4 mbsl; 254.2-263.9 mbsf

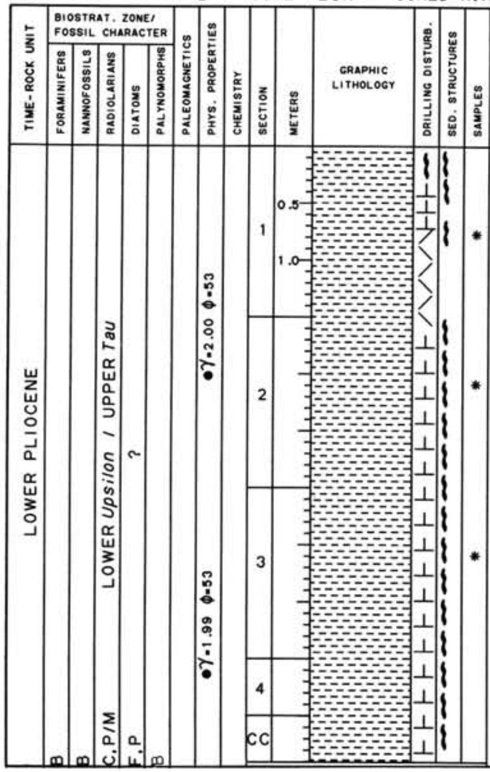

LITHOLOGIC DESCRIPTION

CLAY

Major lithology: Clay, dark gray (N 4/0), biscuited. Small pyritized or partly pyritized burrows in Section 1, 62 cm; Section 3, 34, 93, 109-115, and 145 cm; and CC, 6 cm.

Minor lithologies: Clay, very dark gray (N 3/0), occurs as laminae or burrow fills in Section 1, 15 cm; Section 2, 28, 35, 58, 74, 93, and 97 cm; Section 3, 40, 42, 78, 96, 100, 120, 137, and 144 cm; and Section 4, 4, 10, 28, and 36 cm. Clay, dark greenish gray (5GY 4/1), occurs as laminae in Section 2, 83 and 104 cm; Section 3, 96, 105, 115, 134, and 119 cm; and Section 4, 2, 9, 16, 21, 33, and 39 cm. Silt, gray (N 6/0), occurs as tiny (1-2 mm) clasts, mainly in Sections 3 and 4.

Minor bioturbation.

SMEAR SLIDE SUMMARY (%):

	1, 75 D	2, 58 D	3, 60 D
TEXTURE:			
Silt	19	20	20
Clay	81	80	80
COMPOSITION:			
Quartz	5	10	7
Feldspar	—	Tr	Tr
Clay	81	79	80
Accessory minerals	5	3	7
Amphibole	Tr	—	—
Opaque minerals	2	2	1
Heavy minerals	Tr	1	Tr
Diatoms	7	5	5
Radiolarians	Tr	—	Tr
Sponge spicules	Tr	←	—

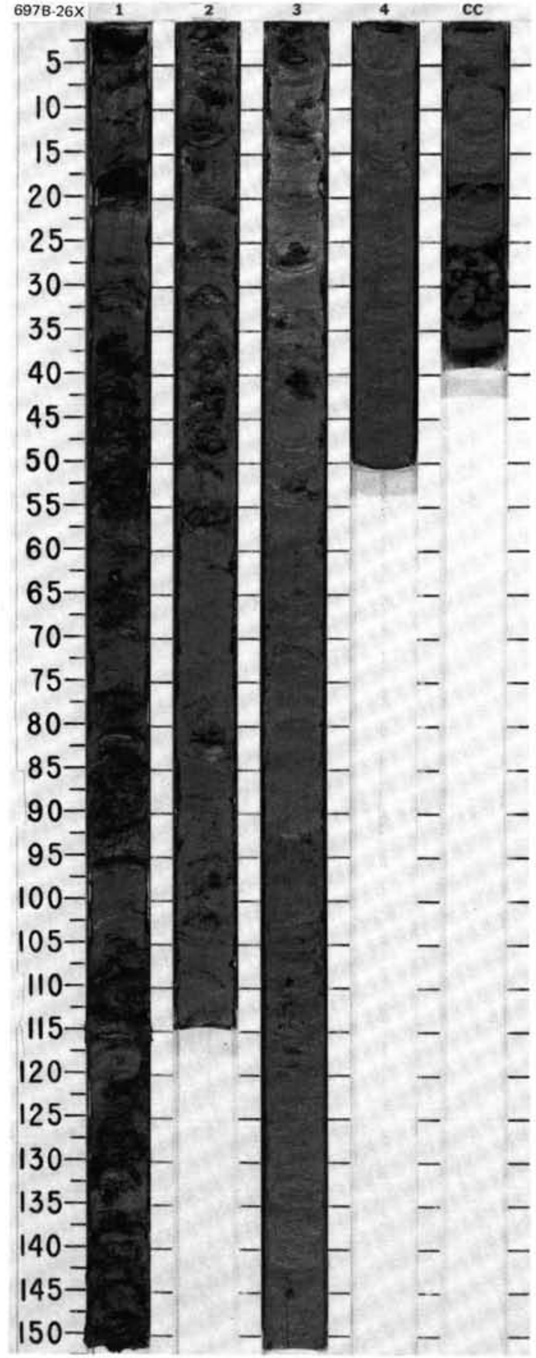

SITE 697 HOLE B CORE 27X CORED INTERVAL 3744.4-3754.1 mbsl; 263.9-273.6 mbsf

TIME-ROCK UNIT	BIOSTRAT. ZONE/ FOSSIL CHARACTER: FORAMINIFERS	NANNOFOSSILS	RADIOLARIANS	DIATOMS	PALYNOMORPHS	PALEOMAGNETICS	PHYS. PROPERTIES	CHEMISTRY	SECTION	METERS	GRAPHIC LITHOLOGY	DRILLING DISTURB.	SED. STRUCTURES	SAMPLES
LOWER PLIOCENE	B	B	C,P/M LOWER *Upsilon* / UPPER *Tau*	R,P ?	B		●γ=2.01 φ=52 V=1615		1	0.5 1.0				*
									2					*
									CC					

LITHOLOGIC DESCRIPTION

CLAYEY MUD and CLAY

Major lithologies: Clayey mud in Section 1, grading down to clay in Section 2, dark gray (N 4/0) to dark greenish gray (5GY 4/1), moderately to highly disturbed, minor bioturbation. Slightly siltier at base of CC. Pyritized burrows in Section 1, 19 and 38 cm.

Minor lithology: Clay, very dark gray (N 3/0), occurs as a few burrow fills in Section 1, and as laminae in Section 2, 46 and 50 cm; and in CC, 12 cm.

Minor bioturbation. Two small dropstones.

SMEAR SLIDE SUMMARY (%):

	1, 50 D	2, 50 D
TEXTURE:		
Sand	2	—
Silt	19	15
Clay	79	85
COMPOSITION:		
Quartz	7	5
Feldspar	—	Tr
Clay	79	85
Accessory minerals	5	1
Amphibole	—	Tr
Opaque minerals	1	1
Heavy minerals	1	1
Diatoms	7	7
Radiolarians	Tr	Tr

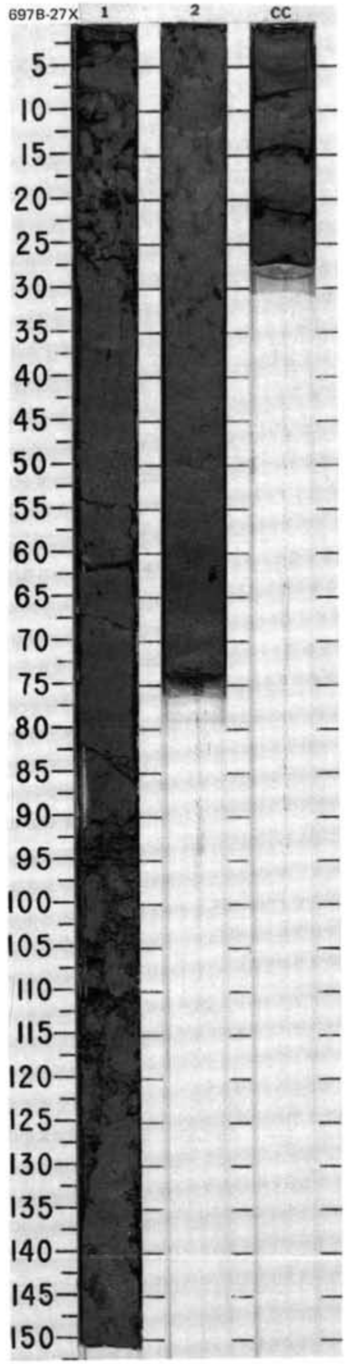

SITE 697 HOLE B CORE 28X CORED INTERVAL 3754.1-3763.8 mbsl; 273.6-283.3 mbsf

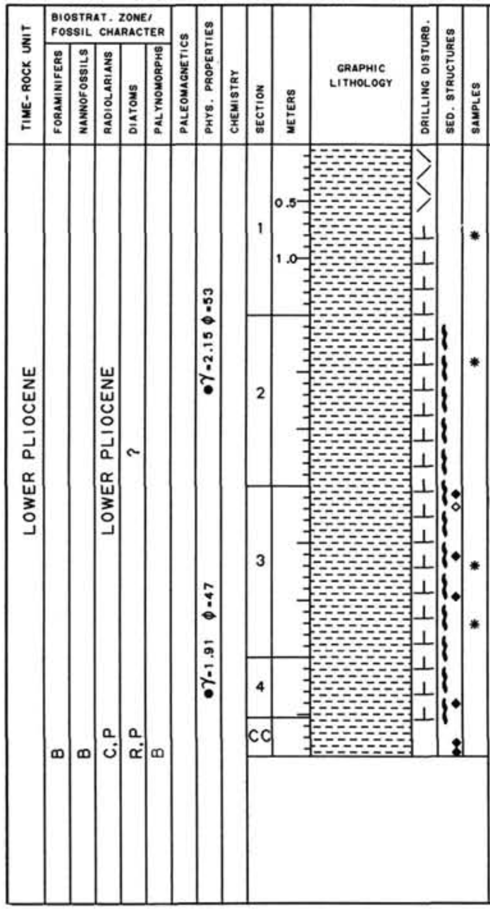

LITHOLOGIC DESCRIPTION

CLAY

Major lithology: Clay, dark greenish gray (5G 4/1), grading to dark gray (N 4/0), in Sections 3 and 4.

Minor lithologies: Altered volcanic ash(?) and clay; very dark gray (N 3/0) laminae, Sections 2 to 4, and dark greenish gray laminae (5G 4/1), Section 3. Silty mud, gray (5Y 5/1), Section 3, 113-114 cm.

Minor bioturbation, Sections 2-4; pyritized burrows, Sections 3 and 4. Dropstones. Section 1, 48 cm (red sandstone), and Section 3, 18 cm. Gray silt clasts, Sections 3, 4, and CC.

SMEAR SLIDE SUMMARY (%):

	1, 80 D	2, 40 D	3, 65 D	3, 118 M
TEXTURE:				
Sand	5	2	1	2
Silt	8	12	19	44
Clay	87	86	80	54
COMPOSITION:				
Quartz	3	5	9	2
Feldspar	Tr	Tr	—	—
Clay	87	86	77	46
Volcanic glass	—	—	1	2
Accessory minerals	7	4	3	8
Glauconite	—	—	Tr	—
Amphibole	—	Tr	Tr	—
Opaque minerals	1	1	4	3
Heavy minerals	1	1	2	1
Unidentified	—	—	—	30
Diatoms	1	3	4	8
Sponge spicules	Tr	Tr	—	—

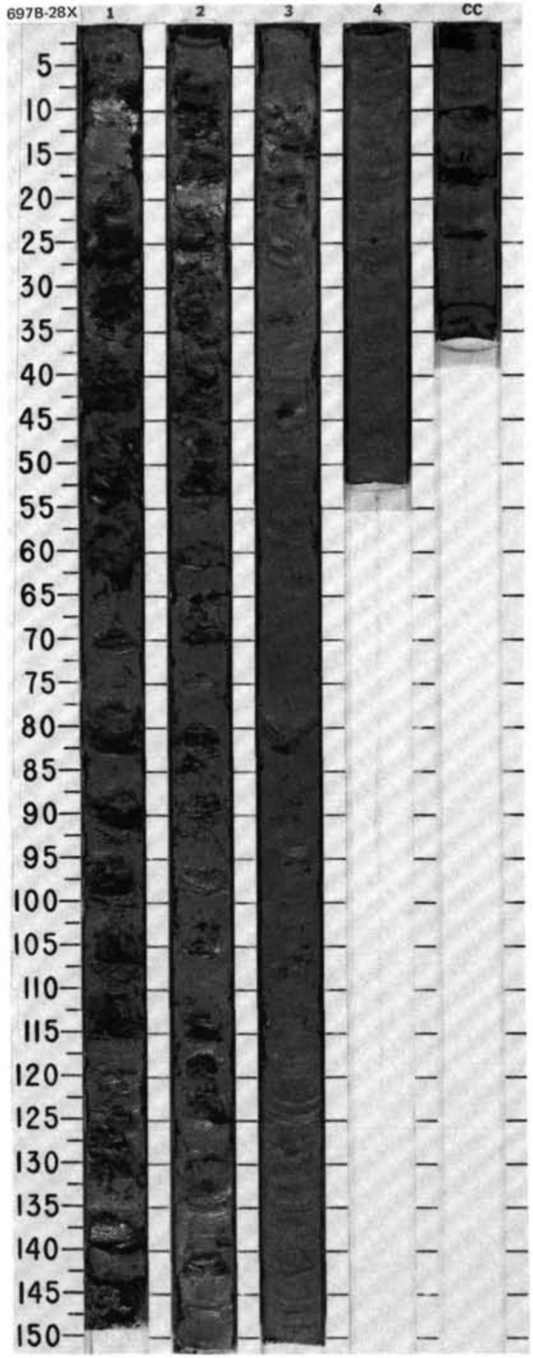

SITE 697 HOLE B CORE 29X CORED INTERVAL 3763.8-3773.5 mbsl; 283.3-293.0 mbsf

TIME-ROCK UNIT	BIOSTRAT. ZONE/ FOSSIL CHARACTER: FORAMINIFERS	NANNOFOSSILS	RADIOLARIANS	DIATOMS	PALYNOMORPHS	PALEOMAGNETICS	PHYS. PROPERTIES	CHEMISTRY	SECTION	METERS	GRAPHIC LITHOLOGY	DRILLING DISTURB.	SED. STRUCTURES	SAMPLES
LOWER PLIOCENE	B	B	PLIOCENE F/C,P	? F,P	B		γ=1.87 ϕ=47 ● γ=1.94 ϕ=50 ●		1, 2, 3, CC	0.5, 1.0				* * * * IW THOG HS

LITHOLOGIC DESCRIPTION

CLAY

Major lithology: Clay, dark greenish gray (5G 4/1), grading to dark gray (N 4/0) at base of Section 3 and CC. Minor bioturbation. Splitting disturbance as well as biscuiting, particularly in Sections 1 and 2.

Minor lithologies: Silty mud, dark gray (5Y 4/1), occurs as burrowed layer in Section 3, 21-26 cm. Altered volcanic ash(?), clay, very dark gray (N 3/0), occurs as laminae or burrow-fills in Section 1, 3, 5, 49, 76, 104, 113, 119, and 131 cm, and Section 3, 16, 47, and 66 cm. Altered volcanic ash(?), clay, dark greenish gray (5GY 4/1), occurs as layers in Section 1, 5-6 and 10-12 cm.

Dropstones in Section 3, 23-25 cm, biotite schist (1 cm in size), angular; and mudstones (0.8 and 0.6 cm in size), rounded.

SMEAR SLIDE SUMMARY (%):

	1, 50 D	2, 50 D	3, 25 M	3, 50 D
TEXTURE:				
Sand	Tr	—	25	—
Silt	12	6	50	18
Clay	88	94	25	82
COMPOSITION:				
Quartz	7	2	54	8
Feldspar	Tr	—	3	1
Mica	1	—	2	2
Clay	87	94	25	82
Volcanic glass	—	—	—	2
Accessory minerals	—	—	3	—
Rutile	—	—	—	Tr
Amphibole	Tr	—	7	Tr
Garnet	—	—	2	—
Opaque minerals	2	2	1	2
Heavy minerals	1	1	3	1
Micronodules	—	—	—	Tr
Glauconite	—	—	—	Tr
Diatoms	2	1	Tr	2
Radiolarians	—	Tr	—	—
Sponge spicules	Tr	Tr	Tr	—

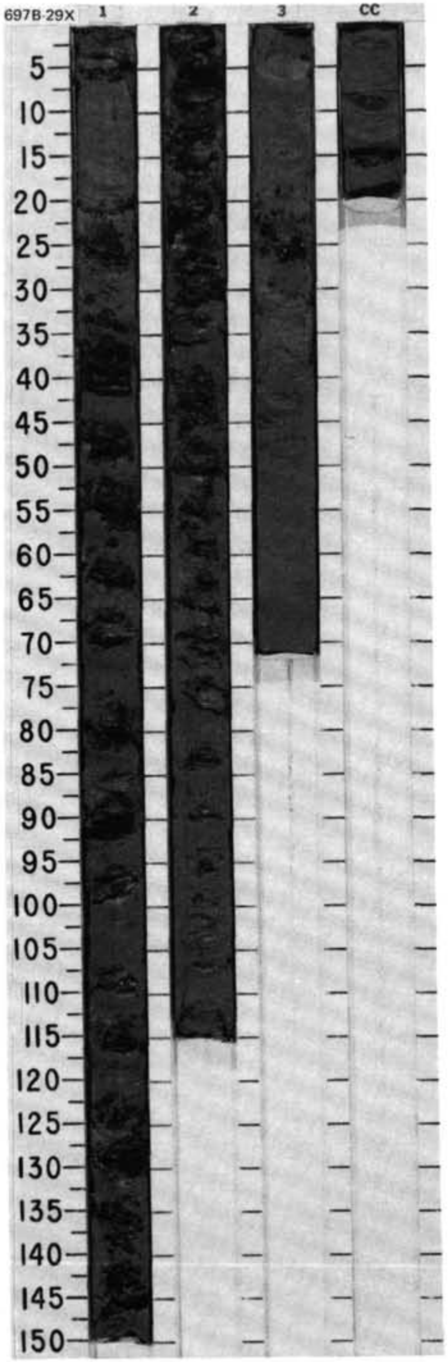

SITE 697 HOLE B CORE 30X CORED INTERVAL 3773.5-3783.1 mbsl; 293.0-302.6 mbsf

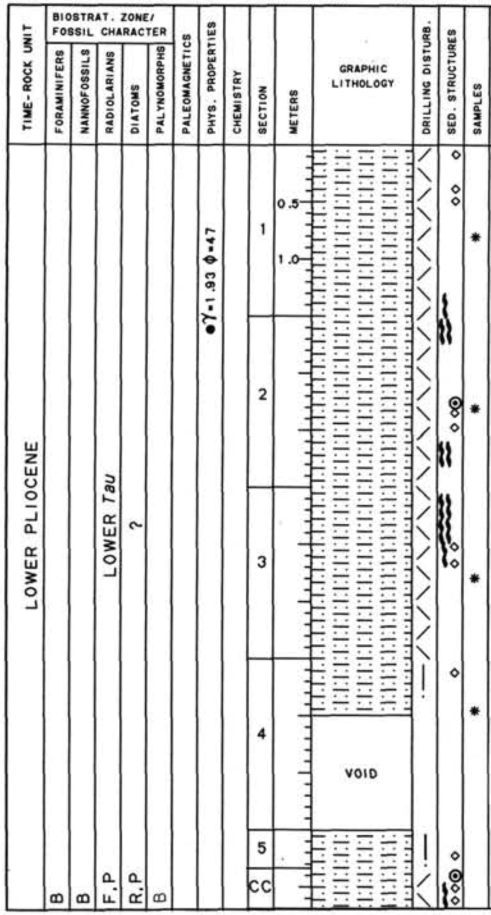

LITHOLOGIC DESCRIPTION

CLAYEY MUD

Major lithology: Clayey mud, dark greenish gray (5BG 4/1), top of Section 1, changing to dark gray (N 4/0) throughout rest of core. Core is highly fragmented and biscuited, so it is difficult to see primary structures.

Minor lithology: Altered volcanic ash(?), silty mud, dark greenish gray (5BG 4/1), as thin layers in Section 1, 65-90 cm(?); Section 2, 70 cm; Section 4, 41-52 cm; and Section 5, 19 and 32 cm.

Ice-rafted dropstones are common throughout. Dropstones greater than 0.3 cm occur in Section 1, 10 cm (2 cm in size), sedimentary, rounded; Section 1, 38 cm (0.5 cm), igneous, rounded; Section 1, 50 cm (0.5 cm), sedimentary, rounded; Section 2, 78 cm (0.3 cm), quartz, subangular; Section 2, 82 cm (0.5 cm), black, subrounded; Section 3, 106 cm (0.8 cm), granite, subangular; Section 3, 108 cm (0.5 cm), sedimentary, rounded; and Section 5, 23 cm (0.5 cm), sedimentary, rounded. A pyrite concretion, 1.5 cm in size, occurs at Section 2, 75 cm. Bioturbation includes *Zoophycos* and *Chondrites*.

SMEAR SLIDE SUMMARY (%):

	1, 80 D	2, 80 D	3, 80 D	4, 50 M
TEXTURE:				
Sand	—	—	—	Tr
Silt	45	45	40	60
Clay	55	55	60	40
COMPOSITION:				
Quartz	21	20	24	32
Feldspar	4	4	5	4
Rock fragments	2	—	—	—
Mica	2	1	—	1
Clay	55	55	60	40
Volcanic glass	—	2	—	2
Accessory minerals:				
Weathered minerals	12	12	7	15
Zeolites	Tr	3	1	—
Opaque minerals	4	3	3	3
Amphibole	—	Tr	—	—
Diatoms	Tr	Tr	—	3

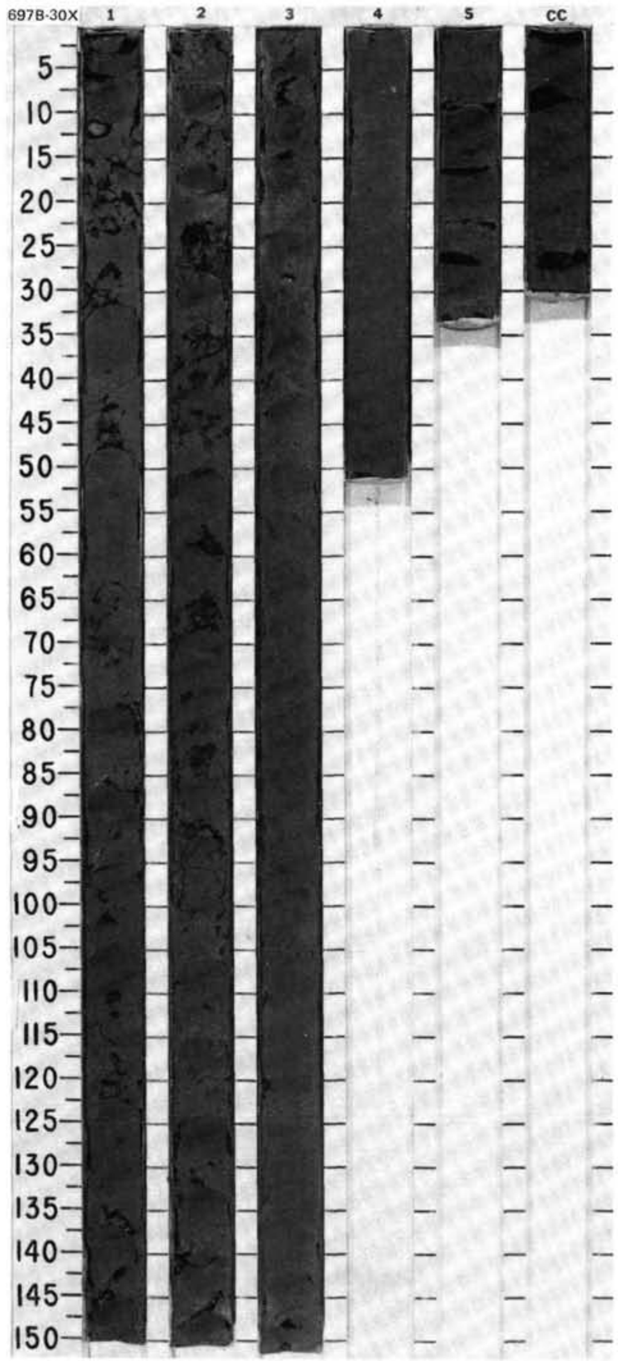

SITE 697 HOLE B CORE 31X CORED INTERVAL 3783.1-3792.7 mbsl; 302.6-312.2 mbsf

TIME-ROCK UNIT	FORAMINIFERS	NANNOFOSSILS	RADIOLARIANS	DIATOMS	PALYNOMORPHS	PALEOMAGNETICS	PHYS. PROPERTIES	CHEMISTRY	SECTION	METERS	GRAPHIC LITHOLOGY	DRILLING DISTURB.	SED. STRUCTURES	SAMPLES
LOWER PLIOCENE	B	B	LOWER Tau C,P	? R,P	B		γ=1.92 φ=53 ●V=1655		1, 2, 3, CC	0.5, 1.0				* * IW *

LITHOLOGIC DESCRIPTION

SILTY MUD

Major lithology: Silty mud, dark greenish gray (5BG 4/1). Extensive coring disturbance making sedimentary structures difficult to observe. Some faint color banding is present.

Minor lithology: Altered volcanic ash(?) and clay; dark gray (N 4/0) in thin beds *in Section 1, 59, 60, 75, and 110 cm.*

Bioturbation is rarely observed; includes *Chondrites*. Sand-sized dropstones are common throughout. Dropstones greater than 0.3 cm are present in Section 1, 128 cm (0.5 cm in size), quartz, subangular; Section 2, 124 cm (0.5 cm), indeterminate, rounded; Section 2, 132 cm (0.3 cm), indeterminate, rounded; Section 3, 93 cm (0.5 cm), volcanic, rounded; and CC, 19 cm (0.8 cm), plutonic, subrounded. Pyrite concretion in Section 3, 106 cm, is 2 cm wide.

SMEAR SLIDE SUMMARY (%):

	1, 80 D	2, 80 D	3, 80 D
TEXTURE:			
Silt	60	55	50
Clay	40	45	50
COMPOSITION:			
Quartz	30	39	32
Feldspar	2	2	3
Mica	2	1	1
Clay	40	45	50
Volcanic glass	2	2	2
Accessory minerals:			
Weathered minerals	15	5	8
Zeolites	Tr	2	1
Opaque minerals	5	2	3
Diatoms	4	2	Tr
Radiolarians	Tr	—	Tr

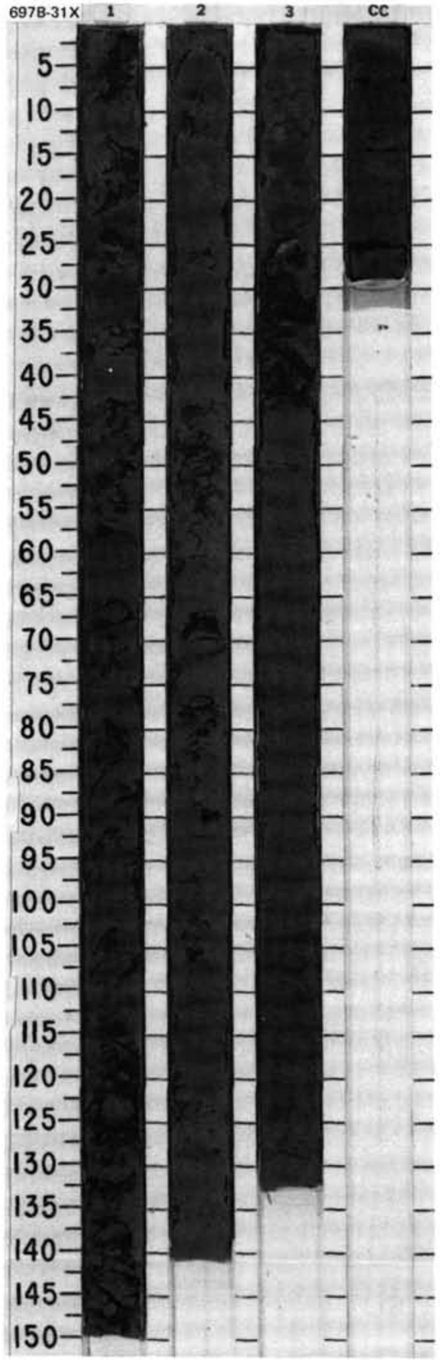

SITE 697 HOLE B CORE 32X CORED INTERVAL 3792.7-3803.4 mbsl; 312.2-322.9 mbsf

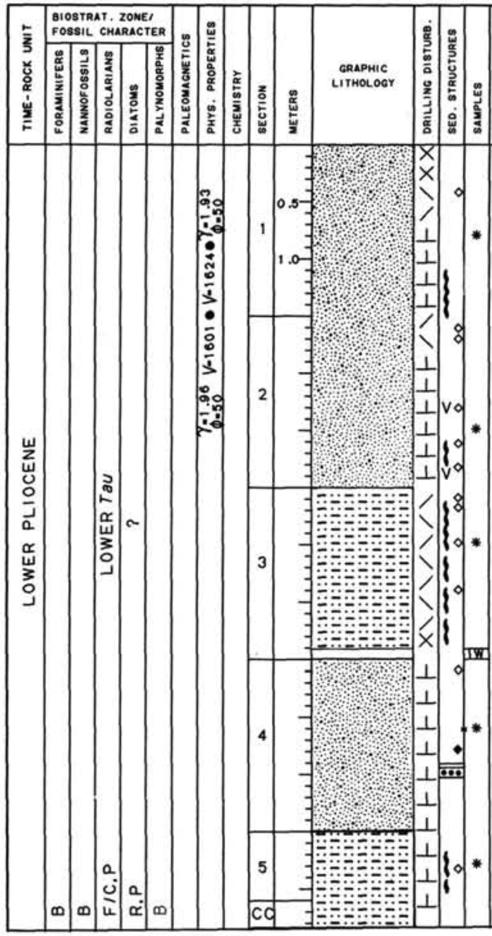

LITHOLOGIC DESCRIPTION

SILTY MUD and CLAYEY MUD

Major lithologies: Silty mud and clayey mud, dark greenish gray (5GY 4/1, 5BG 4/1); colors intermixed and highly disturbed by drilling. In Section 4, 90-100 cm, there is a graded and laminated interval.

Minor lithologies: Altered volcanic ash(?) and clay; dark gray (N 4/0) and dark greenish gray (5G 4/2), thin layers, in Section 1, 101-103 and 144 cm; Section 2, 41-48 cm; Section 4, 26, 28, 80-82, and 137-140 cm; and Section 5, 11, 12, 13, 21, and 30 cm. Volcanic ash, dark grayish brown (2.5Y 3/2), in Section 2, 74-75 and 146-147 cm.

Bioturbation is minor to absent, and includes *Planolites*. In Section 2, 123 cm, there is a pyritized *Planolites* burrow. Dropstones are common. Dropstones >0.3 mm are present in Section 1, 45 cm (2.5 cm in size), sedimentary, rounded; Section 1, 75 cm (2.5 cm in size), metamorphic, subangular; Section 2, 9 cm (0.5 cm), sedimentary, rounded; Section 2, 15 cm (1 cm); metamorphic, rounded; Section 2, 84 cm (0.5 cm), undetermined; Section 2, 99 cm (0.5 cm), quartz, angular; Section 2, 126 cm (0.5 cm), metamorphic, rounded; Section 3, 10 cm (3 cm), igneous, rounded; Section 3, 16 cm (2 cm), shale, rounded; Section 3, 26 cm, sedimentary, angular; Section 3, 88 cm (2 cm), igneous, rounded; Section 4, 8 cm (0.5 cm), sedimentary, rounded; Section 4, 148 cm (0.5 cm), shale, rounded; and Section 5, 45 cm (0.5 cm), igneous, angular.

SMEAR SLIDE SUMMARY (%):

	1, 70 D	2, 90 D	3, 75 M	3, 45 D	4, 60 D	5, 25 D
TEXTURE:						
Sand	4	5	—	1	5	1
Silt	47	42	90	26	44	31
Clay	49	53	10	73	51	68
COMPOSITION:						
Quartz	30	15	5	12	15	10
Feldspar	3	—	7	—	3	2
Rock fragments	2	2	—	—	1	—
Mica	—	3	—	—	—	—
Clay	49	53	10	73	51	68
Volcanic glass	2	1	59	—	2	2
Accessory minerals	1	2	—	3	1	1
Opaque minerals	3	4	25	4	2	2
Weathered minerals	10	20	—	8	25	10
Diatoms	Tr	Tr	—	—	Tr	5
Radiolarians	—	—	—	—	Tr	Tr